The response of NG2-glia after traumatic brain injury

Dissertation

der Fakultät für Biologie

der Ludwigs-Maximilians-Universität München

prepared at the Institute of Physiology, LMU München

submitted by

Axel von Streitberg

The thesis was submitted at the 1st of October 2015

Erstgutachter: Prof. Dr. Benedikt Grothe

Zweitgutachter: Prof. Dr. Christian Leibold

Tag der Einreichung: 01.10.2015

Tag der mündlichen Prüfung: 18.07.2016

I Summary

The mammalian central nervous system (CNS) consists of many different cell types contributing to its complex functional outcome. Its task of controlling essential body functions led to a unique cellular composition of this organ with many tissue-specific properties. One of the resulting consequences is an altered response to tissue damage, leading to insufficient regeneration following CNS injuries or diseases, which yields detrimental outcome for the majority of brain pathologies. A CNS-specific cell type which has just recently been connected to injury response are the NG2-glia. So far, these cells were known to be the major proliferative pool outside the neurogenic niches and are furthermore the progenitors of oligodendrocytes in the adult brain parenchyma. Given their great abundance, it is of major importance to better characterize the behavior and functionality of NG2-glia especially in relation to brain injury. Therefore, the aim of this PhD thesis was to further the knowledge about the course of events and potential functions of the NG2-glia response following traumatic brain injury. A detailed analysis of the cellular events employing *in vivo* two-photon microscopy in stab wounded mice expressing GFP within the oligodendrocyte lineage, revealed a fast and heterogeneous response of the majority of NG2-glia. The cells showed different behaviors like hypertrophy, polarization, migration and proliferation; whereas a small subset of NG2-glia and all mature oligodendrocytes remained static, retaining their initial position and morphology. The intensity of the observed injury response of NG2-glia was dependent on the severity of tissue damage as well as the distance to the injury. During the peak of NG2-glia reactivity that was observed between 2-4 days after injury an accumulation of NG2-glia directly within and in very close proximity to the lesion core could be detected. This cellular amassment led to a transient discontinuity of the homeostatic control of NG2-glia, which had been observed under physiological conditions. While starting from one week after injury, this cellular homeostasis was progressively reinstated and completely restored one month later. These events of cellular accumulation of NG2-glia after brain injury argue for the contribution to a first scaffold that is built after tissue damage, probably participating in wound closure and highlighting their importance in brain pathology.

II Zusammenfassung

Das zentrale Nervensystem (ZNS) der Säugetiere besteht aus einer Vielzahl verschiedener Zelltypen, die alle zu der komplexen Funktionalität dieses Organs beitragen. Insbesondere die Aufgabe überlebenswichtige Körperfunktionen zu kontrollieren und zu regulieren führte zu einem einzigartigen zellulären Aufbau, der einige gewebsspezifische Eigenschaften mit sich bringt. Eine daraus resultierende Konsequenz ist die ZNS-spezifische Reaktion auf Verletzungen, welche sich von anderen Gewebstypen unterscheidet und eine unzureichende Regeneration nach diversen ZNS-Verletzungen sowie Krankheiten zur Folge hat. Dies hat meist schwerwiegende Folgen für die entsprechenden Krankheitsverläufe. Ein ZNS-spezifischer Zelltyp, der erst kürzlich mit einer Reaktion auf Verletzungen in Verbindung gebracht wurde sind NG2-glia. Bis vor kurzem wurden diese Zellen hauptsächlich zwei wichtigen Eigenschaften in Verbindung gebracht: Proliferation außerhalb der neurogenen Nischen und der Vorläuferstatus für myelinisierende Oligodendrozyten im adulten Gehirn. Angesichts der Vielzahl von NG2-glia im adulten Gehirn ist es von großem Interesse das Verhalten dieses Zelltyps nach Verletzungen besser zu charakterisieren. Aufgrund dessen war das Ziel dieser Doktorarbeit den Ablauf und die mögliche Funktionen dieser Verletzungsreaktion näher zu untersuchen. Hierzu wurde der Kortex transgener Mäuse, die GFP nach Rekombination in der Oligodendrozyten-Linie exprimieren, nach Stichwundsverletzung repetitiv mit Hilfe eines Zweiphotonen-Mikroskops visualisiert. Detaillierte Analysen der Zellreaktionen zeigten eine schnelle und heterogene Reaktion der Mehrzahl aller NG2-glia. Das Verhalten der reaktiven Zellen umfasste Hypertrophie, Polarisierung, Migration und Proliferation, wohingegen alle Oligodendrozyten und ein geringer Teil der NG2-glia statisch, bezüglich ihrer Morphologie und Position, blieben. Die Intensität der beobachteten Reaktion der NG2-glia war abhängig von der Schwere der Gewebsverletzung sowie dem Abstand zum Zentrum der Läsion. Während des Reaktionsmaximums, zwischen 2 und 4 Tage nach Verletzung, kam es zu einer Ansammlung von NG2-glia im Zentrum und der unmittelbaren Umgebung der Verletzungsstelle. Diese zelluläre Anhäufung führte dazu, dass die unter physiologischen Bedingungen beobachtete homöostatische Kontrolle von NG2-glia vorübergehend außer Kraft gesetzt wurde. Nach einer Woche gingen die Zellen wieder dazu über sich umzuorientieren, und nach etwa einem Monat war die zelluläre Homöostase wiederhergestellt. Diese Reaktivität der NG2-glia nach Hirnverletzungen deutet darauf hin, dass diese zu einem ersten zellulären Gerüst beitragen, welches eine wichtige Rolle für Wundheilung und Gewebsregeneration spielen könnte. Diese Beobachtungen heben erneut die Bedeutung dieses Zelltyps für Hirnverletzungen hervor.

Table of contents

1 Introduction

1.1 The cellular composition of the brain

During evolution the intricacy of organisms increased, introducing a whole set of different body parts with distinct sets of properties and functions the so called organs. Together, these organs contribute to the different body functions resulting in a division of labor, mainly orchestrated by the brain. This basic principle can be found not just in all organisms but even in single cells tasks are divided between specific parts of the cell. Within cells different cellular components are amongst others responsible for information storage, information gathering, information processing and energy distribution. This basic distribution of tasks can also be seen in groups of cells forming a functional unit like an organ. It is not always easy to understand what each cell is contributing to the functionality, but in many cases the loss of a specific cell type leads to severe phenotypes and even death of the whole organism. Also the central nervous system (CNS), like any other part of the body comprises different cell types. However, in contrast to other organs it has a quite distinct set of cells (Figure 1) which cannot be found in other parts of the body.

1.1.1 Neurons

Neurons, comprising of various distinct subtypes, are the most intensively studied cells in the CNS of higher organisms. These nerve cells have the important capability to be electrically excitable and hence are able to transmit information in form of electrical and chemical signals throughout the body. Typical neurons have an outstretched dendritic network where they receive input from other neurons. If the strength of this signal reaches a specific threshold it will be transformed in an action potential at the axon hillock neighboring the cell soma, which is then transmitted along the axons. Passing the connection between neurons, the so called synapses, the signal can then be transferred to a neighboring neuron. There is a great number of different neuronal subtypes with specialized tasks like sensory neurons in the eye or the ear responding to stimulation of electromagnetic or mechanical waves respectively. Additionally motoneurons that are responsible for muscle contractions as well as excitatory or inhibitory interneurons facilitate the communication between neurons are important parts of the nervous system. The implications that the intelligence of different species is related to the number of neurons in the brain has been a heavily discussed topic for the last decades (Herculano-Houzel, 2009). Rough estimations suggest around 86 billion neurons in the human brain with slightly less non-neuronal cells, whereas the rodent brain comprises of roughly 12 billion neurons and 4 times as many non-neuronal cells

(Herculano-Houzel, 2009). Interestingly, glial cell numbers in human brains are variable between the sexes and while neurons and some glial cells decrease during aging others remain rather constant (Pelvig et al., 2008). It is an accepted view that the amount of cells in the brain are in parts responsible for the cognitive ability of the organisms, but the exact correlative between cellular composition of the brain and the cognitive output is much more complex and has still to be determined (Herculano-Houzel, 2009).

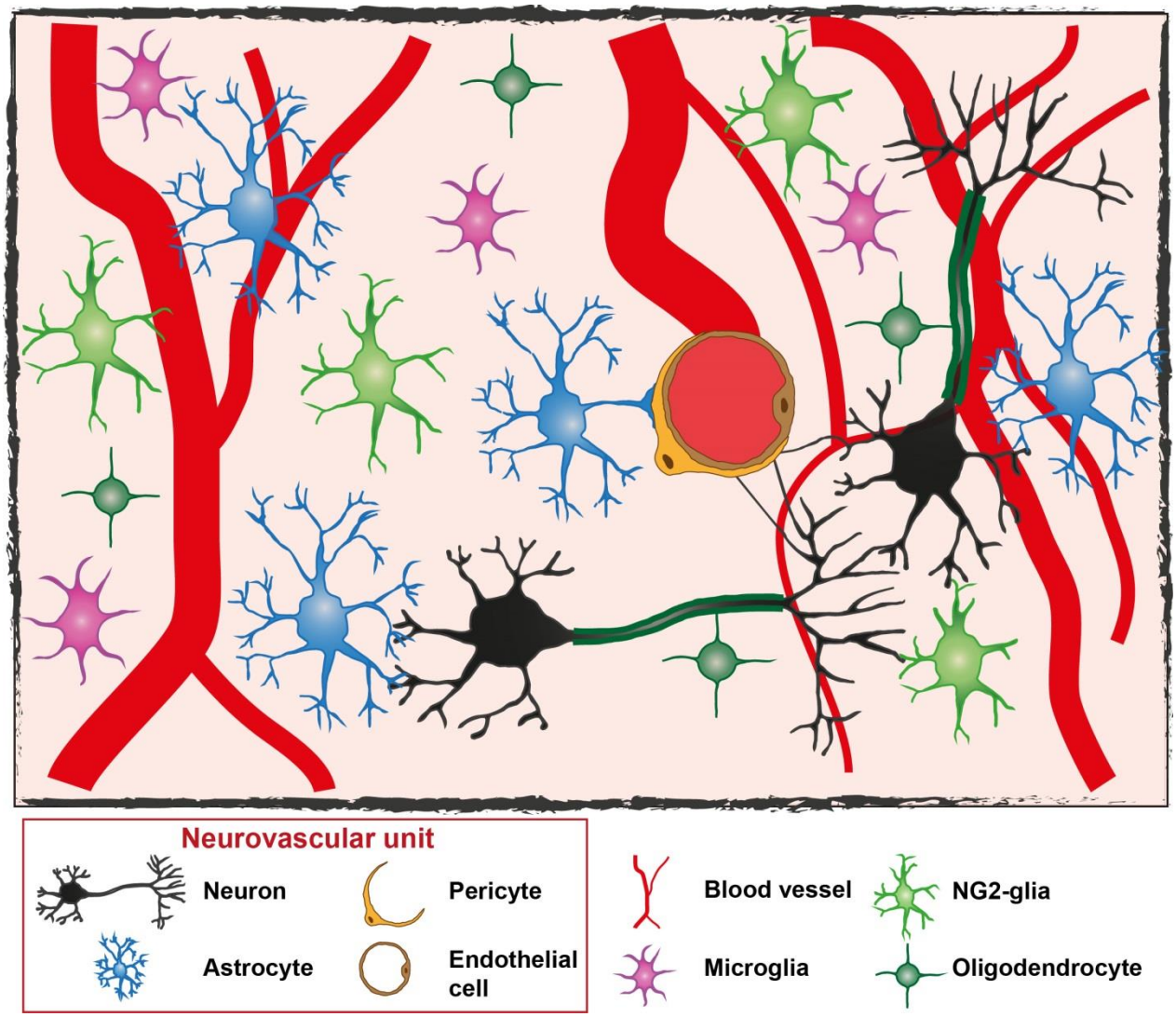

Figure 1 Different cell types in the brain. The major cellular composition of the brain depicting the neurovascular unit, containing neurons, astrocytes, pericytes, endothelial cells and the aligning basement membrane (not depicted here).

Overall, the functionality and network of neurons is seen as the fundamental framework for our mind and the exerted control, supervision and regulation needed for a functional living. The complexity underlying this machinery has fascinated a multitude of researchers over the past decades, however we are still far from understanding how our brains work. Nevertheless, more recent findings have made it intriguingly evident that neurons cannot survive without support and that the surrounding non-neuronal cells are playing a major part in the healthy and diseased CNS.

1.1.2 Astrocytes

The most abundant non-neuronal cells in the brain are the astrocytes which are members of the so called macroglia. First discovered and described as a part of the neuroglia by Rudolf Virchow around 1850, they were thought to merely be the connective tissue between neurons (Somjen, 1988). Now it is known that those cells have a diverse set of important functions which are essential for the CNS. During development astrocytes are the second arising cells, following neuronal cells, to peak around postnatal day (P)2 (Wang and Bordey, 2008). They have a highly complex and diverse morphology with long and fibrous branches which can be in direct contact with synapses and blood vessels. Their contribution to the neuronal network stretches from housekeeping functions like protein synthesizing, ion buffering and neurotransmitter recycling to actively shaping the neuronal network. Thereby they influence maturation of neurons, synapse formation and neuronal survival e.g. via secretion of trophic factors (Wang and Bordey, 2008; Bouzier-Sore and Pellerin, 2013). The second major contribution of astrocytes relate to the vasculature. Being part of the blood-brain barrier (BBB) they influence blood flow regulation, angiogenesis, uptake and buffering of ions, metabolic support as well as control of the penetration ability of various molecules (Wang and Bordey, 2008). Interestingly, more recent findings begin to assign astrocytes an even more active participation in synaptic transmission and formation (Wang and Bordey, 2008). Beside those well described functions it is suggested that they are in close contact with additional cell types and contribute majorly to the orchestration of cell distribution and behavior under physiological conditions as well as after brain injury.

1.1.3 Oligodendrocytes

Oligodendrocytes, the second major macroglial cell type, are best known for their function of myelin formation. This ensheathment emerging from a plasma membrane extension which enwraps axons in regularly spaced segments leads to an insulation and hence accelerated signal conduction velocity in myelinated axons. In vertebrates the area containing densely packed, myelinated fibers, the so called white matter (WM), increased during evolution in relation to the

complexity of the nervous system (Morell and Norton, 1980; Snaidero and Simons, 2014). Beside the improved conduction speed and therefore the possibility of a reduced axon diameter implicating decreased brain volume, myelin is also majorly responsible for the trophic and metabolic support of axons (Funfschilling et al., 2012; Bercury and Macklin, 2015). Therefore loss or disturbance of myelin and myelination, seen in many demyelination diseases like multiple sclerosis (MS) or leukodystrophies, results in reduced conduction velocity, major axonal pathology and neuronal death (Bercury and Macklin, 2015). Another interesting concept being investigated for the last decade is the interplay of neuronal activity and adaptive myelination. Latest findings could demonstrate that reduced neuronal activity due to social isolation led to impaired myelination and hence thinner myelin, whereas a socially stimulating environment increased oligodendrocyte differentiation (Liu et al., 2012). This concept was proven via optogenetic stimulation which elicited increased oligodendrogenesis and myelination in the premotor cortex of mice (Gibson et al., 2014).

Depending on the brain region, oligodendrocytes can extent their thin processes to myelinate up to 80 internodes (myelin segments) of small diameter axons in the cortex or *corpus callosum* (CC; Murray and Blakemore, 1980; Hildebrand et al., 1993), whereas oligodendrocytes in the spinal cord sometimes just generate myelin around one single axon with huge internode lengths up to 1500µm (Remahl and Hildebrand, 1990; Snaidero and Simons, 2014). Although myelination is majorly finished after the first postnatal weeks it still continues in the adult to some extend (Vigano et al., 2013; Wang and Young, 2014). This plasticity of myelin within the WM can also be seen in human adolescents and even adults (Giorgio et al., 2008). Therefore, the investigation of enhanced oligodendrogenesis and remyelination is of great importance, especially regarding demyelinating diseases. These efforts to increase remyelination and to compensate for lost oligodendrocytes and myelin fibers could eventually lead to restored functional integrity.

1.1.4 Microglia

Since their discovery by Pio del Rio-Hortega in 1932 (Kettenmann et al., 2011) the origin of microglia has been subject to much attention. Theories for their neuroectodermal origin, comparable to other neuroglial cells, were standing against the observations of migrating cells from a mesodermal origin (Kettenmann et al., 2011). Nowadays it is an accepted concept that microglia originate from the yolk sac (Ginhoux et al., 2010; Schulz et al., 2012) with erythromyeloid progenitors as precursors (Kierdorf et al., 2013; Gomez Perdiguero et al., 2015). In the mouse brain, microglia start appearing around embryonic day (E)8 via blood circulation dependent migration (Koushik et al., 2001; Casano and Peri, 2015) and their immigration process

lasts until P10 whereupon the exchange between blood and brain parenchyma is heavily diminished under physiological conditions (Kettenmann et al., 2011). Therefore these cells are tissue-resident macrophage-like cells which serve immune-related functions in the brain but also take part in the CNS development and the homeostasis as glial cells (Casano and Peri, 2015). During development they actively phagocyte apoptotic neurons, promote neurogenesis and axonal growth via trophic factors and participate in synaptic refinement as well as vessel patterning (Casano and Peri, 2015). However, especially the phagocytosis of apoptotic neurons and the synaptic pruning still continue to play a role in the adult brain. As part of the immune system microglia are very motile cells scanning their environment for potential detriments and are able to react very quickly after pathological insults by transforming from a ramified to an amoeboid morphology and migrating to the site of injury (Nimmerjahn et al., 2005; Kettenmann et al., 2011). They are able to recognize and phagocytose viruses, bacteria or other pathogenic material and mediate cytotoxicity e.g. via released nitric oxygen (NO; Kettenmann et al., 2011). Signaling to other immune cells as well as other glial cells by the release of cytokines or the presentation of antigens to T-cells are also contributing to their functions within the immune system (Kettenmann et al., 2011). Subsequently they are able to promote wound repair by removing cell debris and recruiting cells to the lesion site (Casano and Peri, 2015).

1.1.5 Neurovascular unit

To provide the brain with nutrients, metabolic support and oxygen together with the clearance of harmful substances like carbon dioxide, the coverage with vessels and blood flow is essential for a functioning brain. The brain is very sensitive to lack of blood and oxygen supply in particular, which becomes tremendously clear in events of stroke where short periods of interrupted or reduced blood circulation can lead to a horrendous outcome (Arai et al., 2011; Go et al., 2014). As the brain is such a sensitive and important organ, it has in contrast to the vasculature of other organs a specific barrier, the blood brain barrier (BBB), to block pathogens and other harmful substances from entering the CNS (Sa-Pereira et al., 2012). The main components forming to the BBB are endothelial cells, pericytes, astrocytes and the intermediate basal membrane (Sa-Pereira et al., 2012).

1.1.5.1 Endothelial cells and the basement membrane

Cerebral endothelial cells like other endothelial cells are forming the interior surface and hence the first barrier of blood vessels. Nevertheless, they can be distinguished by means of their functional, morphological and biochemical properties from other endothelial cells in the body (Sa-

Pereira et al., 2012). They form dense cellular networks with tight and adherens junctions between adjacent endothelial cells resulting in a structure that is 50-100 times tighter, than in peripheral microvessels. This limits the influx of hydrophilic substances but not of small lipophilic molecules like O_2 or CO_2 (Abbott, 2002; Sa-Pereira et al., 2012). Sparse pinocytic vesicular transport systems (Sedlakova et al., 1999) and the endothelial plasma membrane without fenestrations also contribute to the tight regulation of passage (Fenstermacher et al., 1988; Sa-Pereira et al., 2012). To control the uptake of nutrients, hormones and other important molecules, brain endothelial cells have a great number of specific transport systems and receptors with the consequential big amount of mitochondria to cover the resulting energy demand (Oldendorf et al., 1977; Sa-Pereira et al., 2012). The basement membrane, a tightly interwoven protein layer comprising of proteins like collagen, elastin, fibronectin and laminin formed and maintained by endothelial cells, pericytes and astrocytes, aligns the endothelial cells with other cellular components of the BBB (Zlokovic, 2008; Sa-Pereira et al., 2012). Its function relays more on the stability and integrity of the BBB then on additional blockage of molecule influx (Persidsky et al., 2006; Sa-Pereira et al., 2012).

1.1.5.2 Pericytes

Another important component of the BBB situated next to the basement membrane, are the pericytes. Already described in 1873 by Charles Rouget (Sa-Pereira et al., 2012), pericytes are present in a wide range of species and located at the abluminal side of microvessels (Sa-Pereira et al., 2012). In the brain they are located between two layers of basement membranes covering the outer layer of endothelial cells as well as the astrocytes endfeet (Figure 1) which are the outer part of the BBB (Krueger and Bechmann, 2010; Dore-Duffy et al., 2011). They are distributed along walls of pre-capillary arterioles, capillaries and post-capillary venules in a non-regular manner (Krueger and Bechmann, 2010). The number of pericytes covering the different vessel-types seem to be dependent on the tissue type and the degree of tightness of the interendothelial junctions (Shepro and Morel, 1993). Interestingly, the brain has a much higher pericyte-to-endothelia ratio than other organs (Dalkara et al., 2011). Pericytes are polymorphic with mostly spherical or oval cell bodies and long, branching cytoplasmic processes along the axis of the blood vessels which are enwrapping the vessels (Sa-Pereira et al., 2012). This ensheathment is very variable between cells and can be extended to lengths of 800 nanometers (nm; Zlokovic, 2008). Due to their morphological proximity to vessels, most of their discovered functions are therefore also related to the vasculature. First and foremost they are an essential part of the BBB contributing to its maintenance and stabilization as well as its low permeability and molecule-specific transport (Sa-Pereira et al., 2012). During development, but also after brain injury or

hypoxia, pericytes are also contributing to the angiogenic processes of sprout formation, migration, maturation and termination (Dore-Duffy et al., 1999; Sa-Pereira et al., 2012). For this complex process they have to closely cooperate and communicate with other vasculature related cells like the endothelial cells e.g. via secretion of vascular endothelial growth factor (VEGF) or NO (Sa-Pereira et al., 2012). Furthermore, because of the expression of contractile proteins like tropomyosin and myosin (Joyce et al., 1985) pericytes have some features of smooth muscle cells: they are able to contract and hence modulate the blood flow within their covered vessels (Fernandez-Klett et al., 2010; Sa-Pereira et al., 2012). Due to their expression of adhesion molecules which are able to stimulate major histocompatibilty complex-class II dependent antigen presentation and their production of immunomodulatory cytokines *in vitro*, it has been speculated that they are even able to participate in the regulation of immune response within the BBB (Fabry et al., 1993; Verbeek et al., 1995; Sa-Pereira et al., 2012). Additionally, the expression of acid phosphatase in their lysosomes and their ability to take up small and soluble molecules from the blood or brain parenchyma led to the assumption that they are even capable of phagocytosis (Sa-Pereira et al., 2012). Last but not least, the potential of embryonic endothelial cells to transdifferentiate into many different cell types like fibroblasts, smooth muscle cells or endothelial cells has drawn the interest of many researchers to pericytes, trying to investigate the potential of this multipotency (DeRuiter et al., 1997; Sa-Pereira et al., 2012). Latest results showed that after ischemia neuronal progenitors originated from pericytes in the monkey and that it was possible to differentiate primary rat CNS pericytes *in vitro* with the addition of basic fibroblast growth factor (bFGF) into cells of the neural lineage (Yamashima et al., 2004; Dore-Duffy et al., 2006). Therefore, their plasticity could be a great tool for cell-based therapies (Sa-Pereira et al., 2012).

1.1.6 Ependymal cells

Beside the neurovascular unit also the ventricular system is lined by specific cell types. The most prominent cells along the ventricular surface spanning from the lateral ventricles to the *filum terminale* are the ependymal cells. They are ciliated, have a cuboidal to columnar morphology with a fairly round nucleus and their apical surface is covered with microvilli (Del Bigio, 2010). Like pericytes being involved in the BBB, ependymal cells also form a barrier between the ventricular system and the brain parenchyma regulating molecule uptake and exchange. Next to the trophic and metabolic support via an cerebrospinal fluid (CSF) exchange system ependymal cells may also secrete growth factors like fibroblast growth factor (FGF) and VEGF in the surrounding parenchyma, especially influencing the neighboring stem cell niche (Del Bigio, 2010).

Another speculated function involves their coordinated beating of cilia which is suggested to influence the circulation of CSF and the gradients of molecule-concentration within the CSF (Del Bigio, 2010). In the choroid plexus that is the CSF producing organ, choroidal epithelial cells derived from ependymal cells are capable of uptake and secretion of CSF and its containing molecules, metabolites and nutrients (Skipor and Thiery, 2008). Furthermore ependymal cells have been suggested to have neural stem cell capacity (Johansson et al., 1999). However, this was partially revised later on as these cells show only parts of the features of a stem cell like giving rise to neurons and glial cells following stroke but not others as they were not able to self-renew (Carlen et al., 2009).

1.1.7 Progenitor- and stem cells in the adult brain

Endogenous stem or progenitor cells and the question of their capacity to self-renew and to be multipotent within the brain and how this could be exploited for therapeutic purposes have been very hot topics in the last decades. The endogenous progenitors for the most prominent CNS cell type, the neurons, are neural stem or progenitor cells. They still persist after development in the adult mammalian brain and are located in the niches of the subependymal zone in the lateral wall of the lateral ventricle, the subgranular zone in the dentate gyrus of the hippocampus and the hypothalamus (Dimou and Gotz, 2014). The progenitor cells of the subependymal zone, mostly referred to as radial glia during development, proliferate and generate transit-amplifying progenitors and neuroblasts. They are able to migrate along the rostral migratory stream into the olfactory bulb where they finally differentiate into neurons (Dimou and Gotz, 2014). In the hypothalamus, the resident progenitor cells are called tanycytes. They have been classified in two subtypes differing in location and output of cells: α-tanycytes producing few neurons and majorly glial cells and β-tanycytes being majorly neurogenic but lacking self-renewal capacities and multipotency *in vitro*. This combination results in an relatively low neurogenic potential of this area (Dimou and Gotz, 2014). The third neurogenic niche, the subgranular zone of the dentate gyrus is comprised of self-renewing and neurogenic astrocyte-like cells which by producing intermediate progenitors can give rise to differentiating neuroblasts (Ming and Song, 2011). Taken together, those niches would host an ideal reservoir of potential neuronal substitution needed in pathological conditions. Hence a great effort is being made to investigate possibilities to make use of those niches for therapeutic strategies.

1.2 NG2-glia – an underestimated glial cell type

Another interesting cell type persisting in the adult brain, which often has been attributed with progenitor and even stem cell like features, are the NG2-glia or oligodendrocyte progenitor cells (OPC).

1.2.1 Development of the oligodendrocyte lineage

To learn more about a specific cell type, it is very useful to investigate its origin and early development. Oligodendrocytes and hence OPCs or NG2-glia originate from the neuroepithelium at different timepoints during late embryogenesis and until early postnatal periods, like astrocytes (Wang and Bordey, 2008). For years the exact process of oligodendrocyte development was heavily debated in the field, until fate mapping studies clearly showed that those cells arise successively from different areas (Richardson et al., 2006). In the spinal cord the largest proportion of NG2-glia is generated in the ventral cord starting at E12.5 whereas a smaller proportion originates from the dorsal part around E15 (Cai et al., 2005; Vallstedt et al., 2005; Richardson et al., 2006). A similar pattern could also be shown for the development of forebrain oligodendrocytes (Figure 2) via fate mapping of Nkx2.1-, Gsh2- and Emx1-cre mouse strains (Kessaris et al., 2006). Starting at around E11.5 the first wave of cortical NG2-glia is generated from precursors which originate at the ventricular zone of the medial ganglionic eminence (MGE) and the anterior entopeduncular area (AEP). Subsequently the cells migrate into all areas of the telencephalon and enter the cortex around E16 (Kessaris et al., 2006). This is followed by a second wave of cells, coming from an area spanning from the lateral or caudal ganglionic eminence (LGE and CGE) to parts of the MGE. The second together with the third wave of endogenous cortical progenitors, appearing in the cortex around the day of birth, make out the majority of the oligodendrocyte lineage traceable at postnatal stages, whereas the first wave is largely depleted (Kessaris et al., 2006). Even if these two waves of progenitor pools give rise to the majority of the oligodendrocyte lineage in the adult brain there are still possibilities of other sources contributing to the heterogeneous composition of this cell population (Ventura and Goldman, 2006). Interestingly, if one of the populations giving rise to oligodendrocytes is destroyed by the targeted expression of diphtheria toxin the other populations can compensate this event and oligodendrocyte differentiation as well as myelination is proceeding normally (Kessaris et al., 2006).

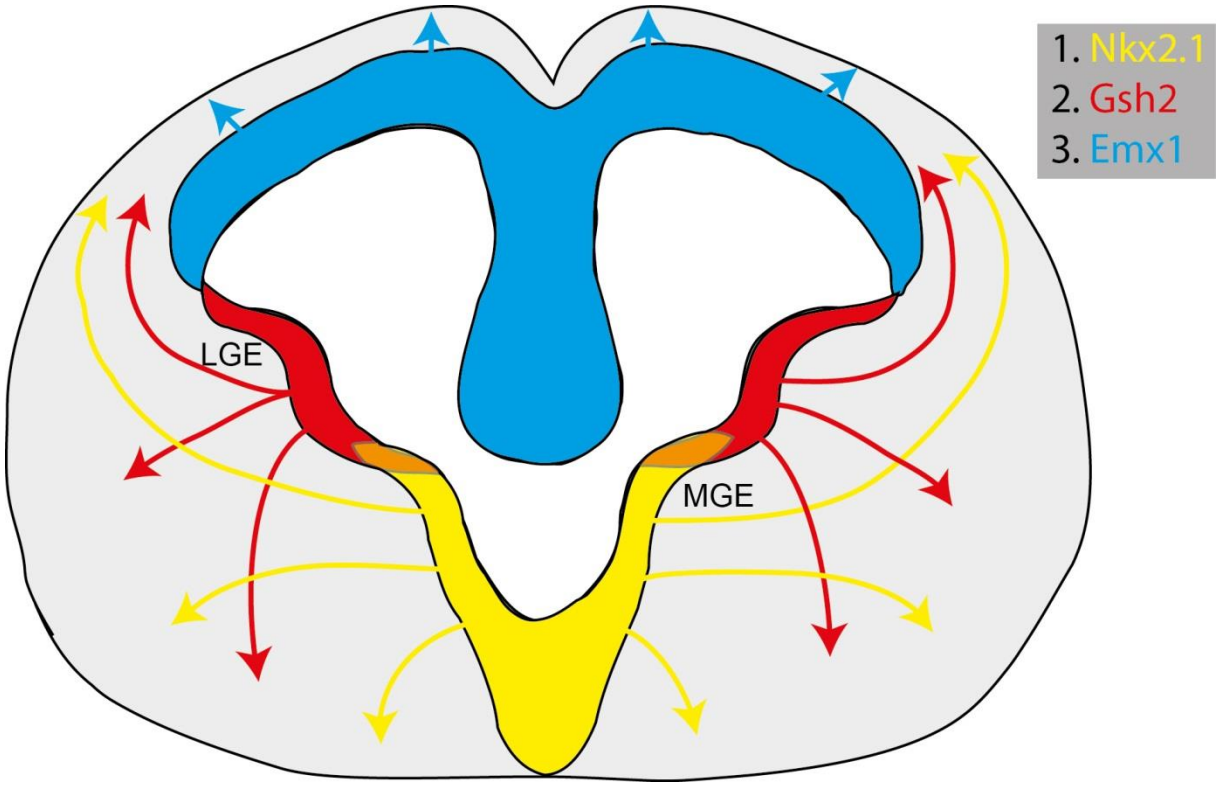

Figure 2 Competing waves of oligodendrocyte progenitors during development. The first wave of NG2-glia arise from Nkx2.1$^+$ precursors located at the MGE arriving at the cortex at around e16 followed by the second wave of Gsh2$^+$ from the areas of LGE and CGE. The third wave of Emx1$^+$ endogenous cortical progenitors starts around the day of birth (modified from Kessaris et al., 2006).

After birth a big proportion of this progenitor pool starts to differentiate into myelinating oligodendrocytes reaching a peak of myelination at the second postnatal week and lasting mainly until the fourth postnatal week (Greenwood and Butt, 2003). Differentiation into oligodendrocytes and myelination are continued also after this period, but to a much reduced extent (Wang and Young, 2014).

Although a large amount of NG2-glia differentiate during this time window, a big proportion of cells remains in the progenitor status even in the adult brain. Because NG2-glia share the same heritage with mature and myelinating oligodendrocytes it is important to distinguish those distinct differentiation stages of the oligodendrocyte lineage. Therefore, specific marker antigens have been identified, demarcating the differentiation steps within the oligodendrocyte lineage (Figure 3). The NG2-glia within the adult as well as the developing brain share the expression of the membrane protein neuron-glia antigen 2 (NG2) which is a chondroitin sulfate proteoglycan and also the name giver of the term NG2-glia (Nishiyama et al., 1997). Other potential markers for this progenitor population, are the membrane proteins platelet-derived growth factor receptor α (PDGFRα; Dawson et al., 2003) and junctional adhesion molecule A (JAMA; Stelzer et al., 2010).

An antigen which has been proposed to also label parts of the progenitor cell population of the oligodendrocyte lineage is the G-protein coupled receptor 17 (GPR17; Boda et al., 2011). Latest results of GPR-17 expressing cells seem to point to a subset of NG2-glia with a slower differentiation rate (Vigano et al., 2015). After differentiation to mature oligodendrocytes, these cells can be labeled with antibodies for the cytoplasmic proteins glutathione-S-transferase pi (GSTπ), adenomatosis polyposis coli (APC, with the antibody CC-1) and the less specific aspartoacylase (ASPA; Moffett et al., 2011). In the case that mature oligodendrocytes are also myelinating, they are able to be detected with antibodies against antigens which are typically expressed inside the myelin sheath like the myelin-associated glycoprotein (MAG), myelin oligodendrocyte glycoprotein (MOG), myelin basic protein (MBP) and myelin proteolipid protein (PLP; Baumann and Pham-Dinh, 2001).

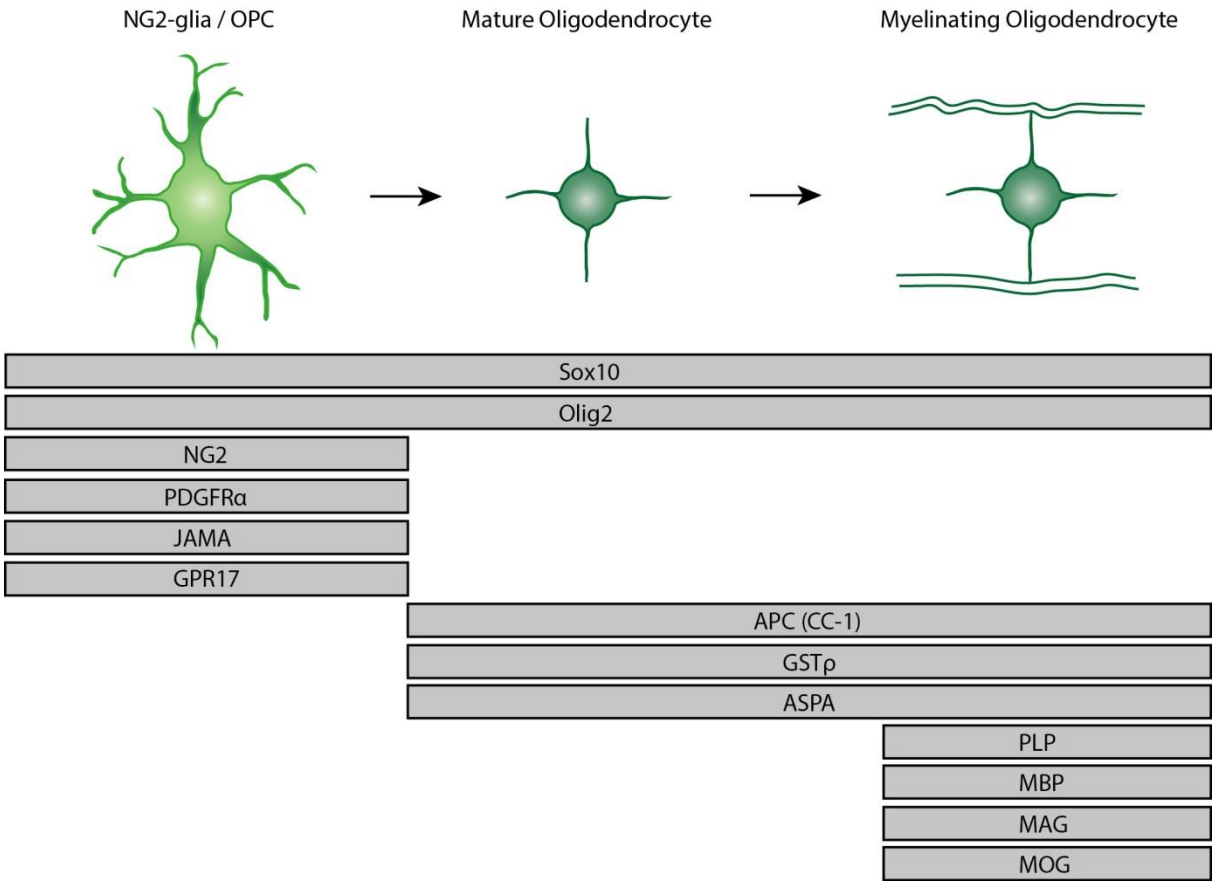

Figure 3 Oligodendrocyte lineage. Illustration of cells within the oligodendrocyte lineage in the adult brain at various differentiation stages with the according expression profiles containing different antigens, which can be used for labeling.

Additionally to these immunohistochemical methods it is also possible to differentiate between NG2-glia and mature oligodendrocytes via morphological discrimination. While NG2-glia have a

rather large, elongated and often bent cell body with thick and ramified processes, mature oligodendrocytes have a round and smaller cell body with thin and less ramified processes.

1.2.2 Fate of NG2-glia

As mentioned at the beginning of this chapter, the multipotency and stem cell potential of NG2-glia has been the subject of many discussions over the last decades. Early observations of this cell type mainly carried out *in vitro* showed their potential to differentiate into oligodendrocytes as well as type-2 astrocytes giving them the term "O-2A" adult progenitor cell (Raff et al., 1983; Wolswijk and Noble, 1989; Wren et al., 1992; Shi et al., 1998). Accordingly, continuous *in vitro* work expanded the possible differentiation/stem cell potential of NG2-glia also for neuronal progenitors. In the neurosphere assay, where dissociated and specifically cultured cells are tested for their potential to form multipotent spheres, enriched postnatal NG2-glia cultures were found to differentiate into oligodendrocytes, astrocytes and neurons (Reynolds and Weiss, 1992; Richards et al., 1992; Belachew et al., 2003; Aguirre and Gallo, 2004; Aguirre et al., 2004; Dimou and Gotz, 2014). In the adult, the general neurosphere-forming capacity decreases, but there are still some studies showing WM derived NG2-glia to form neurospheres (Nunes et al., 2003). Moreover, cells derived from other areas of the brain showing marker expression of NG2 or Olig2 were neurosphere-forming (Dimou and Gotz, 2014). These are promising results in regard to their multipotency and the theoretical use of NG2-glia in cell-therapies, nevertheless clear evidence by genetic fate mapping is still missing (Dimou and Gotz, 2014). Furthermore, lineage analysis carried out *in vivo* are contradictory to the results obtained *in vitro*. In contrast to the generally more plastic progenitors during development, which form oligodendrocytes, astrocytes and some neurons in the spinal cord (Masahira et al., 2006) and oligodendrocytes and neurons in the olfactory bulb (Aguirre and Gallo, 2004), the plasticity of NG2-glia seems to be rather restricted to oligodendrocytes and some astrocytes at later embryonic stages (Zhu et al., 2008; Huang et al., 2014) and to the oligodendrocyte lineage in the adult (Dimou et al., 2008; Kang et al., 2010; Simon et al., 2011; Zhu et al., 2011; Huang et al., 2014). If adult NG2-glia are also capable of generating neurons has been a very controversial topic for the last years. So far, two studies have shown the detection of some labeled neurons in the piriform cortex after recombination in the Plp1-CreER^{T2} (Guo et al., 2010) or PDGFRα-CreER^{T2} (Rivers et al., 2008) mouse lines. However, until now the majority of results were speaking against this neurogenic capacity in adult NG2-glia and the neurogenic observations derived from the PDGFRα-CreER^{T2} mice could not even be reproduced by the lab describing it first (Clarke et al., 2012). Therefore, it is very likely that some

of these data, showing the generation of neurons could have resulted from technical difficulties of fate mapping studies.

These fate mapping studies make use of the CreER/LoxP technique. For this purpose, mouse lines are generated containing the cyclization recombination (Cre) specific DNA recombinase fused with a modified estrogen receptor binding domain (ER) in their genome. This ER domain has a high affinity to the artificial estrogen tamoxifen, but not the endogenously expressed estrogens. After targeted placement of this construct under a specific promotor in the genome transcription occurs in the cell type of interest. Together with this construct two locus of crossover phage (LoxP) sites are introduced, flanking the reading frame (or parts of the reading frame) of a gene of interest. Another possibility is to place the LoxP next to a stop cassette situated in front of the gene encoding a reporter protein. After tamoxifen induction the CreER fusion protein can translocate from the cytoplasm into the nucleus and actively excise the genomic area which is flanked by the LoxP sites. Hereby, cell type specific labelling for fate mapping or selective gene deletion can be achieved (Sauer, 1998).

Ectopic, low level CreER expression or tamoxifen side effects, especially during long treatment phases could be some of the resulting difficulties from these fate-mapping studies (Dimou and Gotz, 2014; Dimou and Gallo, 2015). Overall, the observed plasticity of NG2-glia is certainly dependent on the environment, facilitating multipotency during development or rather restricting it to certain lineages in many areas of the adult brain (Dimou and Gotz, 2014). Also pointing toward this direction is the concept of increased plasticity of cells after injury. Indeed, some studies could detect NG2-glia generating astrocytes after different CNS injury paradigms with the help of fate mapping approaches (Tatsumi et al., 2008; Sellers et al., 2009; Busch et al., 2010; Komitova et al., 2011). Contradictory, others were not able to confirm these results and detected progeny of the oligodendrocytes lineage after injury (Dimou et al., 2008; Barnabe-Heider et al., 2010; Kang et al., 2010; Zawadzka et al., 2010; Simon et al., 2011). Interestingly, the study from Zawadzka et al. (2010) using a fate-mapping approach of PDGFRα- and Olig2-CreER^{T2} mouse lines after a demyelination model showed differentiation of NG2-glia into Schwann cells (Figure 4).Notably, this was seen in toxin induced demyelination, but not after experimental autoimmune encephalomyelitis (EAE; Zawadzka et al., 2010; Dimou and Gallo, 2015). Besides the above mentioned technical issues, these inconsistent results could also be due to different regional input, resulting from variations of the lesion paradigm, technical protocols or mouse lines. So far this leads to the conclusion that NG2-glia, despite having some potential for multipotency, have to be in the appropriate environment for an effective implementation (Figure 4). Consequently, this

yields some great promise for cell-based therapies when NG2-glia are pushed into the right direction as already demonstrated via *in vivo* reprogramming of NG2-glia into neurons after brain injury (Heinrich et al., 2014).

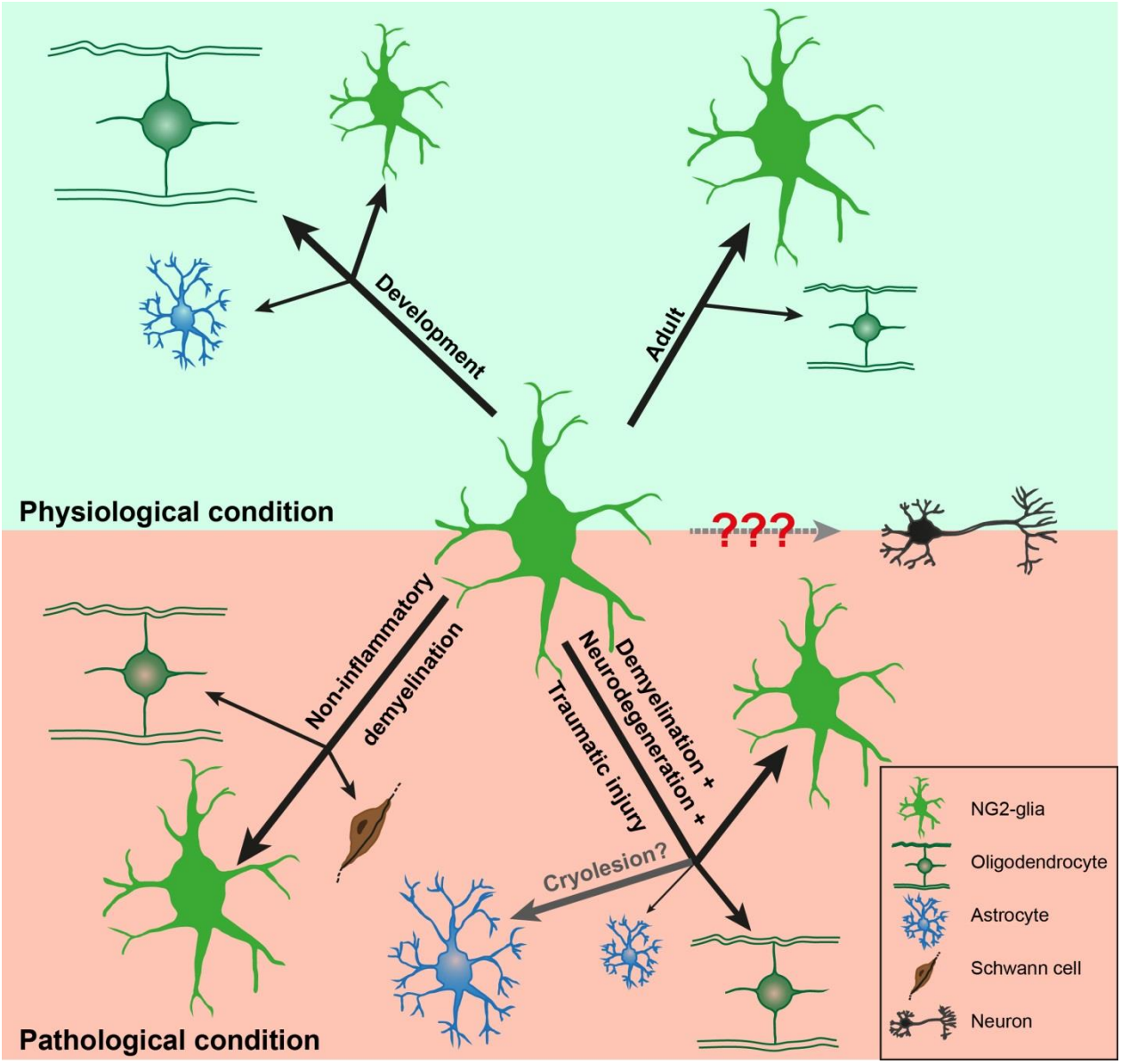

Figure 4 Fate of NG2-glia in health and disease. NG2-glia generate majorly oligodendrocytes and NG2-glia but also a small amount of astrocytes during development. However, they are restricted to the oligodendrocyte lineage in the healthy adult brain. This changes under pathological conditions when NG2-glia are also able to form astrocytes and Schwann cells under certain conditions. If they are also able to differentiate into neurons is still heavily debated and confirming evidence seems to be rather sparse (modified from Dimou and Gallo, 2015).

1.2.3 Properties of NG2-glia

Besides being the major proliferating cell population in the adult brain parenchyma (Gensert and Goldman, 1997; Dawson et al., 2000; Horner et al., 2000; Aguirre and Gallo, 2004; Buffo, 2007; Dimou et al., 2008) and their ability to differentiate into mature oligodendrocytes during development and in the adult brain (Dimou et al., 2008; Rivers et al., 2008), recent studies unraveled more and more roles of NG2-glia contributing to the functionality of the brain. Together with their great abundance in the mammalian brain (5-8%; Horner et al., 2000; Hill et al., 2011), this led to the terminology of NG2-glia as a 4th glial cell population, to highlight their general functionality in the brain beside their progenitor potential that is expressed in the term OPC (Horner et al., 2002). Interestingly, non-myelinating but enwrapping glial cells can be already found in lower invertebrates without myelinated axons, like Drosophila, where they closely interact with axons (Banerjee and Bhat, 2008) also pointing to functions beside their progenitor status (Mangin and Gallo, 2011).

Under physiological conditions the cells are homogenously distributed and form a homeostatic network with distinct territories controlled by self-repulsion, as shown by *in vivo* live-imaging in the somatosensory cortex (Hughes et al., 2013). This cellular homeostasis is even maintained when differentiation or death of one cell occurs, as the neighboring cells are able to counteract these events via proliferation and migration, leading to the restoration of this network (Hughes et al., 2013). To achieve this surveillance of the neighboring area the cells are motile and move with no distinct directionality ~2µm per day, scanning the area with highly motile filopodia (Hughes et al., 2013). Additionally to this cellular behavior within the cell lineage, NG2-glia were shown to be tightly integrated within the astrocytic and neuronal network (Wigley and Butt, 2009). In contrast to their repulsive behavior in respect to cells of the own lineage they have been shown to form contacts with axons (myelinated and unmyelinated), neuronal cell bodies, astrocytes and pericytes (Wigley and Butt, 2009). While there is not so much known concerning their connection to pericytes, besides a potential involvement in blood flow regulation (Wigley and Butt, 2009), many studies have been conducted, investigating the connection between NG2-glia and neurons/axons. The anatomical and functional properties of those connections led to the assumption that NG2-glia form synapses with neurons at positions like the nodes of Ranvier, the dendrites and the neuronal cell soma which could influence functions like differentiation, migration and proliferation of NG2-glia (Mangin and Gallo, 2011). Those neuron-glia synapses were shown to be either glutamatergic mediating excitatory postsynaptic currents (EPSC) via α-amino-3-hydroxyl-5-methyl-4-isoxazole-propropnate (AMPA) receptors or γ-aminobutyric acid (GABA)-ergic mediating

also mainly EPSCs. The GABA-ergic synapses are also able to mediate inhibitory postsynaptic currents (IPSC) via $GABA_A$ receptors under specific circumstances (Lin and Bergles, 2004; Sun and Dietrich, 2013). Several studies could demonstrate that synaptic input and the resulting current lead to locally restricted Ca^{2+} increase in those processes of NG2-glia that are connected to synapses (Blaustein and Lederer, 1999; Bergles et al., 2000; Lin et al., 2005; Mangin et al., 2008; Tong et al., 2009; De Biase et al., 2010). If the EPSC induced opening of voltage-dependent Na^+ channels can lead to a generation of an action potential remains a heavily discussed topic, the evidence, however seems to be dwindling and species-specific (Karadottir et al., 2008; Frohlich et al., 2011; Clarke et al., 2012; Sun and Dietrich, 2013). Nonetheless there are voltage-activated sodium channels expressed in NG2-glia which could at least lead to an amplification of the synaptic input (Sun and Dietrich, 2013).

Alternative possibilities for cell-cell communication are based on released factors or molecules. Adenosine triphosphate (ATP) as a sensor for energy metabolism and cellular homeostasis (Butt, 2011) could be released by neurons or astrocytes and bound by metabotropic P2Y and ionotropic P2X receptors present on NG2-glia leading to intracellular Ca^{2+} increase (Hamilton et al., 2010). Even if direct synaptic release on NG2-glia has just been shown for glutamate and GABA receptors (Gallo et al., 2008), other possible modes of activation could involve muscarinic and nicotinic acetylcholine receptors (AChR; Cui et al., 2006; Velez-Fort et al., 2009), dopamine receptors (Barres et al., 1990), cannabinoid receptors (Mato et al., 2009), glycine receptors, purinergic receptors and like recently discovered N-methyl-D-aspartate (NMDA)- and kainate receptors (Kukley and Dietrich, 2009; De Biase et al., 2010; Sun and Dietrich, 2013). However most of the early work was carried out in O-2A progenitor cell lines (derived from rat optic nerve) which are considered the *in vitro* NG2-glia equivalent but might as well have different characteristics due to the underlying artificial conditions (Barres et al., 1990; Sun and Dietrich, 2013). Via these signaling pathways NG2-glia could be influenced in their differentiation, proliferation or migration behavior (Yuan et al., 1998; Ghiani et al., 1999; Agresti et al., 2005; Gudz et al., 2006; Gallo et al., 2008; Chen et al., 2009; Tong et al., 2009), but to dissect the specific outcome of one of those effectors *in vivo* would be very challenging.

Another interesting aspect of the NG2-glia population is their heterogeneity. So far, the major findings concentrate on the difference between NG2-glia from white matter (WM) and grey matter (GM). Also their electrophysiological properties add to this WM/GM heterogeneity, which was shown via patch-clamp recordings from acute slices demonstrating different membrane properties, channel expression profiles and reaction to depolarization between WM and GM NG2-

glia (Chittajallu et al., 2004). Furthermore different reaction profiles after depolarization could be detected for a subclass of cortical NG2-glia, suggesting an additional heterogeneity within the same region (Chittajallu et al., 2004). The first study investigating heterogeneity of NG2-glia demonstrated that NG2-glia from the WM have a higher proliferation rate compared to the GM (Dawson et al., 2003), which could in part be explained with different responsiveness to PDGF (Hill et al., 2013). Later on, also an elevated differentiation rate was detected for the NG2-glia of the WM (Dimou et al., 2008; Rivers et al., 2008; Kang et al., 2010). To get a better understanding of the underlying mechanisms causing this difference, transplantation experiments have been performed, grafting GM and WM cells in both WM and GM (Vigano et al., 2013). Grafted cells derived from the WM showed much higher differentiation efficiency in both areas compared to their GM counterparts, arguing for intrinsic differences, whereas the improved differentiation capacity of GM derived transplanted cells in the WM indicated an additional environmental effect (Vigano et al., 2013). Taken together, these findings suggest that both intrinsic and extrinsic factors play an important role in the heterogeneous capacity of GM and WM NG2-glia to differentiate (Vigano et al., 2013). However, also within the same area NG2-glia show heterogeneity in expression of the transcription factor achaete-scute homolog 1 (Ascl1) and the receptor GPR17 in just a subset of cells, adding to the complexity of the NG2-glia population (Parras et al., 2007; Boda et al., 2011; Zhang et al., 2014).

1.3 Brain injuries and the evoked cellular response

One essential reason to study the roles and behaviors of different brain cells is to unravel their distinct participation in brain function. This becomes particularly relevant in cases of disease and injury when the cells of the CNS are detained from exerting their tasks. The CNS with its complex networks is the target of many diseases with just a small minority so well investigated that efficient treatments can be carried out. Notably, although some basic wound healing processes are comparable between all tissue types the whole recovery process in the CNS seems to be somehow insufficient. In contrast to other organs CNS tissue regeneration is rather reminiscent of chronic/unresolved wounds resulting in tremendous symptoms and pathologies for the majority of brain pathologies (Shechter and Schwartz, 2013). This leads to a great demand for research to further our understanding of brain function in general and the specific cellular and molecular events discerning physiological from pathological conditions to improve treatment strategies for these severe conditions.

1.3.1 Brain injury models

As it is not possible to study many features of the brain pathologies in human patients, one has to create model systems, in which a comparable outcome can be reconstructed. When it comes to injuries and diseases the medical research has so far always taken advantage of using animals, most favorable rodents like mice and rats. The big advantages of working with the mouse model are their short reproduction cycle, low housing costs and the relatively close genetic resemblance to humans as well as a long history of research and thus already a huge selection of genetically manipulated mouse lines. Basic research on the molecular, cellular or under some circumstances even functional level has also been performed in bacteria, worms or flies (with increasing complexity). However, almost all medical relevant topics are investigated in rodents.

Models for brain injuries together with models for brain diseases share many basic similarities like inflammation, cell death and subsequent functional impairment. Furthermore, the majority of brain diseases are so complex that the only promising option for investigation is the singled out study of specific facets of the disease course, often representing specific cellular or tissue damage. As soon as those different pathological aspects are well understood, they can be assembled to address the pathology as a whole. Therefore, it is essential to understand the cellular and molecular basis of brain injuries and diseases for the challenging aim to improve clinical therapy.

1.3.1.1 Comparison of injury models

For the comparison of different injury models one has to particularly consider three major properties of the individual model: first, the actual methodology and hence how the injury is introduced to the system, second, in which region the injury occurs and third, at what timepoint in life/during development it is carried out. An additional variation, which becomes essential for dissecting the underlying mechanisms, is to manipulate the model system itself by e.g. knocking out genes of interest.

So far, the major region-wise segmentation of CNS injury research has been done between brain (Kermer et al., 1999) and spinal cord (Wrathall, 1992) and within those regions between GM (Reier et al., 2002; Back, 2014) and WM (Fern et al., 2014; Kou and VandeVord, 2014). Concerning the methodology of the injury models the different injury paradigms can be subdivided into indirect and direct injuries with the majority of direct injuries being models for traumatic brain injury (TBI) which will be covered in the next chapter. Indirect injuries are manipulations of the system which then lead to brain damage as a secondary effect. This can be induced via primary injuries like the rupture or occlusion of an artery in stroke/ischemia models leading to severe

lesions in the afflicted areas (Tajiri et al., 2013). Other options are via injection or feeding of toxins like lysolecithin or cuprizone (Blakemore and Franklin, 2008) or injection of viruses like the Theiler´s murine encephalomyelitis virus (Pachner, 2011) leading to cell death of oligodendrocytes, demyelination and axonal damage in these specific MS models (Pachner, 2011). However, those models only mimic the demyelination part of MS and do not address the complex pathology to the full extent. Therefore, other models have been created addressing the immunological part of the disease by active immunization of genetically predispositioned animals against myelin proteins also leading to demyelination (Pachner, 2011). Furthermore, infection with bacteria has been employed to e.g. model white matter injuries in perinatals (Dean et al., 2015). Beside these closely disease linked models, some very specialized and artificial methods have been designed to isolate distinct injury processes. One example would be the very tedious approach invented by Madison and Macklis (1993). For that technique they targeted neurons which have received cytotoxic, photoactivatable beads via retrograde transport along axons from neurons located in the contralateral hemisphere, with laser illumination leading to a rather noninvasive and specific neuronal death (Madison and Macklis, 1993).

1.3.1.2 Traumatic brain injury

Basically all approaches to directly injure the brain are counted as models of TBI. In the clinic, the definition of TBI has been imprecise for a long time, especially regarding the challenging concept of combining the huge variety of causes and pathologies. Together with the changing epidemiologic patterns and an increasing significance of a milder version of TBI which results in a more subtle neurocognitive and neuroaffective deficits finding a precise definition was challenging (Menon et al., 2010). In a recent study, Menon et al. (2010) formulated the following definition: "TBI is defined as an alteration in brain function, or other evidence of brain pathology, caused by an external force" (Menon et al., 2010). In the USA alone 235,000 people are hospitalized for nonfatal TBI, 1.1 million are treated in emergency departments resulting in 50,000 casualties every year (Niemeier et al., 2015). TBI can be classified in open or closed injuries, depending whether the skull and the dura of the patient was penetrated (Morales et al., 2005). This can also lead to different outcome in disease course and symptoms. The resulting pathologies can comprise primary injuries due to direct mechanical disruption which leads to focal or diffuse lesions of brain tissue, hematomas, axonal damage and consequently secondary injuries like intracranial hemorrhage, brain swelling and ischemic damage (Morales et al., 2005). Thus, patients of TBI can show a multitude of neurologic and mental symptoms including weakness, loss of balance, change in vision, dyspraxia paresis, aphasia sensory and memory loss, depression, anxiety,

cognitive deficits or disorientation. Some of these symptoms can become chronic and there is no effective treatment so far (Menon et al., 2010; Niemeier et al., 2015). Being a major cause of death and disability all over the world, finding potential therapeutic strategies for TBI is a very important aim for medical research. Therefore, experimental models for TBI have been created to investigate the progression of the pathology, the underlying mechanisms and in the long run options for therapy. Another benefit of those rather simple lesion paradigms is that they can also be employed for a basic understanding on how the brain reacts to an insult, which can then be translated to almost all brain diseases where tissue damage is occurring.

Marmarou et al. (1994) designed the impact acceleration model where a stainless steel protection plate is attached to the skull of the animal reducing the risk of skull fracture, when a weight is dropped on the head of the animal, mimicking the more complex diffuse brain injury (Marmarou et al., 1994). The diffuse injury model using an air-driven impactor hitting the brain via a protection plate and a molded, gel-filled base supporting the animals head is an alternative model for this complex injury (Cernak et al., 2004; Morales et al., 2005). This is complemented by the classic models for focal TBI: the weight drop model using a guided weight lowered on the skull without any further protection (Feeney et al., 1981), the controlled cortical model with an rigid impactor transmitting mechanical pressure directly on the intact dura (Smith et al., 1995) and the midline fluid percussion model employing a pendulum released impact of a fluid bolus on the intact dural surface (Sullivan et al., 1976; Morales et al., 2005). An even more basic model of focal brain injury with skull and dura penetration is the stab wound injury (SWI) model. In that case a craniotomy is performed followed by a cut or stitch in the somatosensory cortex using a lancet, leading to damage of the dura, blood vessels and the affected gray matter but sparing the white matter (Buffo et al., 2005).

1.3.1.3 Cellular response to brain injury

Parts of the functional and symptomatic pathology after TBI can be explained by the observable tissue damage. However, employing such a simple assessment can hardly contribute to a sufficient comprehension of the responsible events for the resulting pathology. Particularly in the first days after the injury, as illustrated in Figure 5, the evoked response involves complex interactions between cells of numerous lineages, comprising tissue resident cell types and extrinsic cells with various functions infiltrating the CNS after insult (Burda and Sofroniew, 2014). Therefore one has to understand the cellular events first before continuing the analysis on the molecular level to really dissect the cause and consequence of those forced changes in brain tissue.

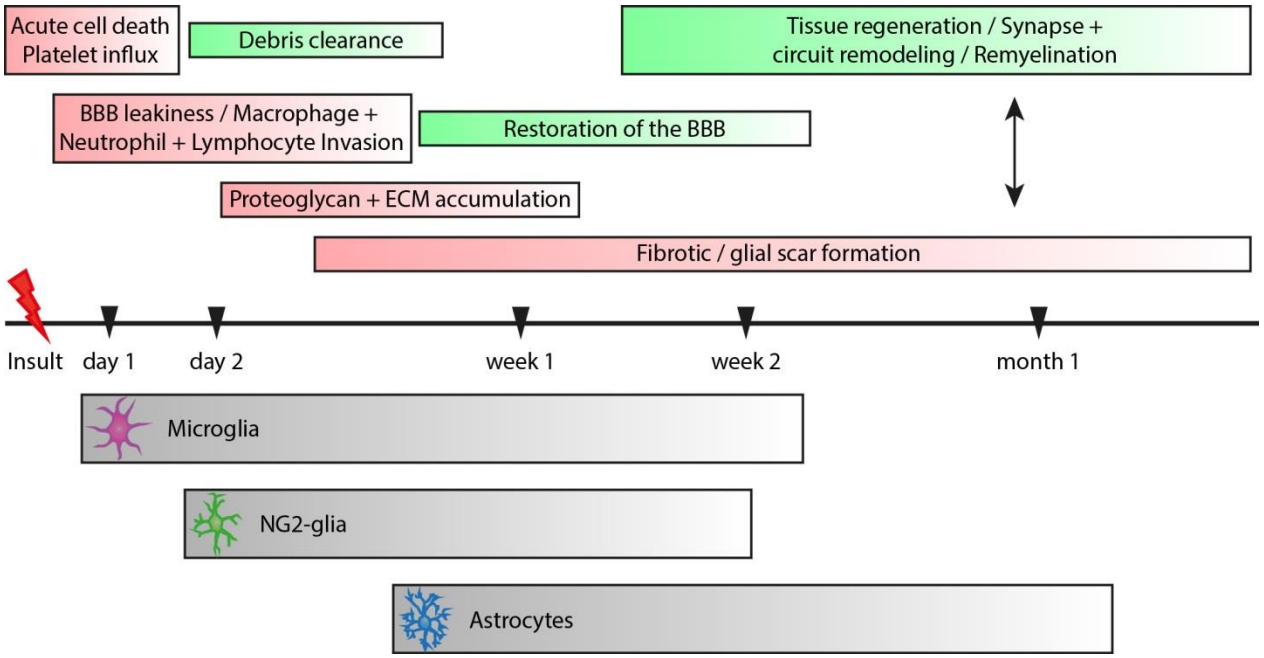

Figure 5 **Time course and cellular reaction after CNS injury.** General events following an insult in the CNS including beneficial (green) and detrimental effects (red), like persisting scar formation or extracellular matrix ECM accumulation, which inhibit the beneficial event of wound healing. Cellular responses depict the main cellular accumulation periods of resident CNS cells following injury (modified from Shechter and Schwartz, 2013; Burda and Sofroniew, 2014)

1.3.1.4 Immune cells

The CNS has been described as an immunologically privileged or specialized site due to the general BBB blockage of immune cell infiltration (Ransohoff et al., 2003; Anthony and Couch, 2014). This is overcome in case of injury or disease when leucocytes are able to migrate into the CNS mediating an immune response, which often leads to a secondary damage (Ransohoff et al., 2003; Anthony et al., 2012). However, compared with the periphery, the active recruitment of leukocytes is delayed and to a reduced extent (Anthony et al., 2012). The majority of research investigating neuroinflammation has been conducted in regard to autoimmune diseases like MS, where inflammation is probably a major cause of this detrimental pathology. Therefore, it is known that mainly T-cells and macrophages but also natural killer cells, mononuclear phagocytes and in some cases even B-cells and neutrophils are able to enter the brain in MS-models like experimental autoimmune encephalomyelitis (EAE; Ransohoff et al., 2003). Nevertheless, also in other cases of brain injury, especially after damage of the vasculature and hence leakage of the BBB, leukocytes are within the first responders to the injury. They fundamentally contribute to the first steps of the damage response: cleaning the damaged sites, protecting against potential infection of the exposed parenchyma and promoting tissue regeneration (Shechter and Schwartz, 2013). The continuous recruitment of immune cells and their detrimental role in subsequent inflammation

and secondary tissue damage has led to the concept of a dual role of the immune system having first beneficial and later on damaging effects on the brain tissue (Shechter and Schwartz, 2013). This dual role was recently connected to the M1 and M2 phenotype of macrophages (Mills, 2015) and this inflammatory response could be a target for manipulation in clinical therapy, e.g. via specific chemokines involved in cell-cell communication (Gyoneva and Ransohoff, 2015). I will outline the combined findings of microglia and macrophages in the next chapter because macrophages, the major responsive elements of the immune system entering the CNS were until recently hard to distinguish from resident microglia.

1.3.1.5 Microglia and macrophages

Microglia, the resident immune cells of the CNS, share many similarities with peripheral macrophages and therefore, have been pooled with this cell type in many studies (Silver et al., 2015). Visualizing cortical microglia after laser lesion with the help of *in vivo* imaging could demonstrate that microglia in close vicinity to the injury site react almost immediately to tissue damage by reorientation and outgrowth of their processes (Nimmerjahn et al., 2005). Subsequently, those cells accumulate in the lesion core via active migration shielding the injury site already starting 1 hour after the injury (Nimmerjahn et al., 2005). Also multiple spherical-shaped inclusions could be observed at 10 to 15 minutes after injury indicating phagocytic activity. These findings emphasize the role of microglia as first responders to the lesion by sealing of the injury site and starting to clear the first tissue debris (Nimmerjahn et al., 2005). Indeed, preventing or reducing microglial activation with the help of pharmacologic or genetic techniques deteriorates lesion pathology and tissue recovery (Lalancette-Hebert et al., 2007; Hines et al., 2009; Silver et al., 2015). Depending on the size of the damage and the consecutive breach of the BBB, it is suggested that infiltrating lymphocytes and especially macrophages additionally contribute to this first immune response (Hanisch and Kettenmann, 2007). Interestingly, a study differentially labeling microglia and macrophages after spinal cord injury (SCI) showed that microglia contact damaged axons earlier then infiltrated macrophages, whereas macrophages have an increased and more effective phagocytic activity (Greenhalgh and David, 2014). The general microglia response, like in macrophages, is dependent on the different activity states which adapt to the severity of the insult and involve signaling to other cells, including neurotrophic factors for neuronal survival, inflammatory mediators in cases of bacterial or viral invasion and anti-inflammatory factors at later stages to reduce tissue damage (Hanisch and Kettenmann, 2007). Beside these mostly initial and rather positive functions, microglia and invaded macrophages are also attributed to be effectors of secondary tissue damage. In this context, the suggested M1

phenotype of "classically" activated macrophages and microglia seems to be more detrimental then the "alternatively" activated M2 type. Even if some of the signaling and activation pathways eliciting those phenotypes are unraveled, the complete picture, especially *in vivo*, remains unclear. Furthermore, since the majority of the *in vivo* work has been conducted investigating axonal recovery after SCI there is still just rudimentary knowledge of the mechanisms in the brain (Silver et al., 2015). Nevertheless, especially in SCI, there are already promising clinical trials ongoing based on the results that *ex vivo* activated macrophages injected into the injured spinal cord promote axonal regeneration and reduce tissue damage, providing hope for future research in this direction (Kigerl and Popovich, 2006; Silver et al., 2015).

1.3.1.6 Astrocytes

The response of astrocytes following neurological disorders and injuries, also called astrogliosis, has been investigated for quite some time. However, the underlying concept and the complete molecular and cellular processes involved are still not fully understood (Pekny and Pekna, 2014). The most prominent features of astrogliosis are hypertrophy, the upregulation of the intermediate filament glial fibrillary acidic protein (GFAP) and proliferation (Pekny and Pekna, 2014). This reactivity is shown after a multitude of neuropathologies like neurotrauma, ischemia, brain hemorrhage, perinatal asphyxia, CNS infections, epilepsy, CNS tumors, diabetic retinopathy, Alzheimer's disease (AD), Parkinson's disease, amyotrophic lateral sclerosis (ALS) and MS (Hostenbach et al., 2014; Pekny and Pekna, 2014). The modes of activation could involve cytokines like transforming growth factor (TGF)-α (Rabchevsky et al., 1998), interleukin (IL)-6 (Klein et al., 1997), ciliary neurotrophic factor (CNTF; Winter et al., 1995), leukemia inhibitory factor (LIF) and oncostatin M (Balasingam et al., 1994) as well as signaling pathways like the gp-130/signal transducer and activator of transcription 3 (STAT3; Sriram et al., 2004; Hostenbach et al., 2014; Pekny and Pekna, 2014). Therefore, it is very likely that cell-cell communication via secreted molecules between astrocytes, microglia, NG2-glia, neurons, endothelial cells or other cell types in the environment plays an important role in the emerging reactive states of these cells. This glial reaction and the consequential tissue alterations following brain pathologies are often referred to as glial scar. Latest results employing *in vivo* imaging of astrocytes after cortical stab wound injury site contradict the long leading assumption that astrocytes are the only contributors to this event, because it was demonstrated that they do not migrate towards the injury (Bardehle et al., 2013). Nevertheless, reactive astrocytes show hypertrophic and polarized morphologies and proliferate to some extent. However, this injury response occurs at a rather late phase after lesion (5-7 days). Interestingly, astrocytes in direct contact to blood vessels, the so

called juxtavascular astrocytes, showed a higher proliferation capacity compared to the remaining astrocyte population (Bardehle et al., 2013). Overall it is clear that astrocytes participate in the glial reaction to injury by forming a border region between the lesion and the surrounding tissue. This favors relatively quick tissue stabilization due to demarcation of the lesion but also potentially impedes the regenerative process later on (Voskuhl et al., 2009; Pekny and Pekna, 2014). Other positive effects of astrocytes within and surrounding the lesioned area during the acute phase of the injury include the restoration of the homeostasis and the BBB, regulation of the blood flow, recycling of neurotransmitters as well as synapse and neuronal protection, which could be demonstrated via ablation of reactive and proliferating astrocytes (Bush et al., 1999; Sofroniew et al., 1999; Faulkner et al., 2004; Pekny and Pekna, 2014). In contrast, at later and chronic stages of brain pathologies, reactive astrocytes and thus astrogliosis together with the so called glial scar are majorly connected to numerous undesired effects. The majority of these effects result from the expression or secretion of molecules like ephrin-a5 (Overman et al., 2012) leading to deteriorated synaptic and axonal regeneration, impeding functional recovery (Lee et al., 2010; Pekny and Pekna, 2014). Interestingly, many therapeutic approaches for diseases like epilepsy or stroke already target astrocytes both to improve astrocytic function in the early recovery process as well as to reduce their detrimental effects at more chronic stages to ameliorate functional recovery (Pekny and Pekna, 2014; Freitas-Andrade and Naus, 2015). Another interesting finding connected to reactive astrocytes was their capability to form neurospheres *in vitro* (Lang et al., 2004; Buffo et al., 2008). This stem cell like response seems to be elicited via the sonic hedgehog pathway and is only induced by invasive injuries disrupting the BBB like stab wound injury or ischemia, whereas noninvasive injuries like chronic amyloidosis or induced neuronal death do not elicit this response (Sirko et al., 2013). This points to a more diverse role of astrocytes depending on the pathology and the affected region, which could also be demonstrated with a gene expression analysis of astrocytes in models of SWI, ischemia and neuroinflammation showing a large amount of injury-specific gene expression (Zamanian et al., 2012; Sirko et al., 2015). Taken together astrocytes seem to play an essential role in events following a multitude of brain pathologies but also inhibit complete tissue recovery at later stages.

1.3.1.7 Other cell types

Over the last years more and more cell types were connected to the cellular response after CNS injuries. As a general feature of the wound healing and scarring process in all tissue types and organs, it is suggested that fibroblasts depositing extracellular matrix (ECM) proteins are major components of the emerging connective tissue (Gurtner et al., 2008). Even without fibroblasts as

a source, ECM proteins can also be found after CNS injuries which are considered to inhibit tissue recovery especially in regard to neuronal survival and axonal growth (Shechter and Schwartz, 2013). In addition, connective tissue with a non-glial origin has been reported as a component of the glial scar after SCI (Krikorian et al., 1981; Fawcett and Asher, 1999; Camand et al., 2004) but the origin of these fibroblast-like cells in the CNS is still unclear. So far, multiple sources of origin like resident fibroblasts, endothelial cells, bone marrow-derived circulating progenitor cells, monocytes or fibrocytes have been suggested (Krenning et al., 2010). One fate-mapping study could at least demonstrate that the fibroblast-like progeny of perivascular collagen1α1 cells are a main source of the fibrotic component of the scar tissue after contusive SCI (Soderblom et al., 2013). Another contributor to the glial scar after SCI was identified via fate-mapping of a subset of pericytes using a Glast-CreER mouse-line. These pericytes and their progeny outnumbered astrocytes within the glial scar in the spinal cord and were essential for the formation of connective tissue and thus the primary regeneration step following injury (Goritz et al., 2011). Noteworthy, the origin of the fate-mapping studies of Göritz et al. (2011) and Soderblom et al, (2013) could be partially overlapping due to the claim that both lineage tracings represent the major population of the connective tissue after SCI (Soderblom et al., 2013). Also massive proliferation of PDGFRβ$^+$ and CD105$^+$ stromal cells originated from the neurovascular unit and their deposition of ECM-molecules could be demonstrated within the brain (Fernandez-Klett et al., 2010). Interestingly, they appear directly within the lesion core aligning next to the GFAP$^+$ area of the glial scar (Fernandez-Klett et al., 2010). Latest findings complemented the list of cell types contributing to the glial scar after SCI with specifically recombined ependymal cells in the FoxJ1-CreER mouse-line. These neural stem cells are multipotent and give rise to astrocytes which then migrate to the lesion core after SCI (Barnabe-Heider et al., 2010), restricting secondary lesion enlargement, improving axonal regeneration as well as neuronal survival and hence are an important factor for spinal cord integrity after injury (Sabelstrom et al., 2013). So far, the majority of these findings focused on the spinal cord. Because there is a multitude of regional differences in injury response one cannot simply transfer these results to brain pathologies (Schnell et al., 1999; Batchelor et al., 2008; Zhang and Gensel, 2014). Nonetheless, some basic similarities like deposition of extracellular matrix proteins could be confirmed so far, in part because of the comparable cellular composition in both regions (Burnside and Bradbury, 2014). Therefore, it is important to investigate the related questions regarding tissue recovery in an appropriate injury model.

1.3.1.8 NG2-glia

Since the last 10 years also NG2-glia, came more and more into the focus of many researchers investigating CNS injuries. The first pathological context those cells were studied in, was their capacity to give rise to new oligodendrocytes and thus lead to remyelination after demyelinating events (Keirstead et al., 1998; Di Bello et al., 1999) or diseases like MS (Chang et al., 2000; Chang et al., 2002; Zhao et al., 2005)and ALS (Kang et al., 2013). For those pathologies it could be demonstrated that NG2-glia react upon a demyelination event with proliferation, accumulation in the lesion area and hence differentiation into myelinating oligodendrocytes (Redwine and Armstrong, 1998; Levine and Reynolds, 1999; Sim et al., 2002; Penderis et al., 2003). The resulting remyelination efficiency differs between species and affected regions, spanning from almost total regeneration and functional recovery in a mouse model of focal demyelination (Penderis et al., 2003) to the wide array of remyelination failure in chronic human MS lesions (Hartley et al., 2014). As there is no effective treatment strategy for MS patients so far, a great endeavor has been put into the search of the underlying mechanisms to improve therapy and eventually prolong the life span of the patients (Franklin and Ffrench-Constant, 2008; Kremer et al., 2015). On the contrary in the recovery phase after SCI, NG2-glia are considered a rather detrimental player after injury (Filous et al., 2014; Levine, 2015). Especially the name-giving molecule NG2 is a part of growth inhibitory chondroitin sulfate proteoglycans (CSPGs) which can be expressed by NG2-glia and to some extent by astrocytes following injury and participate in deteriorated axonal and neurite outgrowth, resulting in impaired tissue recovery (Tang et al., 2003; Tan et al., 2005; Tan et al., 2006). In general, NG2-glia accumulate in the injury core and react with increased proliferation following SCI (Levine et al., 2001; McTigue et al., 2001). Interestingly, abrogation of β-catenin signaling in NG2-glia led to reduced glial scarring and improved axonal regeneration after SCI. However, as the microglia and astrocyte reactivity was also reduced under these conditions it is not yet clear which cells were mainly causing the impediment for regeneration (Rodriguez et al., 2014). Also models of intraspinal hemorrhage (Sahinkaya et al., 2014) and chronic cerebral hypoperfusion (McQueen et al., 2014) led to oligodendrocyte loss with consecutive NG2-glia reactivity, proliferation and differentiation into mature oligodendrocytes. Furthermore, a mouse model of AD plaque deposition led to increased NG2-glia numbers which was however not observed in postmortem human AD brain tissue where NG2-glia numbers were reduced (Behrendt et al., 2013). Comparable to the reactivity after SCI, NG2-glia respond to TBI in the brain with increased proliferation, accumulation in the injury core and some limited degree of differentiation (Levine et al., 2001; Simon et al., 2011; Dimou and

Gotz, 2014), whereas the majority of cells did not differentiate but remained NG2-glia (Dimou et al., 2008; Komitova et al., 2011). Also NG2-glia labeled in an Olig2-CreER^{T2} mouse line proliferated and accumulated around the lesion core following cryolesion. However, this lesion paradigm led to their differentiation into astrocytes (Tatsumi et al., 2008). Remarkably, not all CNS pathologies lead to NG2-glia reactivity as it was demonstrated after massive induction of neuronal death (Cruz et al., 2003) which did not evoke an altered proliferation in NG2-glia (Sirko et al., 2013). Overall, these results show that NG2-glia participate globally in responses after different forms of brain injury and their reactivity in non-demyelinating lesions like TBI indicate that they exert additional functions besides their differentiation and remyelination capacity. Therefore, it is essential to get a better understanding of the cellular and molecular events following CNS injury to characterize the contribution of NG2-glia to the post-lesion processes and tissue regeneration.

1.3.2 Potential factors regulating NG2-glia migration

As the study of Hughes et al. (2013) could demonstrate via live *in vivo* imaging, NG2-glia are motile cells which are also able to exert directed short range migration in case of cell death or differentiation of neighboring cells (Hughes et al., 2013). In all higher organisms cell migration plays essential roles throughout the whole life starting from early development, for general tissue surveillance, maintenance and repair following injury and disease. Studies in cell culture systems and invertebrates have greatly advanced the understanding of physiology and mechanisms involved in migration (Lehmann, 2001; Raftopoulou and Hall, 2004). The previously mentioned *in vivo* imaging technique has created the possibility to observe migrating mammalian cells in the living animal. In brief, extracellular cues like soluble factors or matrix proteins elicit an intracellular response leading to coordinated reorganization of the cytoskeleton and ultimately the movement of the cell (Raftopoulou and Hall, 2004). Therefore, analysis of the responsible mechanisms involved in the NG2-glia migration could contribute to a better understanding of general migratory mechanisms, but also NG2-glia functionality and even possible techniques to manipulate migration and hence their injury response.

1.3.2.1 The Rho GTPase Cdc42 and its involvement in cell polarity and migration

Many factors and signaling molecules, like molecules of the mitogen-activated protein kinase (MAPK) cascades, lipid kinases, phospholipases, Ser/Thr and Tyr kinases and scaffold proteins, have been suggested to be involved in the intracellular mechanisms leading to migration (Raftopoulou and Hall, 2004). Another crucial component of the regulating pathways seems to be

the ubiquitously expressed Rho GTPase-family acting as a molecular switch, by changing from a Guanosine diphosphate (GDP)-bound, inactive to a Guanosine-5'-triphosphate (GTP)-bound, active form or vice versa (Raftopoulou and Hall, 2004). One family member of the Rho GTPase proteins is cell division control protein 42 homolog (cdc42), which has been shown to be a key regulator in cellular events like polarization (Etienne-Manneville and Hall, 2002; Cau and Hall, 2005; Garvalov et al., 2007), migration (Raftopoulou and Hall, 2004) and proliferation in yeast, *Drosophila* and *C.elegans* cells (Fuchs et al., 2009; Wang et al., 2009; Warner et al., 2010). Modes of action could include cdc42 mediated activation of downstream signaling pathways like mechanistic target of rapamycin (mTOR; Wang et al., 2009) and c-Jun N-terminal kinases (JNK)/MAPK as well as targets like Wiskott-Aldrich Syndrome protein (WASp)/Arp2/3 complex and partitioning defective 6 homolog alpha (Par6)/atypical protein kinase C (aPKC; Raftopoulou and Hall, 2004; Cau and Hall, 2005; Hall, 2005; Cappello et al., 2006). Those findings have been conducted in cell types like macrophages (Allen et al., 1998), fibroblasts (Nobes and Hall, 1995; Hall, 1998), astrocytes (Holtje et al., 2005; Etienne-Manneville, 2006) and neurons (Cappello et al., 2006; Garvalov et al., 2007) but were majorly performed *in vitro*. Especially in astrocyte cultures many intrinsic functions of cdc42 signaling have been analyzed using the so called scratch assay, mimicking cellular reactivity after injury *in vitro* (Holtje et al., 2005). The obtained observations could demonstrate effects of cdc42 on polarization (Osmani et al., 2006) and directed migration towards the scratch (Robel et al., 2011). An attempt to transfer those findings *in vivo*, employing live imaging of cortical astrocytes after stab wound injury, could confirm an effect of cdc42 on astrocyte polarization and proliferation. However, as cortical astrocytes did not migrate after injury, alterations in migratory behavior could not have been detected (Bardehle et al., 2013). Other *in vivo* studies in targeted genetic ablation models of cdc42 in neurons showed effects on neuronal polarity, axon formation, cytoskeletal organization and filopodial dynamics (Garvalov et al., 2007) as well as altered polarity of mitosis and a consecutive change of cell fate of neural progenitors (Cappello et al., 2006). Assessing the influence of cdc42 in postnatal NG2-glia, specific cdc42 ablation did not affect proliferation, migration or differentiation *in vitro* (Thurnherr et al., 2006) even if it was suggested that the Rho GTPase-family generally controls cytoskeleton remodeling, process protrusion and migration of NG2-glia (Bacon et al., 2007; Bauer et al., 2009). Also *in vivo* no developmental effects, besides a stage-specific myelination phenotype with abnormal accumulation of cytoplasm at the inner tongue of the oligodendrocyte process, could be detected (Thurnherr et al., 2006). Nevertheless, it is not yet unraveled if cdc42

is able to influence the *in vivo* behavior of NG2-glia especially in regard to their elevated reactivity ensuing injury.

1.3.2.2 The chondroitin sulfate NG2 as a potential regulating factor for migration and polarization

Another factor which was just recently connected to the migratory behavior of NG2-glia is the name giving transmembrane proteoglycan NG2. Phosphorylation of NG2 via protein kinase c (PKC) led to redistribution of the protein from the apical cell surface to the lamellipodia, polarization and increase of cell motility, which was demonstrated *in vitro* with a scratch wound assay of human astrocytoma cells (Makagiansar et al., 2004). Also binding of soluble NG2 to the surface of endothelial cells induces cell motility *in vitro* and angiogenesis *in vivo* (Fukushi et al., 2004). Additionally, connections of chondroitin sulfate proteoglycans to cdc42 (Eisenmann et al., 1999) and another Rho GTPase, Rac (Majumdar et al., 2003) have been found in melanoma, implicating an involvement in cell motility and polarity. Comparable to the effect of cdc42 in neural progenitors, NG2 is connected to asymmetric cell division in NG2-glia (Sugiarto et al., 2011) and its targeting to cellular retraction fibers in glioma cell lines has been connected to fiber formation and polarization (Stallcup and Dahlin-Huppe, 2001). A recent study by Biname et al. (2013) investigated the connection between NG2 and Rho GTPases in NG2-glia. They could demonstrate an influence of NG2 on cell polarity via Ras homolog gene family member A (RhoA) activity and the multi-PDZ domain protein MUPP1/syntaxin 1 (Syx1) signaling pathway, leading to decreased polarization *in vitro* and *in vivo* as well as *in vitro* migration after depletion of NG2 (Biname et al., 2013). To further our understanding of these processes in NG2-glia it is essential to investigate those effects *in vivo* and in more detail. Since most of the *in vivo* analysis, so far, have been conducted in still images, live two-photon laser scanning microscopy (2PLSM) is an essential addition to this tool box, especially concerning the migratory behavior to follow cells over time.

2 Aim of the study

As the brain is such an important but complex organ, brain pathology leads to detrimental and often life threatening consequences. The overall treatment strategies are very limited and in most cases symptomatic. Therefore, it is of great importance to get a better characterization of the cellular and molecular events during brain pathology. NG2-glia just recently got more attention of neuroscientists and is thus not well characterized. Especially under pathological conditions preliminary findings suggest a great potential in tissue and functional recovery. To improve the understanding of NG2-glia behavior following brain injury these questions were addressed in my study:

1. How is the cellular response of NG2-glia after injury in detail?
2. What is the timeline of this response behavior?
3. What is the function of NG2-glia response following brain injury?
4. How could this behavior be altered?

To investigate the cellular events after brain injury in more detail and in a consecutive manner repetitive *in vivo* imaging with two-photon laser scanning microscopy (2PLSM) was performed following stab or punctate wound injury in the somatosensory cortex of mouse lines with green fluorescent protein (GFP)-labeled NG2-glia. The obtained time series were analyzed to follow the cellular behavior in the phase following brain injury. For a better understanding of the underlying mechanisms and as an attempt to achieve altered NG2-glia behavior after injury, cdc42- and NG2-deficient mice were investigated employing the same protocol. Additionally, immunohistochemical and with my colleague Sarah Schneider NG2-glia depletion studies were performed for a better characterization of their functions in wound closure and tissue repair.

3 Results

3.1 The cellular changes of NG2-glia following injury

For analysis of the cellular reaction of NG2-glia after injury repetitive *in vivo* 2PLSM of adult Sox10-iCreER^{T2} x CAG-eGFP mice was performed. In this mouse line the GFP-reporter protein labels cells of the oligodendrocyte lineage, spanning from NG2-glia to mature oligodendrocytes, after tamoxifen induction. Some of the early experiments have been performed by my colleague Christoph Straube and three resulting image stacks have been included in the analysis for this thesis.

Following induction in 3-5 months mice of both sexes, a craniotomy followed by a small punctate wound injury was performed (PWI, ~100µm long and 700µm deep) in the somatosensory cortex. Subsequently, the craniotomy was sealed with a cranial window, Texas-Red-conjugated dextran was injected into the tail vein for vessel labeling and the first imaging session was performed usually around 45 minutes after injury (0 days post injury[dpi]; Figure 6A). At this timepoint, most NG2-glia showed their typical distribution and morphology with ramified branches. To resolve the behavior of NG2-glia in more detail, the same cortical area of interest was repetitively imaged at different timepoints after injury and their cellular reaction analyzed. Specific areas and cells were identified at later timepoints with labeling of the relatively stable vessels as landmarks (Figure 6B-D) and NG2-glia were discriminated from mature oligodendrocytes based on their morphology.

Already after 2dpi dramatic changes in the morphology and the position of many NG2-glia around the lesion site could be observed. This also led to an accumulation of cells within and in direct proximity to the lesion core, while only a small subpopulation of NG2-glia remained static in terms of morphology and position (Figure 6B, C, E). In case the image quality was not impaired due to increasing background the majority of the cells could be traced at the consecutive timepoints (Figure 6B-D), arguing against the occurrence of massive NG2-glia cell death between 0 and 4dpi. In contrast to the majority of NG2-glia, mature oligodendrocytes did not show any observable cellular responses following this injury paradigm but remained rather stable (white arrows in Figure 6B-D). For a better characterization of the behavior of NG2-glia, their detectable responses were classified in the following categories: (a) Hypertrophy, representing the enlargement of the volume of cell bodies and/or processes (Figure 6B´), (b) Polarization, describing the change in cell morphology toward an elongated cell (process/es or cell soma) in a certain direction (Figure 6C´), (c) migration, defined as the movement of the cell body for at least 10µm (Figure 6C´) and (d) proliferation (Figure 6D´).

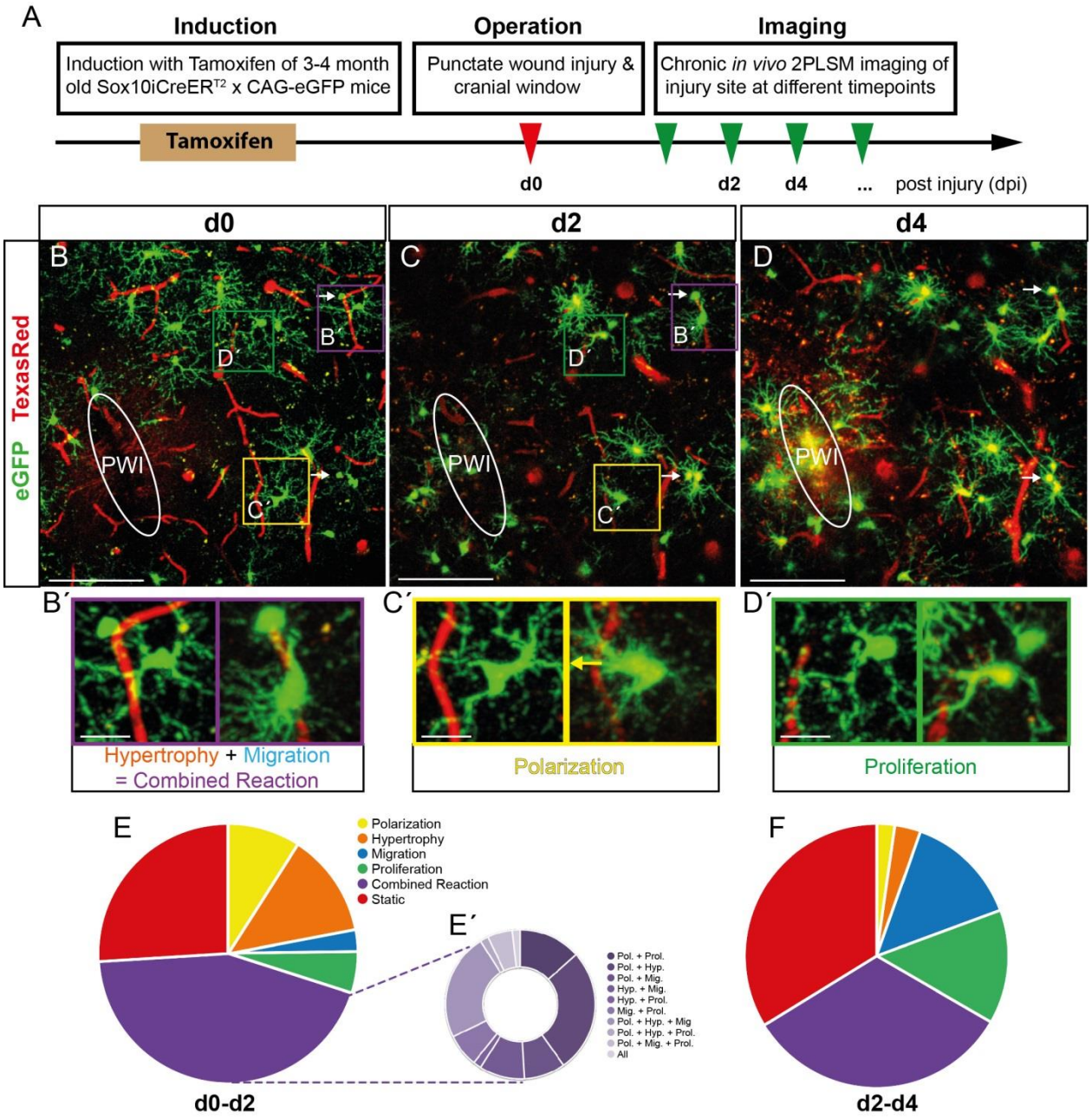

Figure 6 Fast and Heterogeneous reaction of NG2-glia after injury. (A) Schematic illustration of the experimental procedure. (B-D) Images of GFP$^+$ NG2-glia and oligodendrocytes (white arrows) surrounding a punctate wound injury (PWI; white ellipse) at d0, d2 and d4 after lesion. Blood vessels are labeled with Texas-Red dextran (red). (B´-D´) Examples of cells (higher magnification from B-C) showing the combined reaction of hypertrophy and migration (B´), polarization toward the injury (C´; yellow arrow indicates the direction) and proliferation (D´). (E-F) Pie charts represent the heterogeneous reaction of all NG2-glia surrounding the injury site between 0 and 2dpi (E; Polarization represents the cells polarizing toward the injury; the classification of the multiple reactions is represented in pie E´) and 2 and 4 dpi (F; n=220 cells from 8 animals for d0-d2 and n=180 cells from 6 animals for d2-d4). Images show maximum intensity projections of 30µm deep stacks. Scale bars represent 100µm in B-D and 25µm in B´-D´.

The observed response of the majority of NG2-glia was fast and heterogeneous (188 of 254 cells from 8 mice; Figure 6E) in the direct surrounding (up to 500µm) of the lesion already at 2dpi,

with cells showing one or more of these behavioral categories. The majority of reactive cells showed a combined reaction, comprising of at least two of these reaction types between 0 and 2dpi (Figure 6E, E´). Interestingly, the degree and type of this heterogeneous reaction was not drastically altered at 4dpi (Figure 6F).

To assess whether a reduced induction rate led to selected recombination in a specific subtype of NG2-glia with a diverse reaction profile, animals with low induction rates (1x gavaging with ~20µg/ml tamoxifen) were compared with animals receiving a higher induction rate (3x gavaging with 40µg/ml tamoxifen; Figure 7). As expected, the high induction rate led to a massive increase of GFP-labeled cells compared to the low induction protocol (Figure 7A, B). Analyzing the NG2-glia response in both groups revealed some small alterations in polarization and proliferation at 2dpi (Figure 7C) as well as migration at 4dpi (Figure 7C´). However, these differences were not significant due to rather big variations between the animals receiving the same induction treatment. Overall, the cellular response of the recombined NG2-glia seem to be comparable between the two experimental groups (Figure 7C), also considering the heterogeneous reaction profile between 0 and 2dpi (Figure 7D-D´). Therefore no subclass with a specific reaction profile seemed to be preferentially recombined at lower tamoxifen levels and subsequently animals with low and high induction rates were pooled for further analysis.

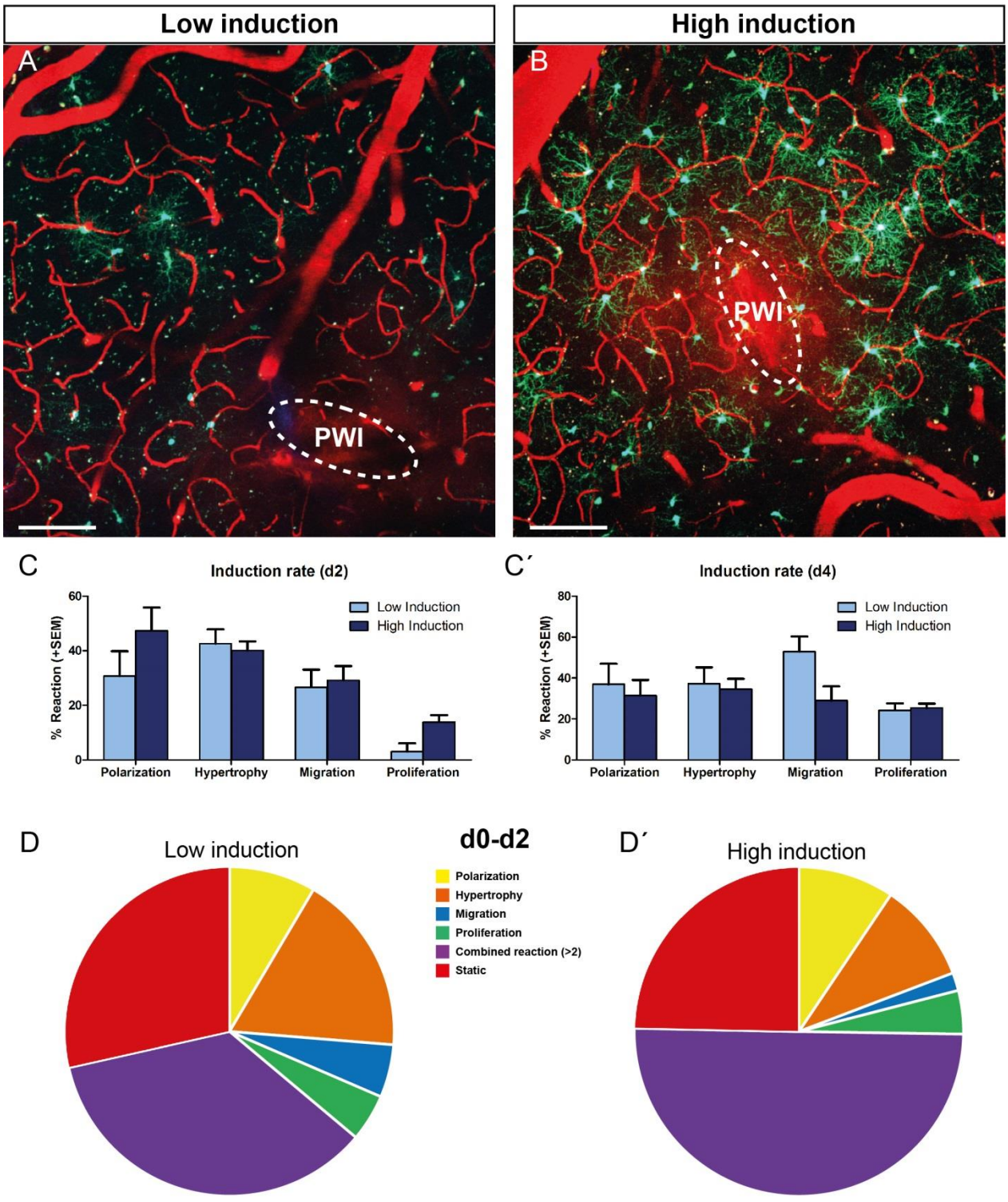

Figure 7 Alterations in induction rates do not change the overall reactivity of NG2-glia. (A, B) Images of recombined cells of the oligodendrocyte lineage with induction rates of 1x gavaging with ~20µg/ml tamoxifen (A) and 3x gavaging with 40µg/ml tamoxifen (B) at 0dpi after PWI (indicated with a white dashed ellipse). (C, C´) Comparison of the different reaction categories at 2dpi (C; n=3 animals for low induction and n=5 for animals for high induction) and 4dpi (C´; n=3 for each induction variant) for animals with low and high induction rates. (D, D´) Pie charts of the reactivity after low (D) and high induction (D´) between 0 and 2dpi. Images show maximum intensity projections of 30µm deep stacks. Scale bars represent 100µm.

3.1.1 NG2-glia undergo morphological changes following brain injury

The next point of interest was to follow the response and reaction profiles of NG2-glia for a longer period after injury. Therefore the results from the analysis of the short timepoints (0-4 dpi) were combined with results from experiments carried out to specifically investigate the consecutive timepoints (4-28 dpi). Due to decreasing reactivity at these later timepoints, increasing gaps between the imaging sessions were introduced for this long experimental period.

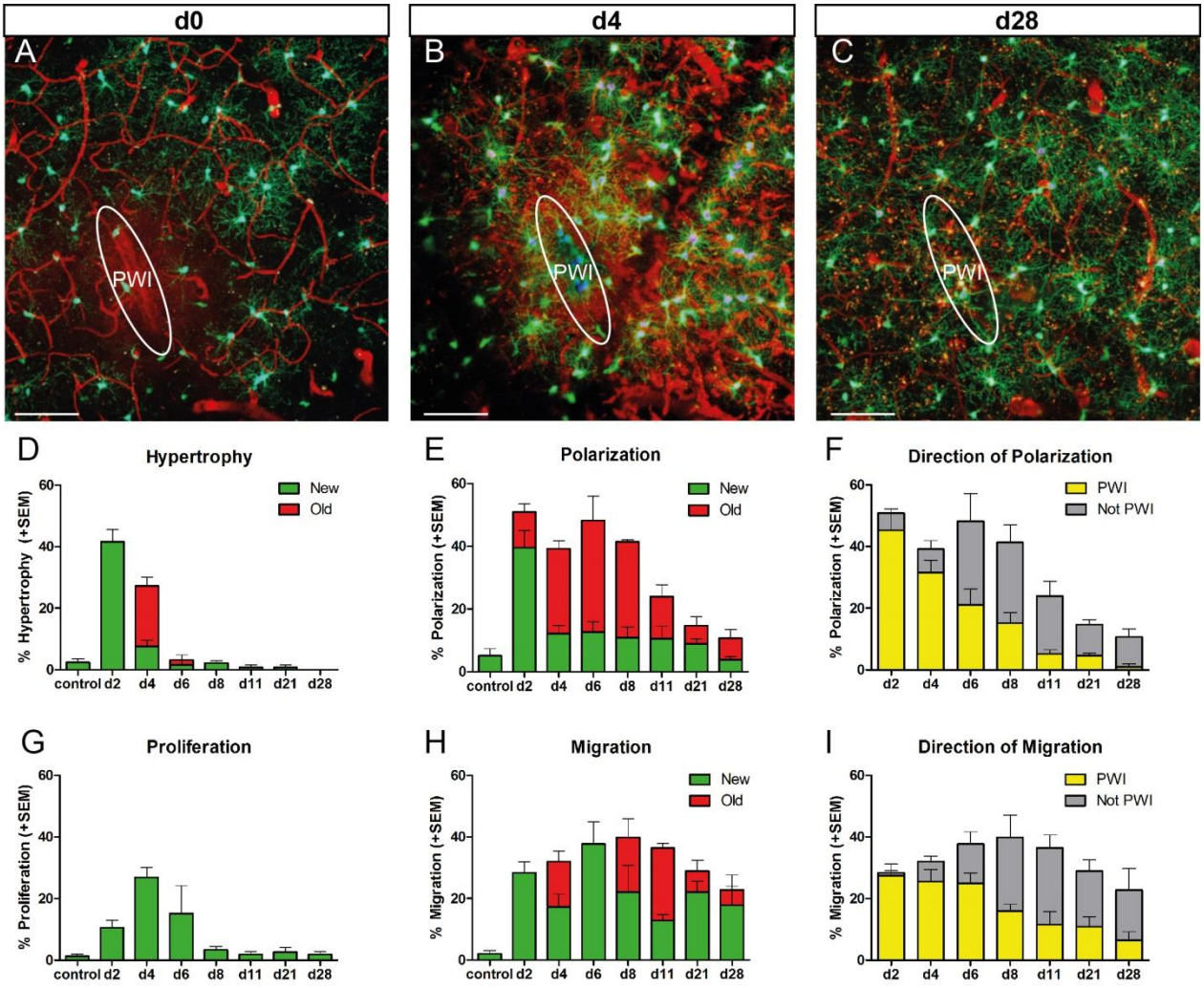

Figure 8 Temporal reaction of NG2-glia after injury. (A-C) Images of cells of the oligodendrocyte lineage around the injury site at d0 (A), d4 (B) and d28 (C) after PWI. (D, E, G, H) Graphs depict the percentage (mean+SEM) of cells showing hypertrophy, polarization, proliferation and migration at given timepoints (n=3-8 animals per timepoint). "New" (green bars) represent the cells showing hypertrophy (D), polarization in any direction (E), proliferation (G) and migration (H) for the first time at the indicated timepoint. "Old" (red bars) represent cells which showed this behavior already at the previous timepoint (for detailed statistical evaluation see chapter 9.1). (F, I) Directionality of polarized (F) or migrated (I) cells (mean+SEM; yellow bars: toward the PWI; grey bars: all other directions) over time. N=9 animals for d4, n=8 for d0 and d2, n=4 for d6, d8 and d21, n=3 for all other timepoints; mostly 20-30 cells per animal. Images show maximum intensity projections of 30µm deep stacks. Scale bars represent 100µm.

The analyzed NG2-glia reactivity peaked during the first days after injury (until 4dpi), followed by a decrease of the reactivity and a stabilization of the overall morphology between three and four weeks after the insult (Figure 8). Especially when comparing the images of 0 and 28dpi the distribution and morphology of NG2-glia appeared very similar with just a slight increase of NG2-glia cell number persisting at the lesion core (Figure 8A and C).

3.1.1.1 Hypertrophy of NG2-glia

Following the hypertrophic response of NG2-glia over time revealed hypertrophy to be a rather quick but transient event. It was observed in 42% of the NG2-glia at 2dpi (106 out of 254 cells from 8 mice), decreasing to 27% at 4dpi (63 out of 222 cells from 6 mice) and almost no hypertrophic cells at 6dpi (4 out of 114 cells; Figure 8D). Notably, 75% of hypertrophic NG2-glia at 4dpi have been already hypertrophic at 2dpi and hence kept their altered morphology for this period (47 out of 63 cells; red bar). In contrast, only 7% of the traceable NG2-glia population became hypertrophic for the first time between 2 and 4dpi (16 out of 222 cells; green bar; Figure 8D). To further validate the observation of hypertrophy, volume analysis of selected cells at different timepoints was performed in collaboration with Felix Buggenthin and Carsten Marr from the Institute of Computational Biology of the HelmholtzZentrum Munich. This analysis showed that hypertrophic cells had a 3-fold bigger volume than non-hypertrophic or control cells (144 cells from 13 animals). The existence of a hypertrophic and a non-hypertrophic subpopulation of NG2-glia and a high overlap between analog and digital classification for hypertrophy could be confirmed with a systematic statistical evaluation (see Figure 23). To assess how the different behavioral categories were interrelated, the cells were clustered according to their reaction at 2dpi. The resulting cell clusters were then analyzed concerning their subsequent reaction at 4dpi. Concerning the behavior of hypertrophic cells, migration and polarization seemed to be not affected of preceding hypertrophy, as hypertrophic and not hypertrophic cells showed comparable responses regarding those two behavioral categories (Figure 9D). Interestingly, almost half of the hypertrophic cells at 2dpi (47±7%) lost their hypertrophy at the 4dpi. However, the likelihood for this population remaining hypertrophic at 4dpi was still higher compared to non-hypertrophic NG2-glia at 2dpi becoming hypertrophic at 4dpi for the first time (Figure 9D). Notably, hypertrophic NG2-glia at 2dpi were more prone to proliferate at 4dpi compared to the non-hypertrophic NG2-glia (42±6% vs. 15±3%; Figure 9D) arguing for a tendency for increased size of the cell soma before cell division (Figure 9B). However, around half of the hypertrophic population of NG2-glia at 2dpi (58±6%; Figure 9D) did not show any detectable cell division at the consecutive timepoint (Figure 9D; examples Figure 9A and C).

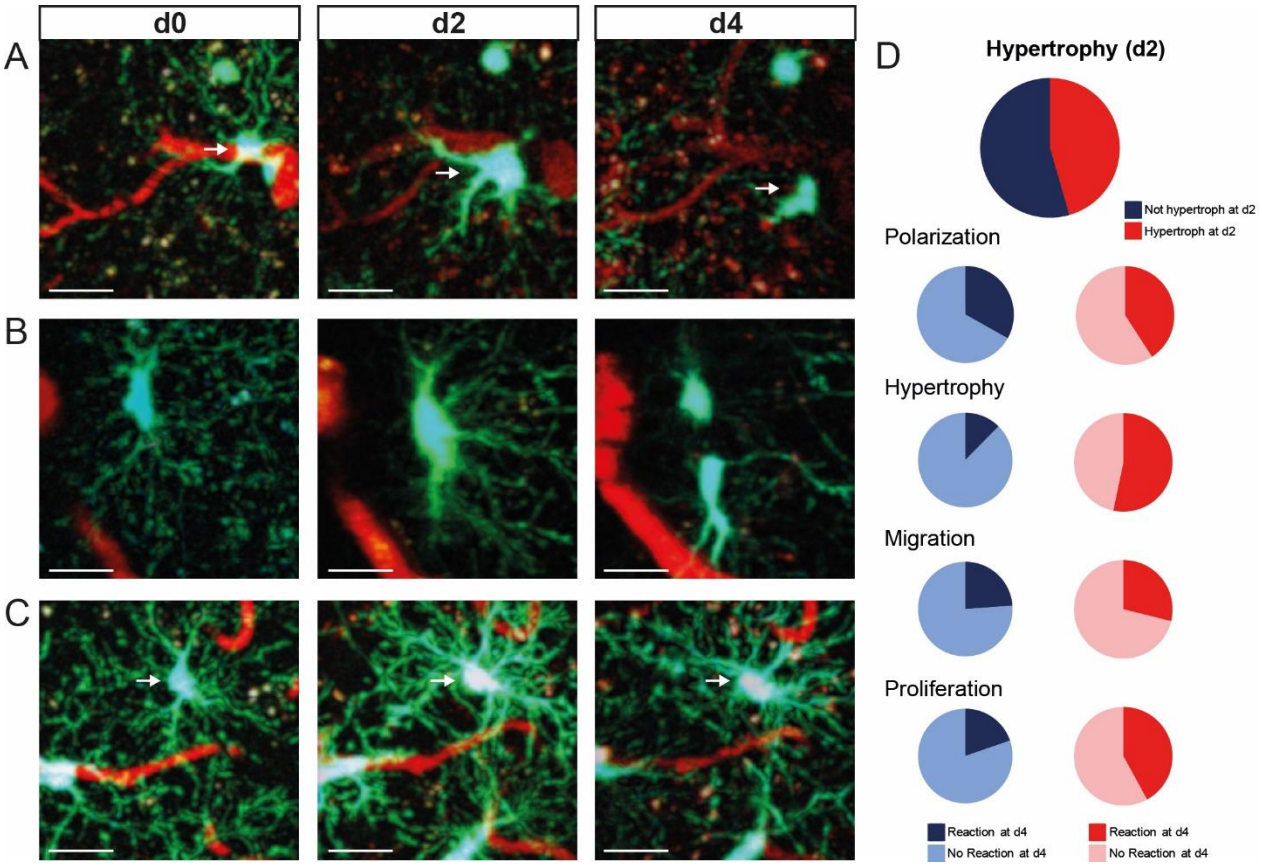

Figure 9 Examples of hypertroph NG2-glia and their further behavior. (A) NG2-glia (white arrow) next to a vessel, moving away from the vessel and showing a hypertroph morphology at 2dpi migrates further and loses its hypertroph morphology at 4dpi. (B) Hypertrophy at 2dpi can also be followed by cell division. (C) Example of a cell (white arrow) getting hypertroph at 2dpi and remaining hypertroph until 4dpi without any further detectable reaction. (D) Proportion of cells that were hypertroph (red) or not (blue) at 2dpi and their further reaction at 4dpi (n=6 animals; mean; unpaired t-test: Polarization: p=0.3095; Hypertrophy: p=0.0012; Migration: p=0.5684; Proliferation: p=0.0116). Images show maximum intensity projections of 30 (A: d0 and d2, C) or 40 (A: d4, B) µm deep stacks. Scale bars represent 20µm.

3.1.1.2 Polarization of NG2-glia

Polarization was defined as a change in morphology of NG2-glia leading to an accumulation of processes or an elongated cell soma at one side of the cell, reflecting a (re-) orientation toward this direction. The directionality of these morphological changes was assigned to one of four quadrants surrounding the area of the cell, with one of the quadrants comprising the lesion area. Like hypertrophy, polarization levels started increasing already at 2dpi and a decrease could first be detected at 8dpi (Figure 8E). Analysis of the direction of the polarization showed that most NG2-glia were polarized toward the injury site until 4dpi, while they shifted more and more from the injury directed to a rather random orientation (with a tendency to orientate away from the injury site) later on (Figure 8F). Assessing the interrelationship between a polarized morphology and the consecutive behavior, showed as expected that NG2-glia with a polarized morphology had a higher tendency to migrate (40±7%) than cells without this morphological characteristic

(12±4%; Figure 10D). Interestingly, more than half of the NG2-glia showing polarization at 2dpi (60±7%) did not migrate subsequently or even lost their polarized morphology at 4dpi (48±7%; Figure 10D), an observation uncoupling polarization from migration. Importantly, this solely states that some polarized cells did not show any migratory behavior at the consecutive timepoints (Figure 10A and B). However, it cannot be stated that migration can occur without polarization as a prerequisite behavior, due to the non-visualized time between each imaging session when potential polarized morphology of cells preceding the detectable migration would have been undetected. In contrast to polarization and migration, hypertrophy and proliferation seemed to be rather independent of a preceding polarized morphology (Figure 10D).

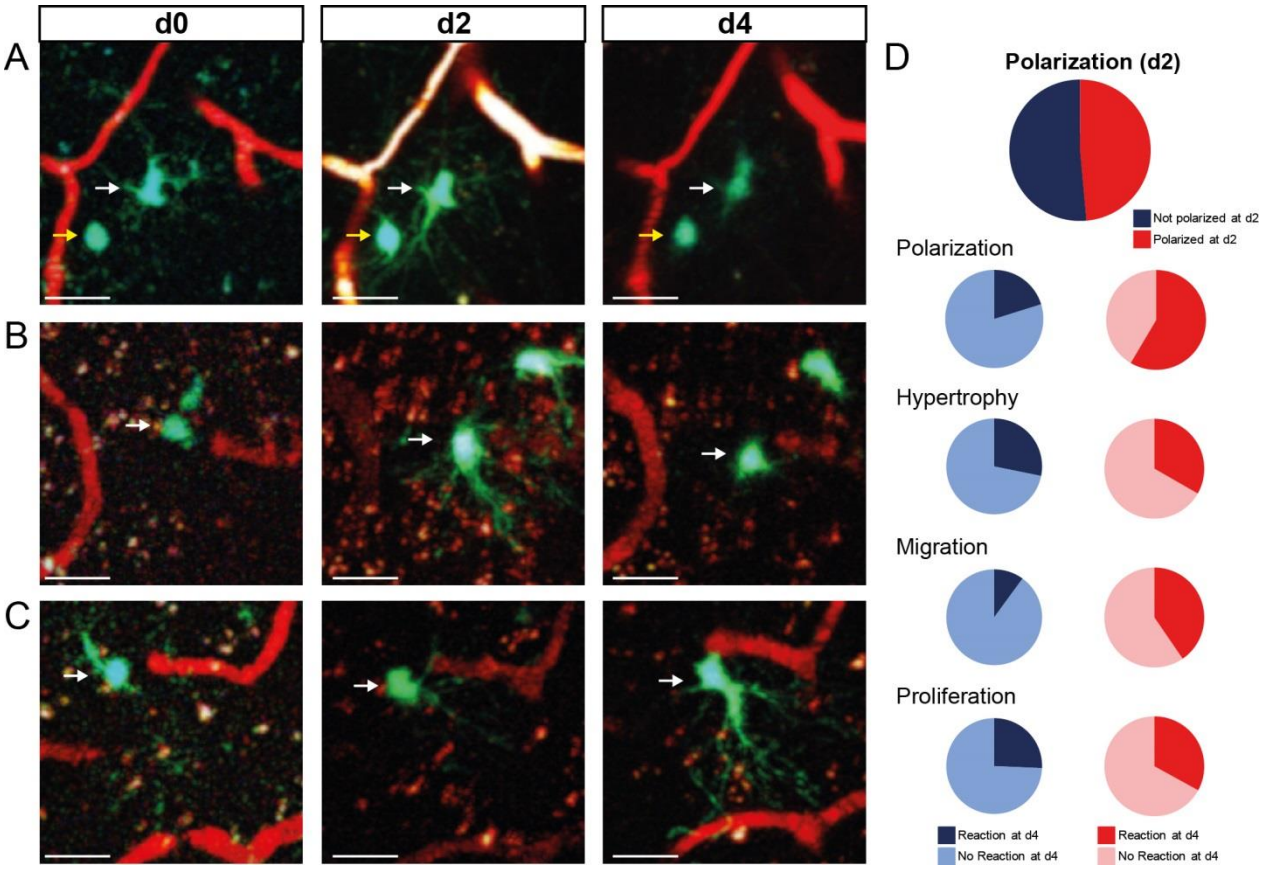

Figure 10 Examples of polarizing NG2-glia at 2dpi and their reaction at 4dpi. NG2-glia showing polarization at 2dpi can retract their processes and not show any further reaction (A, B) or changes its polarization (C) at 4dpi. (D) Proportion of cells that showed polarization toward the injury (red) or no polarization (blue) at 2dpi and their further reaction at 4dpi (White arrows indicating NG2-glia; yellow arrows indicating oligodendrocytes; n=6 animals; mean; unpaired t-test: Polarization: p=0.001; Hypertrophy: p=0.5954; Migration: p=0.0065; Proliferation: p=0.3307). Images show maximum intensity projections of 30 (A, C) or 40 (B) µm deep stacks. Scale bars represent 20µm.

The results for the morphological changes (hypertrophy and polarization) of NG2-glia highlight fast and transient morphological alterations which were already observed shortly after injury followed by a relatively quick return to physiological levels. This is in particular the case for

hypertrophy whereas polarization levels were decreasing not as fast, also pointing to a longer lasting reorientation phase until the homeostatic control of NG2-glia was reestablished after acute tissue damage.

3.1.2 The migratory response of NG2-glia following brain injury

Comparable to the quick events of polarization and hypertrophy, NG2-glia migration was an early response following injury (Figure 6C´and Figure 8H). The question remained if the observed migration was an active cellular process or if the cells were just displaced due to tissue remodeling after injury. Therefore, images of the same cells at different timepoints were registered according to the channel of the relatively stable blood vessels by Felix Buggenthin and Carsten Marr from the Institute of Computational Biology of the HelmholtzZentrum Munich. The resulting superimposed images of the stacks confirmed active migration of NG2-glia (see Figure 24).

Comparable to polarization and in contrast to the fast and transient hypertrophy after injury, migratory behavior of NG2-glia was relatively stable between 2 and 11 dpi, while it declined thereafter (Figure 8H). Due to the longer imaging periods after 11 dpi, slow moving cells had more time to cover the threshold distance for migration of 10 µm. Therefore, they were also considered as migrating cells as long as they kept the direction of their movement constant. As a consequence, the amount of migration did just slightly decrease from 8dpi on and did not reach control levels. However, the maximum migration distance and the velocity (Figure 11E and F) returned to control, uninjured levels already between 11 and 14dpi. Remarkably, both already migrating cells at 2dpi that kept moving until 4dpi (red bars at Figure 8H) as well as cells that initiated a migratory behavior only at 4dpi could be observed (green bars at Figure 8H).

Evaluating the consecutive behavior of cells which migrated at 2dpi, revealed a stronger reactivity at 4dpi compared with the non-migratory NG2-glia. Whereas proliferation was not drastically changed, migratory NG2-glia showed a higher likelihood of being hypertrophic, polarized or migratory at 4dpi (53±7%, 51±4% and 45±9% respectively; Figure 11D). As expected, the directionality of migrating NG2-glia correlated with the orientation of the observed polarization. In the reorientation phase, polarization was even preceding migration in terms of change of directionality. This resulted in the majority of polarized NG2-glia orientating away from the injury already at 6dpi (Figure 8H). The major shift of directionality of the migrating cells appears with one timepoint delay at 8dpi (Figure 8I). These results revealed that NG2-glia indeed respond with quick migration directed toward the lesion site during the first week after injury contributing to an increase of cells within the lesion core before the migration direction returned to a more randomized orientation, which is comparable to physiological conditions.

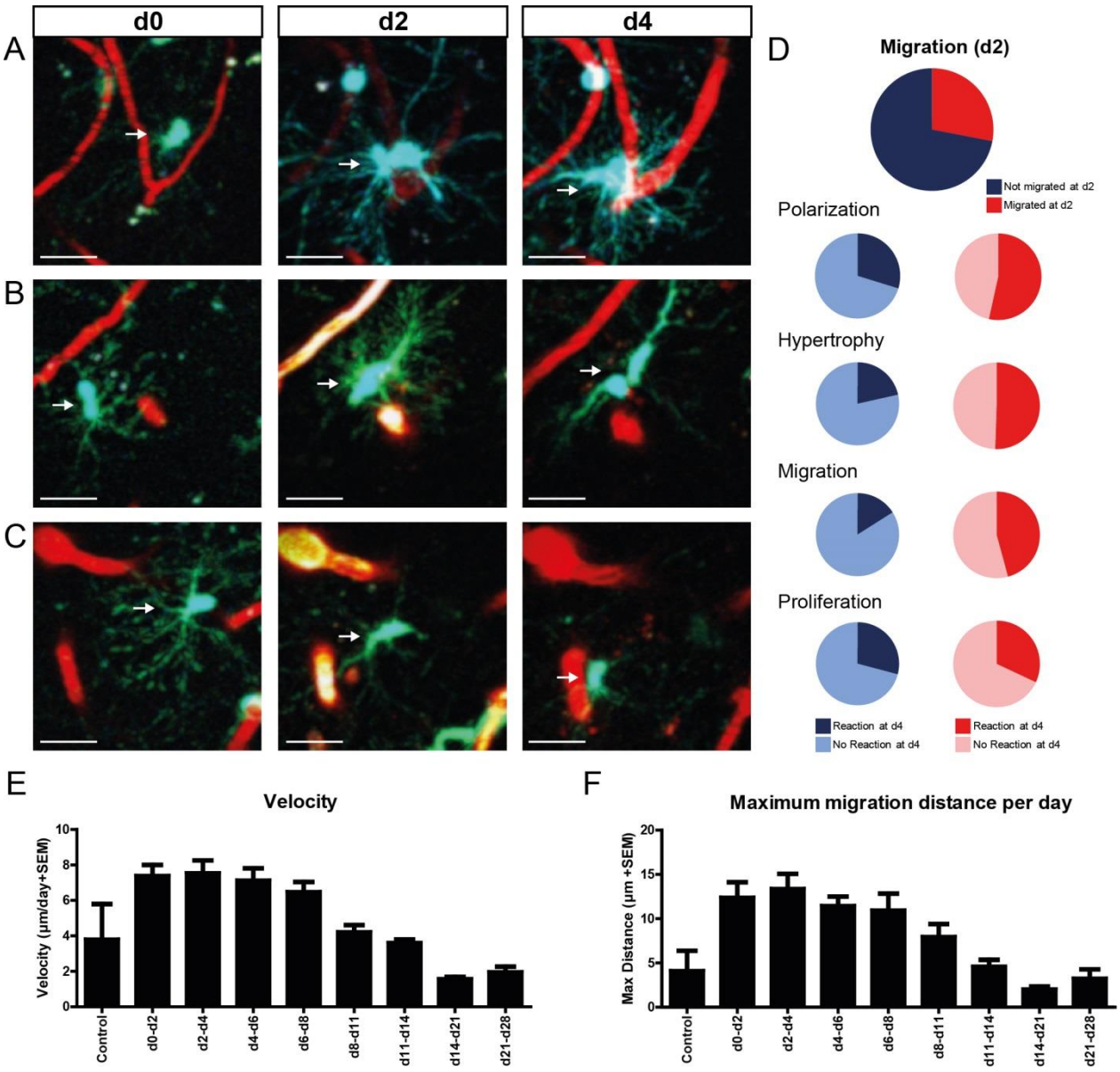

Figure 11 Examples of migrating NG2-glia and their further reaction. (A) NG2-glia (white arrow) migrating over a vessel and showing a hypertroph morphology. (B) Cell migrating until d2 followed by a cell division at 4dpi. (C) NG2-glia that keeps migrating over time. (D) Proportion of cells that showed a migratory behavior (red) or not (blue) at 2dpi and their further reaction at 4dpi (n=6 animals; data are presented as mean; unpaired t-test: Polarization: p=0.0112; Hypertrophy: p=0.0015; Migration: p=0.0197; Proliferation: p=0.5253). Images show maximum intensity projections of 30µm deep stacks. Scale bars represent 20µm. (E) Mean velocity (n=3-8 animals per timepoint; mean+SEM; µm per day) of migrating cells. (F) Maximum migration distance (n=3-8 animals per timepoint) of migrating cells (for detailed statistical evaluation see chapter 9.1).

3.1.3 The injury-induced proliferative behavior of NG2-glia

Even though proliferation of NG2-glia already appeared at 2dpi, it represented a rather late response following injury with its peak at 4dpi. Thereafter the percentage of dividing cells declined and reached control levels already between 8 and 11dpi (Figure 8G). Even if no cell could be

detected that proliferated twice at two distinct timepoints (0 out of 72 dividing cells at all timepoints analyzed; Figure 12D), some NG2-glia (especially in close proximity to the injury core) underwent more than one round of cell division between 2 and 4dpi because they resulted in 3 cells as progeny (2 out of 72 proliferating cells from 6 animals; Figure 12E). Moreover, the massive increase of NG2-glia within and in very close proximity to the injury core between two consecutive timepoints (e.g. Figure 15B) argued for repetitive cell division of those cells. However, migration was also contributing to this accumulation. For cells in close proximity and directly within the lesion core it was in most cases not possible to re-identify them at later timepoints due to the high cellular density and reactivity in this region. Nonetheless, none of the analyzed NG2-glia in the periphery of the lesion did proliferate more than once after brain injury. As expected for self-repulsive cells following cell division, the majority of daughter cells started to polarize in opposite directions (Figure 12A and B). Another explanation could be that the processes of the mother cell are distributed during cell division to both daughter cells according to their position on the cell surface. However, also proliferative events with both progenies orientating approximately toward the same area (polarized toward the quadrant comprising the PWI; 5 out of 72 cell divisions; example Figure 12C) could be seen. Also the degree of migration of daughter cells after proliferation was quite variable, with some progeny migrating away from each other and others staying in close proximity during the subsequent timepoints (Figure 12). As the proliferation of NG2-glia peaked at 4dpi, the behavior-specific clustering was not performed at 2dpi due to the low number of cells which proliferated until 2dpi. Therefore, the proliferative cells at 4dpi were clustered according to their preceding reactivity at 2dpi. Cells undergoing cell division later on were more likely to be hypertrophic than non-hypertrophic at the preceding timepoint (63±6% and 14±6%; Figure 12D), whereas polarization and migration seemed to be rather independent of consecutive proliferation (Figure 12D).

Overall these results could demonstrate that the increase in NG2-glia number during the first phase after injury descended from directional migration and enhanced proliferation, whereas repetitive cell divisions were rather restricted to the injury core. Moreover, no increase in cell death of NG2-glia was observed at those early timepoints.

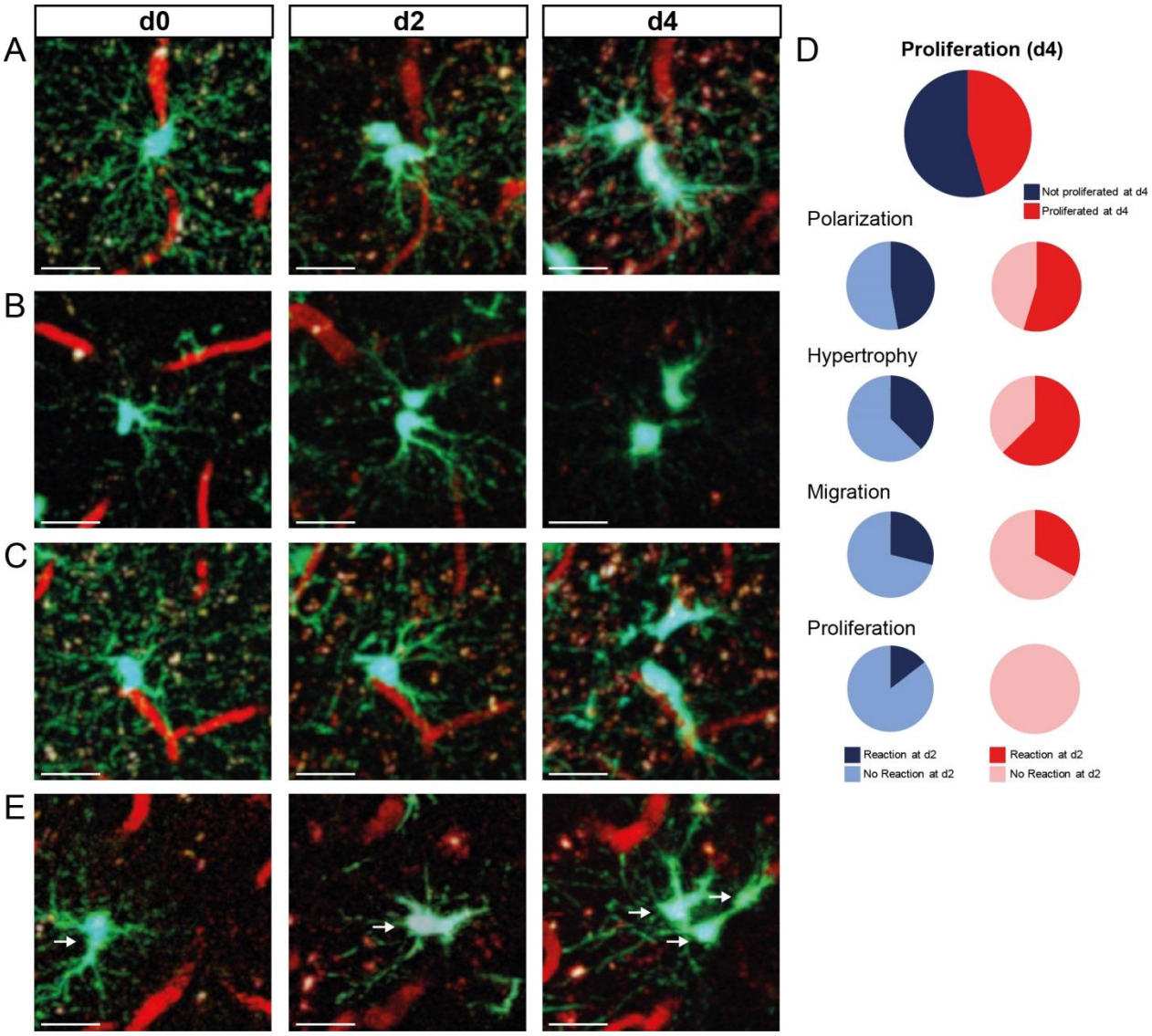

Figure 12 Examples of proliferating NG2-glia and their further reaction. (A-C) NG2-glia dividing at 2dpi mostly remain close to each other at 4dpi and partially polarize to opposite directions. (D) Proportion of cells that proliferated (red) or not (blue) at 2dpi and their further reaction at 4dpi (n=6 animals; mean; unpaired t-test: Polarization: p=0.2748; Hypertrophy: p=0.0123; Migration: p=0.6477). (E) Migrating NG2-glia (white arrows) proliferating twice between 2 and 4dpi. Images show maximum intensity projections of 30 (A, C) or 24 (B) µm deep stacks. Scale bars represent 20µm.

3.1.4 Influence of direct blood vessel contact on NG2-glia behavior

To assess if close contact to blood vessels influences NG2-glia behavior after injury the co-labelling of blood vessels was included in the analysis. Even if all NG2-glia have most likely some processes or filopodia in very close or direct contact to a blood vessel, only a subgroup of cells were in direct proximity to a vessel with their cell soma (Figure 13A). Due to active migration of NG2-glia it was of interest whether the cells showed a preferential movement toward the vessels or even away from them following acute injury. Therefore, the direct contact of NG2-glia to the blood vessels was assessed at several timepoints after TBI as well as under control conditions. As the percentage of NG2-glia in direct contact to the vessels was around 30% at all analyzed timepoints, no preferential movement, neither towards nor away from the blood vessels, was evident. A slight increase could be observed between 0 and 2dpi (30±3% vs. 36±4%), but this increase was not significant (Figure 13B). Due to the high variation between animals and the low animal number it cannot be excluded that there could be a slight preference of NG2-glia to get closer to vessels following an acute injury. However, this tendency would be relatively small. To further investigate if the cells in close proximity to the vessels are a subclass of NG2-glia with distinct response mechanisms after injury, the cells were sorted according to their direct blood vessel contact at 0dpi and their reaction to the injury at 2dpi was analyzed. The vast majority of cells with direct contact to the vessels also maintained this contact at the consecutive timepoint (89±4%), whereas just a minority migrated away from the vessels (11±4%; Figure 13C). Along the same line, from the cells with no direct contact only 15±5% moved their cell body in close contact to a blood vessel, whereas 85±5% of NG2-glia did not come in close proximity the vasculature. Regarding the possibility of different subclasses of NG2-glia with or without direct contact to vessels, no strong alterations of the general injury response could be observed in any of the analyzed behavioral categories (Figure 13C). Therefore, in contrast to the juxtavascular astrocytes with their preferential proliferation after injury, no such subset of NG2-glia seems to exist.

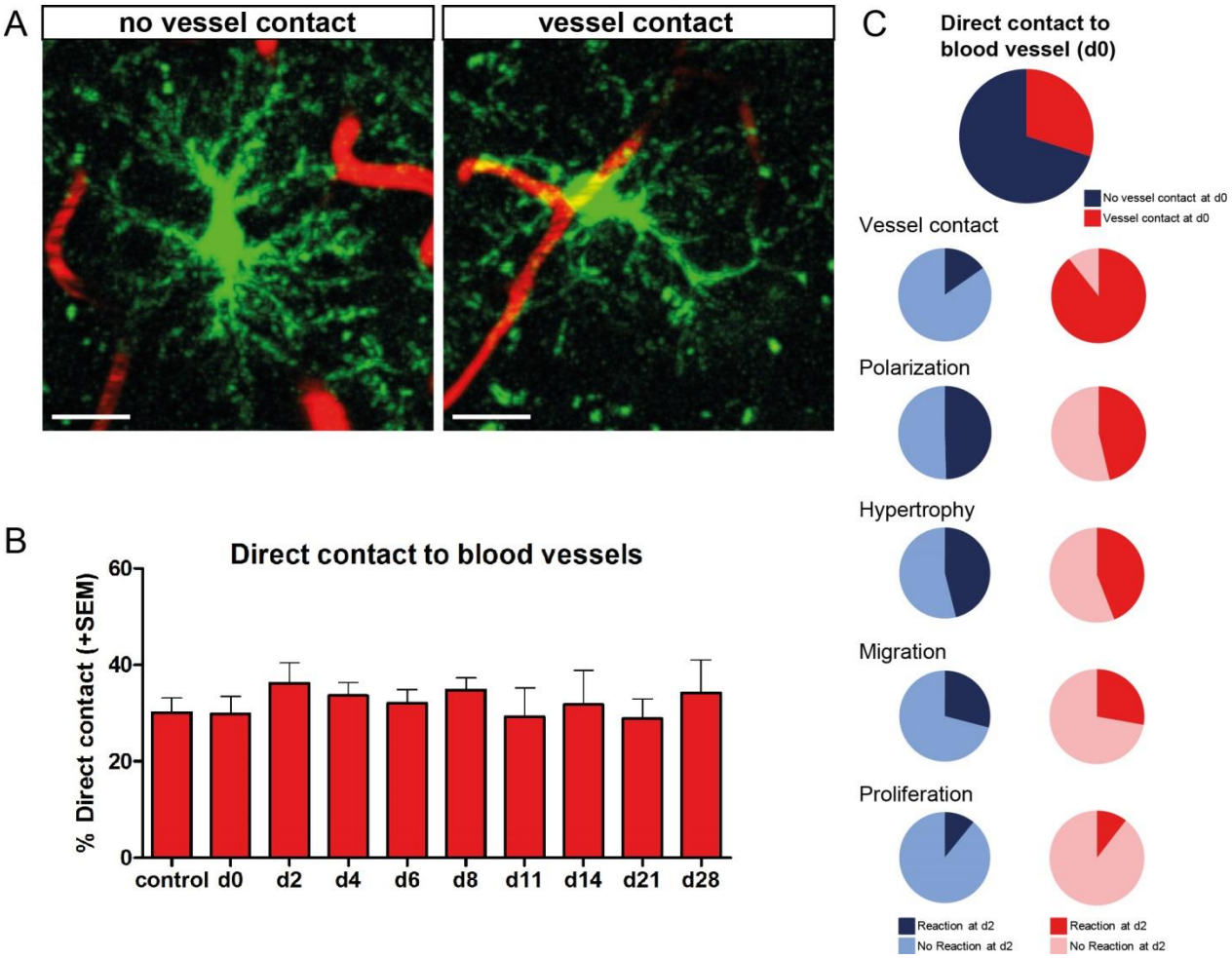

Figure 13 NG2-glia with direct contact to blood vessels. (A) Example of two NG2-glia with direct or no direct contact to a blood vessel. (B) Graph depicts the percentage (mean+SEM) of NG2-glia being in direct contact to blood vessels between 0 and 28dpi as well as under control conditions without lesion (n=9 animals for d4, n=8 for d0 and d2, n=4 for d6, d8 and d21, n=3 for all other timepoints; ~20-30 cells per animal). (C) Proportion of cells that had direct (red) or no direct contact to blood vessels (blue) at 0dpi and their further reaction at 2dpi (n=6 animals). Images (A) show maximum intensity projections of 20µm deep stacks. Scale bars represent 20µm.

3.2 NG2-glia response in relation to injury size and distance to the injury

3.2.1 Increasing injury size reduces static cells

As stated previously, approximately one quarter of the analyzed NG2-glia did not show any detectable cellular response upon PWI (Figure 6E and F). This posed the question if a subpopulation of quiescent NG2-glia exists that does not respond after injury or if the relatively small PWI did not provide sufficient cues for activation of all surrounding NG2-glia. Therefore, a larger stab wound injury (SWI; ~1mm in length; Figure 14B and B' and Figure 15D-F) was performed and the resulting NG2-glia response was then compared with the smaller PWI (~100µm

in length; Figure 14A and A'). Indeed, after SWI a decreased amount of static NG2-glia at 2dpi could be observed (13±2% vs. 26±5% after PWI; Figure 6E and Figure 14D). Comparison of the different reaction categories at 2dpi showed a slight increase in hypertrophy, migration and proliferation of NG2-glia, however this effect was not significant due to high variation within the experimental groups (Figure 14C).

3.2.2 Cells close to the injury show the strongest reaction

Another property related to the concentration of injury-released stimuli is the distance to the lesion site. Due to an augmented diluting effect with increasing distance in the parenchyma, one would expect far off cells to be less responsive compared with cells close to the injury core. Indeed, when the reaction of NG2-glia was analyzed in relation to their distance to the lesion core, a positive correlation between the strength of the reaction and the distance could be detected (Figure 14E-G), with cells showing a stronger response within 200µm of the lesion site at 2dpi than further distant NG2-glia (Figure 14F). This strong correlation decreased at 4dpi with only the proportion of polarization and migration of NG2-glia maintaining slightly elevated levels within the first 150µm compared with cells further away from the injury core (Figure 14E). In contrast to all other reaction categories, the proportion of proliferating NG2-glia showed no dependency on the distance to the injury within the analyzed area at 2 and 4dpi (Figure 14E and F). Nonetheless, NG2-glia in close proximity proliferated slightly more than cells further away and also proliferation rates decreased to physiological levels when the distance to the injury was big enough (data not shown). Comparing cells closer to the dura mater (visualized via second harmonic signal) to cells deeper in the tissue also revealed a stronger reaction of cells closer to the brain surface (data not shown). This also points to a non-negligible influence of the stimuli released in the injury core on NG2-glia behavior due to larger tissue damage (lancet-shaped knife) and heavier bleeding on the brain surface.

Taken together, these results revealed a general ability of the total NG2-glia population to respond after injury if their threshold is reached by the stimuli released from the lesion site. However, as proliferation showed less dependency on the distance to the injury, with the exception of the highly reactive cells directly in the lesion core, triggering cell division of NG2-glia seems less influenced by the cues released after injury.

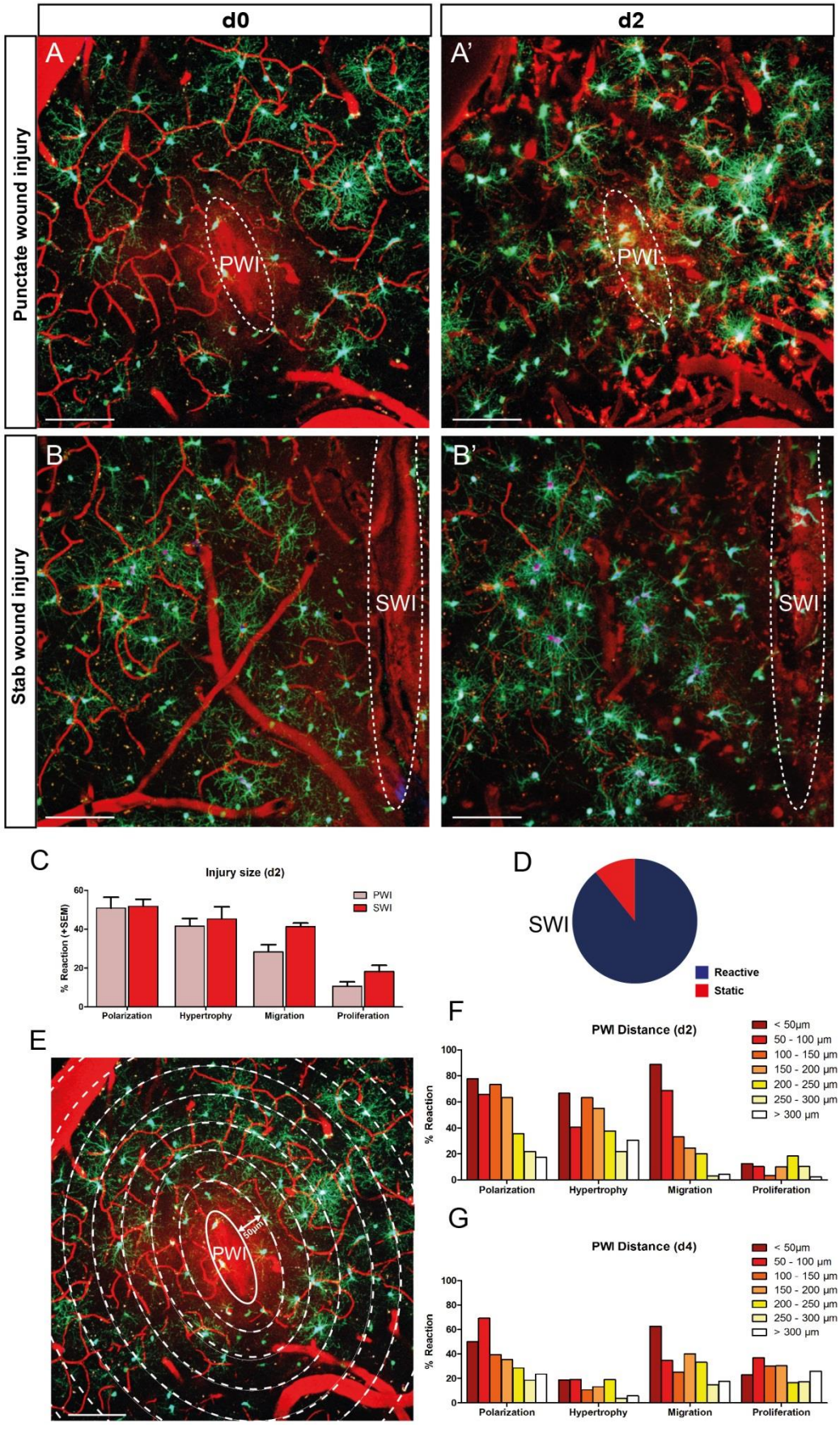
d0
d2
A
A'
Punctate wound injury
PWI
PWI
B
B'
Stab wound injury
SWI
SWI
C
Injury size (d2)
% Reaction (+SEM)
PWI
SWI
Polarization
Hypertrophy
Migration
Proliferation
D
SWI
Reactive
Static
E
PWI
50µm
F
PWI Distance (d2)
% Reaction
< 50µm
50 - 100 µm
100 - 150 µm
150 - 200 µm
200 - 250 µm
250 - 300 µm
> 300 µm
Polarization
Hypertrophy
Migration
Proliferation
G
PWI Distance (d4)
% Reaction
Polarization
Hypertrophy
Migration
Proliferation

Figure 14 The degree of NG2-glia reaction depends on the size and proximity to the injury. (A, B) Images of the NG2-glia reaction between d0 and d2 after PWI (A, A´) and the bigger stab wound injury (SWI) (B, B´). (C) NG2-glia show a stronger reaction after SWI compared to PWI (mean+SEM; n=8 mice for PWI and n=3 mice for SWI) (D) with a lower percentage of static cells at 2dpi (compare to Fig. 6E). (E-G) Cells in closer proximity to the injury show increased reactivity compared to the ones further away from the lesion core at d2 (E, F) while this difference was less pronounced at 4dpi (G, polarization represents cells directed toward the injury; n=220 cells from 8 animals at d2 and n=180 cells from 6 animals at d4). Images show maximum intensity projections of 30µm deep stacks. Scale bars represent 100µm.

3.3 NG2-glia fill the injury core

As the intensity of the NG2-glia response correlated with the proximity of the cells to the lesion core, NG2-glia in the lesion core or in direct proximity (~50µm) to the lesion displayed the strongest reaction. The reaction of these lesion-core NG2-glia were too intense in the majority of cases and even within the first 2dpi (Figure 15A and A') to trace those cells over time. The accumulation of cells in this area exacerbated the re-identification of some cells at later timepoints. Due to these difficulties just 20 cells from 7 animals were traceable between 0 and 4dpi. All of those traceable NG2-glia located within the lesion core showed a response behavior until 2dpi (Figure 15B and C) mainly with high levels of hypertrophy, migration and proliferation. Polarization, which was still observed at 2dpi (29%) could not be detected any more at 4dpi because the cells located in the core of the lesion developed rather bulky, hypertrophic shapes with no clear orientation of cell soma or processes (Figure 15B). It is worth mentioning, that the observed preference of NG2-glia to orientate themselves towards the injury site would rather be redundant for cells which are already located in the lesion center. Intriguingly, no cell, even considering the non-analyzable cells, in very close proximity to the injured area could be observed which showed a static behavior (Figure 15C). Even if individual cells could not be clearly re-identified at the consecutive timepoints, it can be stated, that the cells are not at their previous position any more, therefore arguing for a response of all these cells. This further emphasizes the general ability of NG2-glia to react to the events following brain injury if they receive enough input to trigger their response.

In contrast to the very fast accumulation of NG2-glia in the injury core of a PWI already after 2dpi (Figure 15A'), NG2-glia needed longer to fill up the larger lesion area after a SWI (4 days; Figure 15D-F).

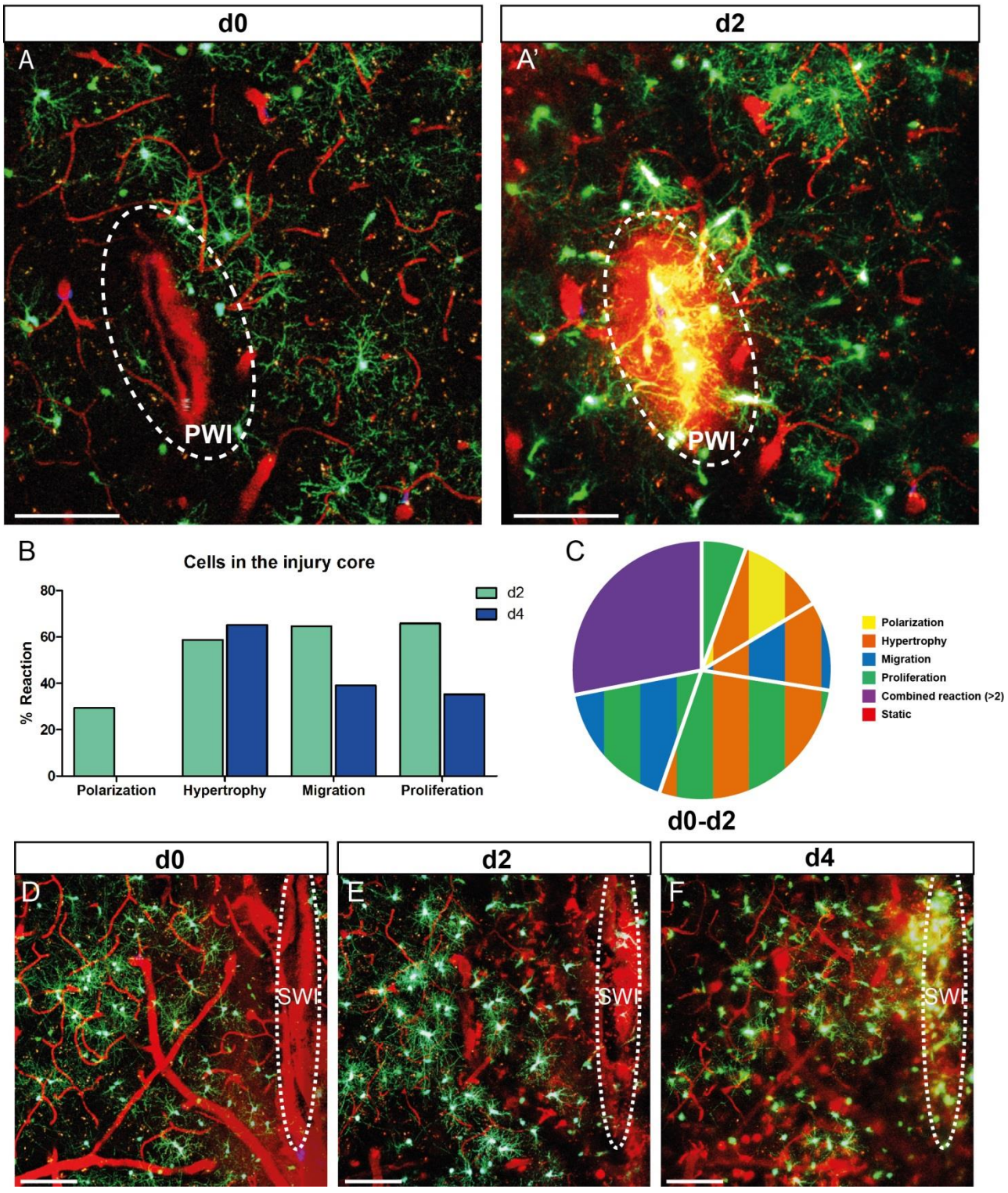

Figure 15 NG2-glia fill the injury core. (A) Images of GFP$^+$ cells at d0 (A) and d2 (A´) after PWI. Dotted circle indicates the core of the injury that corresponds to the analyzed area. (B) Graph showing a very high reactivity of NG2-glia for all criteria (except polarization) at d2 and d4 after injury (Polarization represents cells directed toward the injury; n=20 cells from 7 animals for d0, n=34 cells due to proliferation from 7 animals for d2 and n=23 cells from 4 animals at d4). (C) Pie chart of the heterogeneous reaction between 0 and 2dpi of NG2-glia showing no static cells (n=18 cells from 7 animals). Images show maximum intensity projections of 20µm deep stacks. Scale bars represent 100µm. (D-F) Images of 0, 2 and 4 days after SWI showing NG2-glia only filling up the injury core at 4dpi. White ellipse represents the injury site. Images show maximum intensity projections of 30µm. Scale bars represent 100µm.

3.4 NG2-glia number return to physiological levels one month after injury

Following the intense response until 4dpi, NG2-glia reactivity started to decline. At later timepoints, NG2-glia began to slowly diminish in number and by 28dpi the area around the lesion core resembled an uninjured region in terms of morphology and distribution of NG2-glia. This could be shown with *in-vivo* imaging of the smaller PWI (Figure 8C) and with immunohistochemistry of the larger SWI (Figure 16). Therefore, the cell number of $NG2^+$ and GFP^+ cells in the SW injured Sox10-iCreER^{T2} x CAG-eGFP mice receiving the maximal induction rate (3x gavaging with 40µg/ml tamoxifen resulting in a very high recombination rate) were analyzed. The analyzed area spanning 50µm around the lesion core (visualized with a GFAP staining) showed a slight increase of $NG2^+$ (from 331±32 to 437±19 cells/mm^2) and GFP^+ (from 451±49 to 533±34 cells/mm^2) cells compared with the non-injured control situation already after 2dpi (Figure 16A and F). Also in line with the observed migration behavior and the peak of proliferation at 4dpi, the cell numbers roughly doubled at 4dpi for GFP^+ cells (from 451±49 to 781±74 cells/mm^2) and $NG2^+$ cells (from 331±32 to 812±100 cells/mm^2; Figure 16A, B and F). Interestingly, at 7dpi GFP^+ cells still slightly increased in number (from 781±74 to 825±60 cells/mm^2), whereas $NG2^+$ cells already started to decrease at this timepoint (from 812±100 to 670±156 cells/mm^2; Figure 16B, C and F). At 14dpi also GFP^+ cell numbers started to decrease (from 825±60 to 699±62 cells/mm^2) and $NG2^+$ cells decreased even further (from 670±156 to 441±41 cells/mm^2; Figure 16D and F). Like mentioned earlier, GFP^+ and $NG2^+$ cell numbers were comparable to control levels at 28dpi (GFP: 451±49 vs. 457±44 cells/mm^2; NG2: 331±32 vs. 316±15 cells/mm^2; Figure 16E and F).

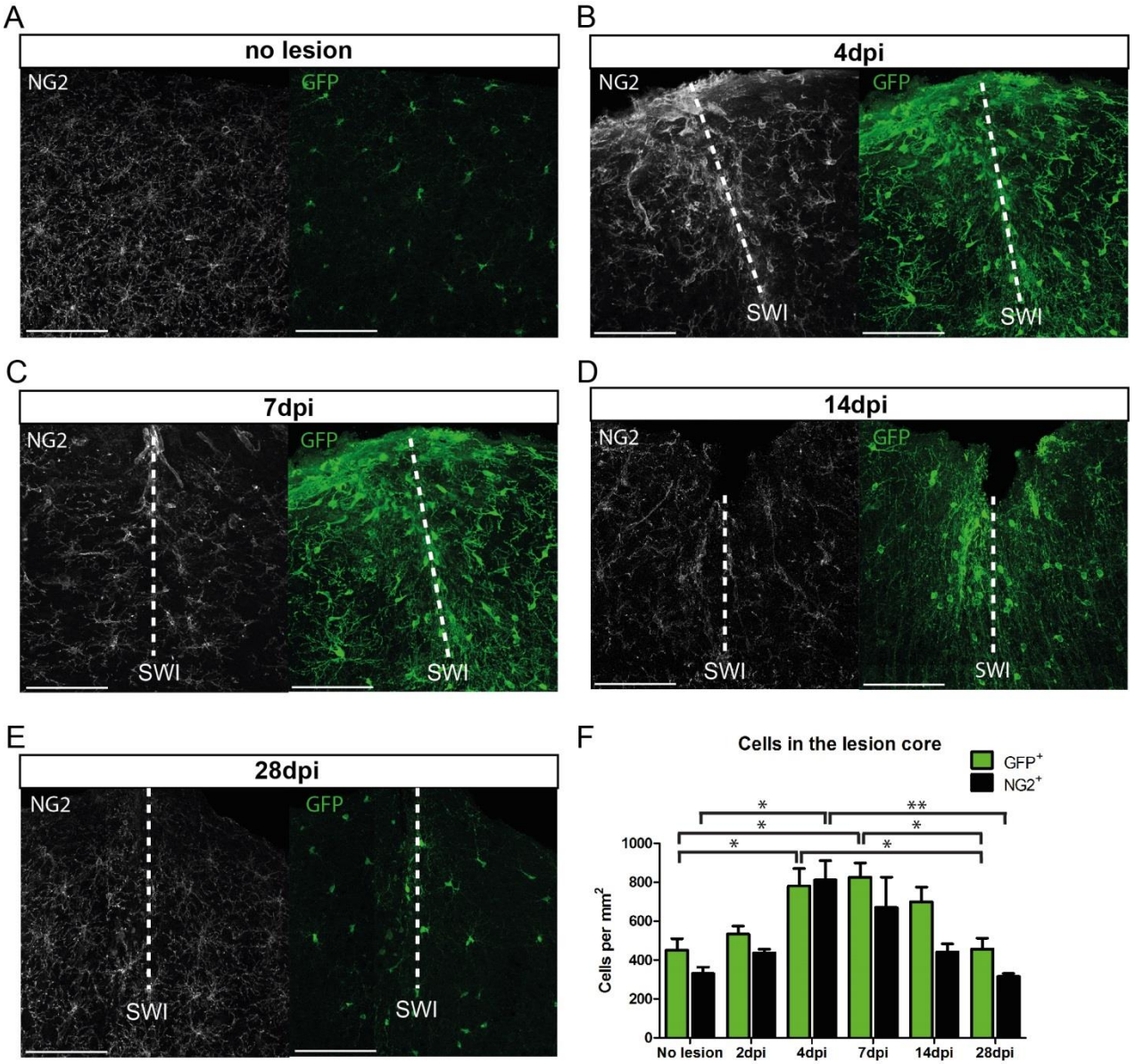

Figure 16 Number of NG2+ cells in the injury core over time. (A-E) Confocal images of NG2$^+$ and GFP$^+$ cells at 4 (B), 7 (C), 14 (D), and 28 (E) days after SWI as well as a non-lesioned area (A) demonstrating the accumulation of NG2-glia between 4 and 7dpi and the decrease of cell number until 28dpi. (F) Cell counts of NG2$^+$ cells per mm^2 in the injury core (and in 50µm surrounding; 1way ANOVA+Tukey post-test: ** indicates significance of $p<0.001$ and * for $p<0.05$; dF=17). Images for the 4dpi timepoint were kindly provided by Sarah Schneider. Images show maximum intensity projections of 10µm. Scale bars represent 100µm.

As described above, the NG2-glia numbers in and around the injury core reached their maximum between 4 and 7 days and decreased thereafter, analyzed by post-mortem still analysis. Visualizing NG2-glia via live imaging made it possible to follow this cellular decrease over time. Especially within the core cells started already to disappear between 4 and 6dpi (two cells of the five cells marked with a yellow arrows; Figure 17A and B). In some of those cases it was not possible to reliably identify which specific cells disappeared because NG2-glia are motile and due to their close proximity it could not be excluded that they took the position of a neighboring cell, while this cell disappeared. Therefore it could solely be stated that from the group of cells in close proximity to each other some were lost at the consecutive timepoint and thus the number of cells in that area decreased. As there were still high levels of cell division and migration at 6dpi (see Figure 8G) the total cell numbers were still at a relative high level around that timepoint (7dpi; Figure 16F). Between 6 and 8dpi another 3 cells disappeared (yellow arrows; Figure 17B and C). Therefore the majority of cells which were located directly in the core of the injury vanished already between 4 and 8dpi (Figure 17A-C). Comparing these results with the data obtained with immunohistochemistry (see Figure 16) the disappearance of cells seemed to be shifted toward an earlier timepoint. One possible explanation could result from the smaller injury type (PWI vs. SWI) and therefore a reduced recovery time. Between 8 and 11dpi, only one more cell disappeared in the periphery (yellow arrow; Figure 17C and D). From 11dpi onwards, the cells re-orientated themselves but major cell disappearance could not been detected (Figure 17D-G). At 21dpi the cellular distribution and morphology already started to resemble the physiological condition (Figure 17G).

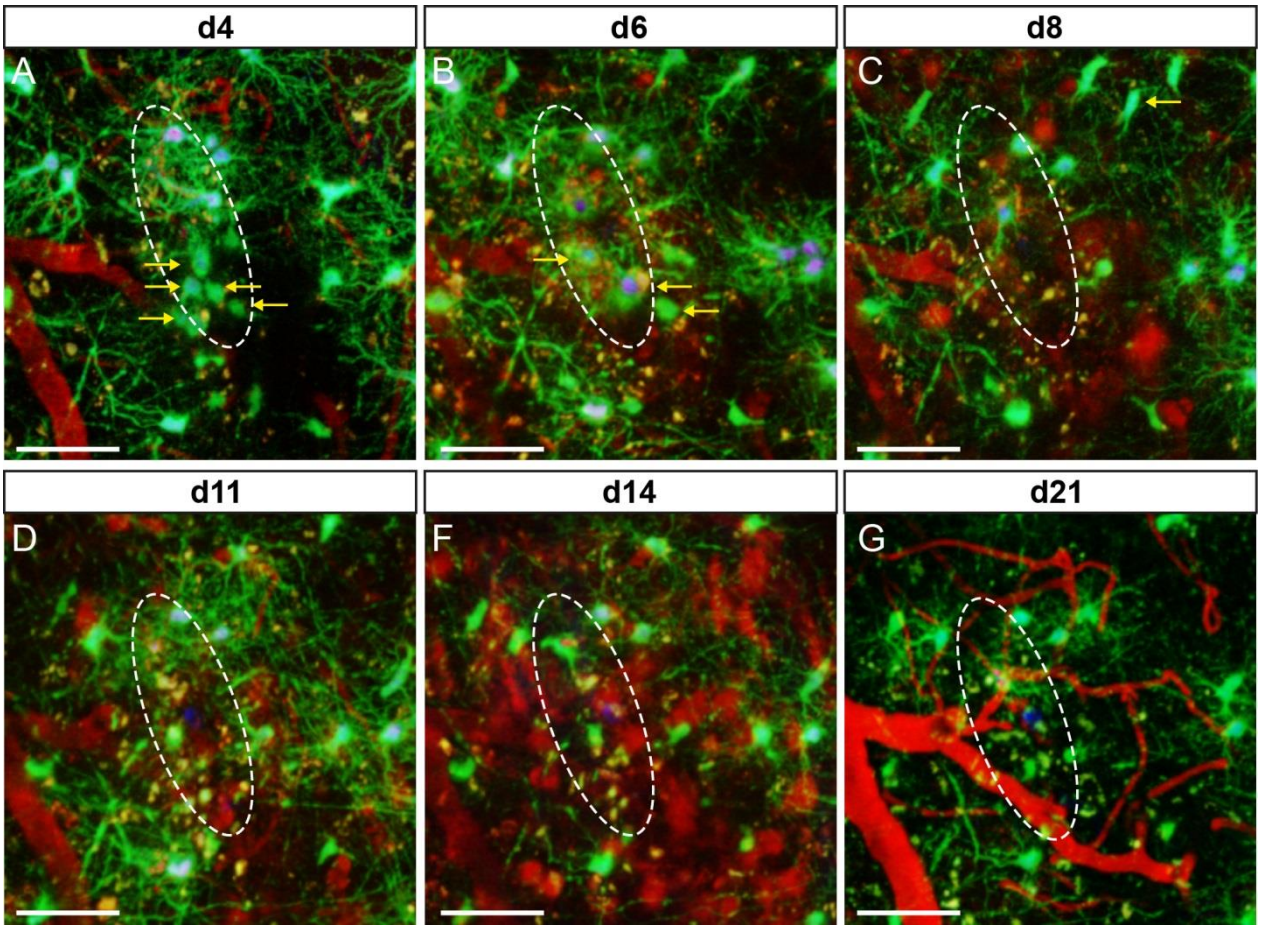

Figure 17 Cells disappearing from the injury core over time. (A-G) Images of GFP^{+} cells of a Sox10-iCreER^{T2} x eGFP animal in and around the injury core (white, dotted ellipse) at 4 (A), 6 (B), 8 (C), 11 (D), 14 (F) and 21dpi (G). Cells disappearing at later timepoints are marked with yellow arrows. Images show maximum intensity projections of 40µm. Scale bars represent 50µm.

Due to the occurrence of cell division after 4dpi, when other cells have already started to disappear (see Figure 17A and B), it posed the question about the fate of the progeny of these late cell divisions. Even if proliferation levels were decreasing to almost physiological levels after 6dpi, there was still some "late" proliferation (6dpi-28dpi) occurring, especially between 4 and 6dpi (see also Figure 8G). Therefore 20 of those late proliferating cells from 3 animals were analyzed for a period of at least 15 and maximal 22 days post proliferation (dpp; Figure 18A and B). As total cell number was decreasing it is also very likely that not all progeny survived after cell division. Analysis of the progeny after late proliferation, showed that in 35±7% of the analyzed cell divisions just one cell survived whereas in 65±7% both progeny survived (Figure 18B). Interestingly, it was never observed that both daughter cells disappeared. Therefore, the majority of cell divisions produced two viable daughter cells, at least surviving for the analyzed time window (example: upper panel of Figure 18A). Nevertheless, the large amount of cell divisions with only one daughter

cell surviving (example: lower panel of Figure 18B) raised the question for the purpose of these cell divisions. The timing of the observed cell deaths was either relatively short after proliferation (between 2 and 5dpp) or at a later phase (between 10 and 15dpp), whereas the longest timepoints (20-22dpp) showed no more disappearance of progeny (Figure 18C), suggesting a critical time window for the survival of NG2-glia progeny.

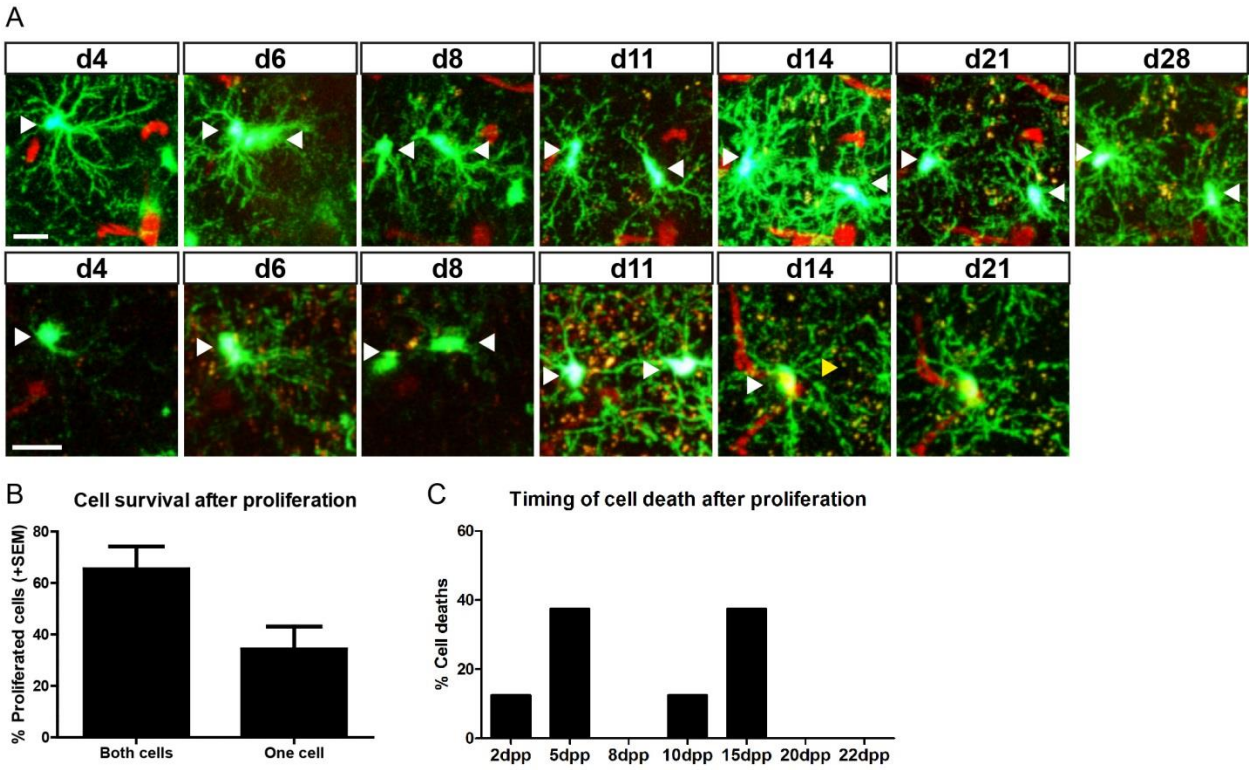

Figure 18 Cell survival after late cell division. (A) Images of "late" proliferating NG2-glia (after d4) of Sox10-iCreER^{T2} x eGFP animals between 4 and 28dpi. Upper panel showing a cell division followed by the survival of both daughter cells (white arrowheads). Lower panel showing a proliferation with the subsequent death of one progeny (yellow arrowhead), whereas the other one survives (white arrowhead). (B) Percentages of cell survival after cell divisions (survival of one or both daughter cells respectively). (C) Timing of cell death after proliferation (dpp=days post proliferation). Images show maximum intensity projections of 30µm. Scale bars represent 20µm.

3.5 Potential differentiation of NG2-glia following tissue damage

A cellular event which is expected to occur at later stages after brain lesion is the differentiation of NG2-glia into mature oligodendrocytes. This is primarily the case in pathologic events like demyelination, when mature oligodendrocytes undergo cell death and thus have to be replaced by the pool of oligodendrocyte progenitors. Nevertheless, also after injuries without any specific demyelination effect, cell death occurs and potentially lost oligodendrocytes could be replaced. Therefore, the morphological changes of NG2-glia during the later phases after PWI were assessed. Even if morphological criteria are not enough to successfully prove differentiation, they

could give a first hint to which extent differentiation of NG2-glia after TBI might occur. Therefore 112 cells in 3 animals were followed from 4dpi until a minimum of 3 weeks after injury. In total 15±2% of the analyzed cells developed an oligodendrocyte-like morphology (examples: yellow arrowheads in Figure 19A and B), whereas 85±2% kept their NG2-glia-like morphology (Figure 19C). Interestingly, those morphological changes were only observed after cell division (white arrowheads; Figure 19A and B). Therefore a small proportion of cells might potentially undergo differentiation following traumatic brain injury. However, whether these cells are really differentiating, actively myelinating and integrating into the persisting network remains to be determined.

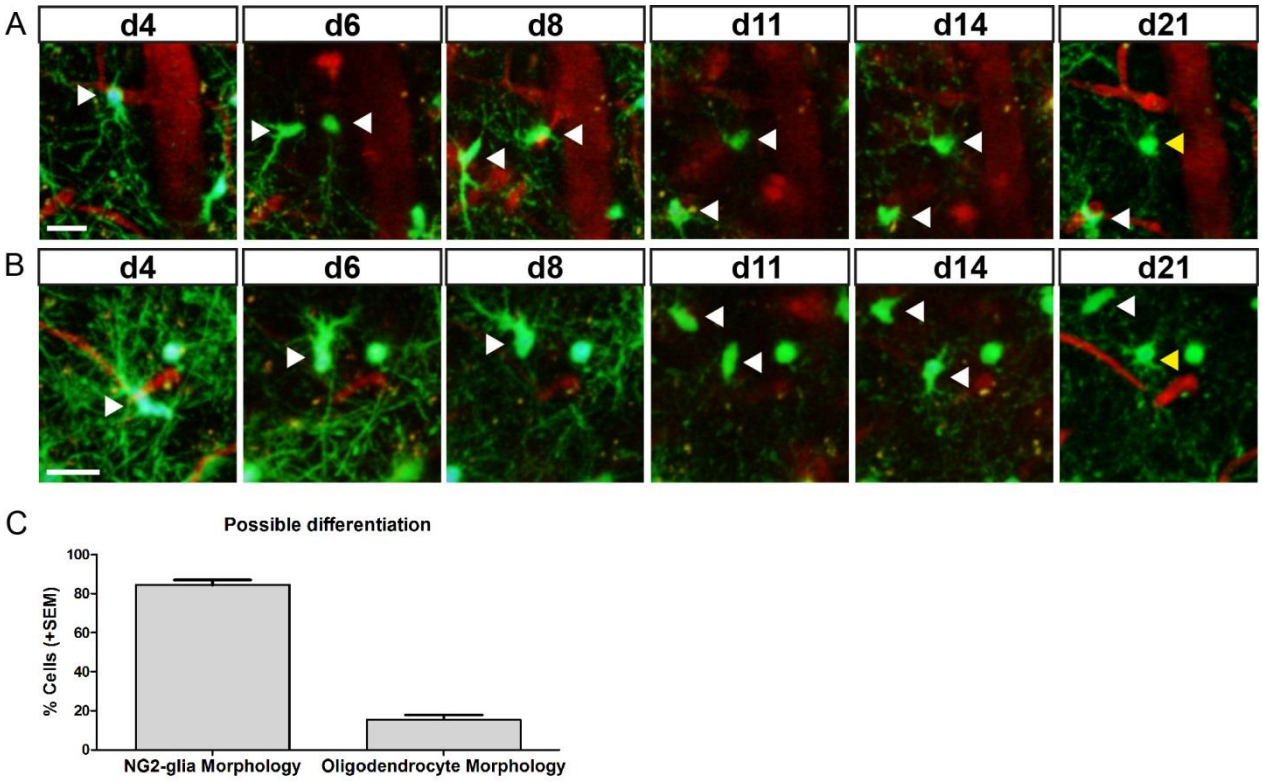

Figure 19 Potential differentiation of NG2-glia following PWI. (A and B) Examples of NG2-glia developing an oligodendrocyte-like morphology between 14 and 21dpi (yellow arrowheads) after previous cell division (white arrowheads). (C) Quantification of NG2-glia with NG2-glia or Oligodendrocyte morphology of cells, followed at the later timepoints (4-28 dpi) after brain injury, at the latest timepoint analyzed (21, 27 or 28 dpi; mean+SEM% of cells; n=3 animals). Scale bars represent 20µm.

3.6 Attempts to alter the NG2-glia response following injury

To further access the mechanistical insight underlying NG2-glia reactivity after brain injury two different approaches were used to specifically manipulate gene expression in NG2-glia (specific

deletion of cdc42 and NG2) and analyze the resulting behavior of those cells after PWI using repetitive live *in vivo* imaging.

3.6.1 The effect of the Rho GTPase cdc42 on the NG2-glia response after brain injury

The first approach targeted the Rho GTPase cdc42 that is suggested to be involved in migration and polarization of different cell types. Therefore, cdc42$^{fl/fl}$ mice were crossed with Sox10-iCreER^{T2} x eGFP mice, resulting in the deletion of cdc42 in cells of the oligodendrocyte lineage after recombination with tamoxifen in adult animals. Unfortunately, all experimental mice displayed a nervous behavior during animal handling, rendering an adequate anesthesia more difficult. Therefore heavy breathing artefacts, which unfortunately could not be avoided, derogated the image quality (Figure 20A-C and A'-C'). Nevertheless, the cellular behavior categories comprising polarization, hypertrophy, migration and proliferation could be analyzed with some reservations. As there is no working antibody for cdc42 and the stability of the protein in NG2-glia is not known the analysis was performed in animals at a longer time (4 months) beside the 1 month timepoint which was based on previous studies with astrocytes. The cellular response of NG2-glia at the 4 months timepoint (long term; LT; Figure 20A-C) was then compared with the original setting of a 1 month interval after induction (short term; ST; Figure 20D and E). In mice with ST recombination NG2-glia responded to a PWI within a short time window (0-2dpi) with hypertrophy, polarization, migration (white arrows in Figure 20A-C) and proliferation (Figure 20A, B; examples of migrating and proliferating cells Figure 20A'-C'). This reactive behavior was also maintained until 4dpi (Figure 20C). However, due to the heavy breathing artifacts, clear analysis about migration distance and velocity could not be performed. As no obvious difference in the reactivity could be detected between the two experimental groups with altered recombination periods (ST vs. LT; Figure 20D and E), the results were pooled and compared to the WT control, for which Sox10-iCreER^{T2} x eGFP animals were used (Figure 20F and G). Beside a non-significant augmentation of hypertrophy at 2dpi (55±12 vs. 42±4 % of analyzed cells) the reactivity of NG2-glia lacking cdc42 were quite comparable to control NG2-glia (Figure 20F and G). Together with the accumulation of NG2-glia in the injury core, which was also comparable to the control situation (Figure 20 B and C), the general cellular reactivity of NG2-glia seemed to be not majorly affected by cell-specific deletion of cdc42.

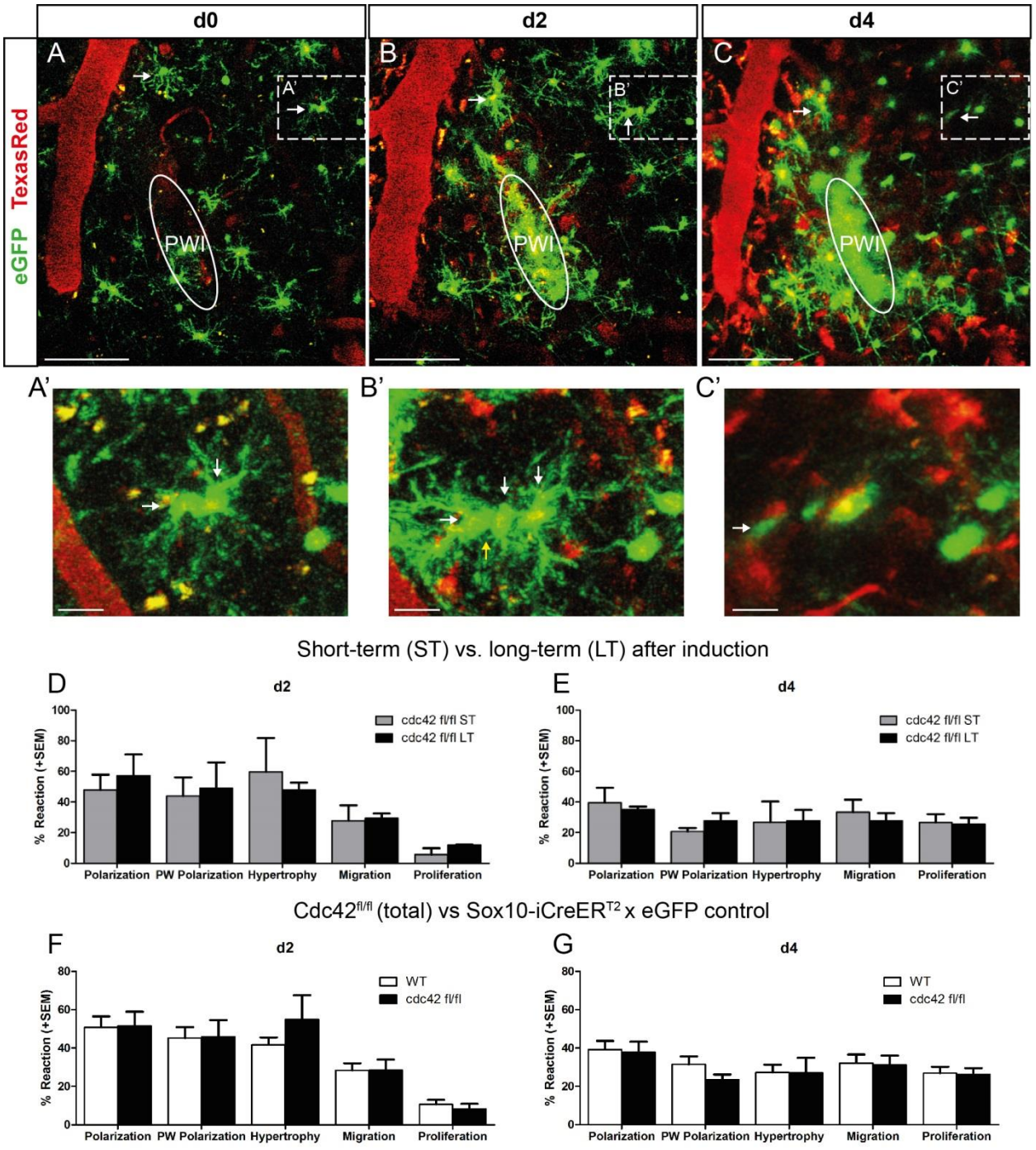

Figure 20 The effect of cdc42 on NG2-glia reaction. (A-C) Images of GFP-labelled cells of the oligodendrocyte lineage (green) and TexasRed labelled blood vessels (red) in cdc42$^{fl/fl}$ x Sox10-iCreERT2 x eGFP animals 4 months after induction at 0 (A), 2 (B) and 4 (C) days after PWI (single images; white arrows indicate migrating and proliferating cells, scale bars represent 100µm). (A'-C') Examples for cells (higher magnifications from A-C) showing migration (white arrows) and proliferation (yellow arrow; images show a maximum intensity projection of 26µm deep stacks; scale bars represent 20µm). (D, E) Comparison of reaction profiles from NG2-glia 1 month (ST) and 4 months (LT) after induction at 2 (mean+SEM; D) and 4dpi (mean+SEM; E). (F, G) Reaction profiles from NG2-glia of pooled cdc42 deficient animals compared to control cells of Sox10-iCreER^{T2} x eGFP animals at 2 (mean+SEM; F) and 4dpi (mean+SEM; G).

3.6.2 The effects of NG2-glia-specific deletion of the proteoglycan NG2 following TBI

The second approach to alter the NG2-glia response after injury targeted the proteoglycan NG2 itself, which was also linked to cell migration and polarization (see introduction). To further analyze possible effects of NG2 on NG2-glia, two different mouse-lines were used: the NG2-enhanced yellow fluorescent protein (EYFP) line (Karram et al., 2008) and the NG2-CreER^{T2} x CAG-eGFP line (Huang et al., 2014). In the NG2-EYFP "knockin" mouse line EYFP was expressed under the NG2-promotor and homozygous knockout mice lacked expression of NG2 (Karram et al., 2008). The NG2-CreER^{T2} x CAG-eGFP mouse line was based on the NG2-EYFP line comprising a substitution of EYFP with the open reading frame of CreER^{T2}, which was then crossed with an eGFP reporter line (Huang et al., 2014). Therefore recombination in homozygous animals led to cell specific eGFP expression. As already observed in the cdc42-deficient NG2-glia, also NG2-deficient NG2-glia showed a fast and heterogeneous response behavior after PWI, accumulating in the injury core already at 2dpi (Figure 21A-C). The cellular behavior included hypertrophy, polarization (white arrows; Figure 21A'), migration (white arrows; Figure 21A' and B') and proliferation (white arrows; Figure 21A-B and B') which was observed in all analyzed mouse lines. However, a strong increase of cells due to enhanced proliferation at 2dpi together with sparse repetitive cell division (also visible in Figure 21B') was detected in both mouse lines, however the proliferation in total (0-4dpi) was not significantly different from control animals. Beside the increase in proliferation already at 2dpi, the general reactivity was comparable to the Sox10-iCreER^{T2} x CAG-eGFP control animals (Figure 21D and E). Pooling the data from all NG2-knockout animals resulted in a significant shift to an earlier proliferation already at 2dpi (26±1 vs. 11±2%; Figure 21F) while the tendency of reduced hypertrophy at 2 (30±2% vs. 42±4%) and 4dpi (15±4% vs. 27±4%) as well as the slight decrease of proliferation at 4dpi was not significant (19±4% vs. 27±3%; Figure 21F and G). Interestingly, also the heterozygous animal showed a tendency for a time-shift in proliferation (Figure 21D and E). Overall, the NG2-glia response after injury in mice lacking NG2 was comparable to the control animals in terms of migration, the general cellular behavior and NG2-glia accumulation in the injury core. Nevertheless, small alterations of NG2-glia behavior after loss of NG2, especially concerning proliferation, cannot be excluded.

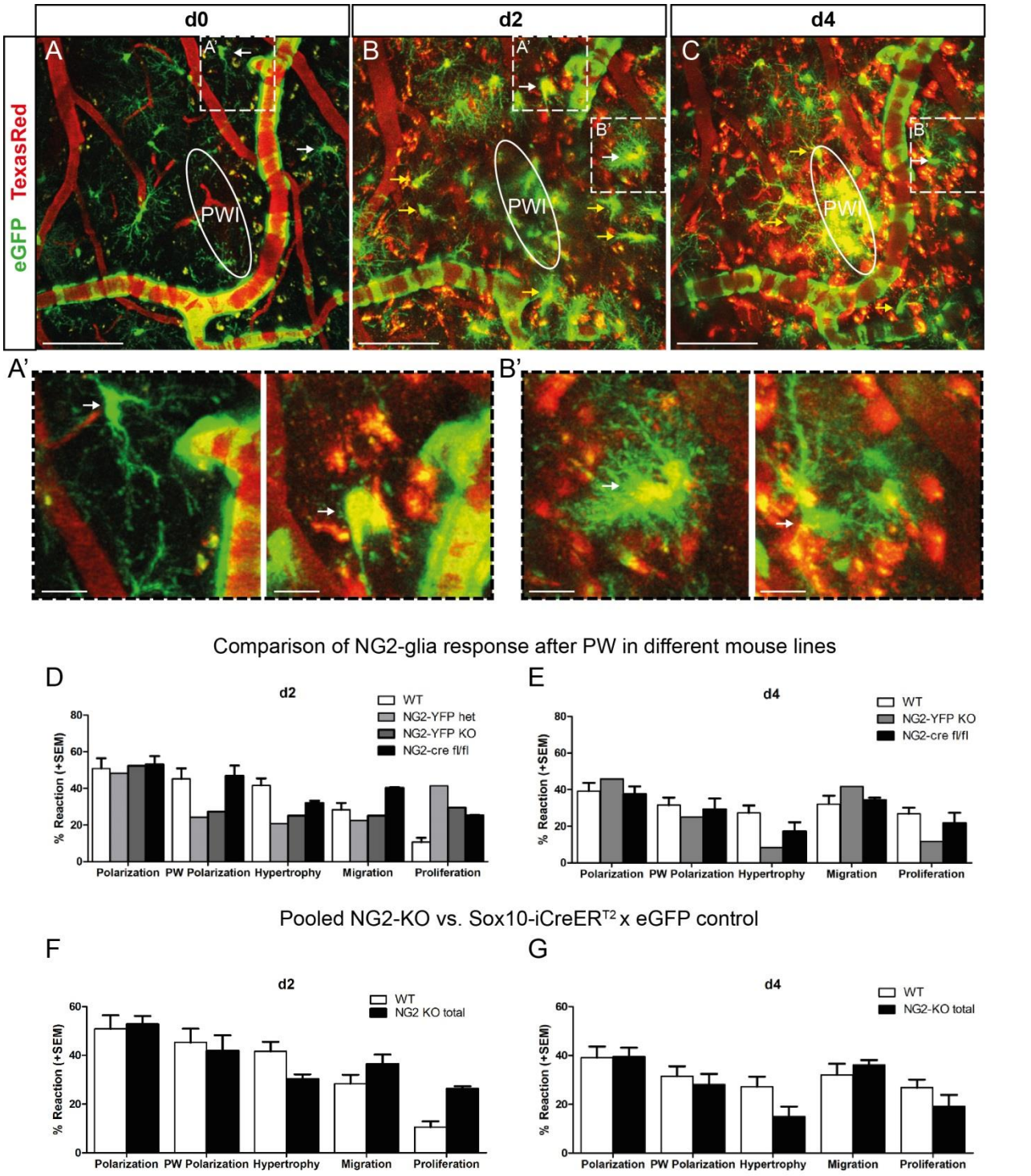

Figure 21 NG2 and its effect on NG2-glia reaction following injury. (A-C) Image stacks of GFP^{+} NG2-deficient NG2-glia and pericytes (green) and TexasRed labelled blood vessels (red) of NG2-cre animals at 0 (A), 2 (B) and 4dpi (C; white arrows indicate migrating cells; yellow arrows indicate polarized cells; images show maximum intensity projection of 20µm deep stacks; scale bar represents 100µm). (A' and B') Examples for cells (higher magnifications from A-C) showing migration and polarization (white arrow; A') and migration after proliferation (white arrow; B'; images show a maximum intensity projection of 22µm deep stacks; scale bars represent 20µm). (D, E) Comparison of NG2-glia responses in different mouse lines at 2dpi (mean+SEM; D) and 4dpi (mean+SEM; E). Reaction profiles of pooled NG2-KO animals compared to Sox10-iCreER^{T2} x eGFP control animals at 2dpi (mean+SEM; F) and 4dpi (mean+SEM; G).

4 Discussion

NG2-glia in the adult brain have gotten more and more into the focus of researchers since they were shown to be more than just progenitors for oligodendrocytes, but also associated with additional functions and interesting abilities (Vigano et al., 2013; Young et al., 2013; Dimou and Gallo, 2015). Amongst others, they have been shown to be the major proliferating cells in the healthy adult brain parenchyma (Dimou et al., 2008; Kang et al., 2010) and to react after acute or chronic injuries in the adult CNS (Levine and Reynolds, 1999; Hampton et al., 2004) with overexpression of the proteoglycan NG2 (Levine, 1994), morphological changes and increased cell division (Keirstead et al., 1998; Buffo et al., 2005; Zawadzka et al., 2010; Behrendt et al., 2013). The observed changes in proliferation rate are achieved by shortening of their cell cycle length and very likely via recruitment of more quiescent NG2-glia into the cell cycle (Simon et al., 2011). Also demyelination in postnatal forebrain slice cultures influenced NG2-glia proliferation and led to the acceleration of differentiation after evoked cell division (Hill et al., 2014). Along that line another recent study showed that after single cell ablation of NG2-glia with focal laser lesion, neighboring NG2-glia reacted relatively homogenously with proliferation and migration to replace the ablated cell (Hughes et al., 2013). However, if the proliferative and migratory response of NG2-glia is solely restricted to replacement of depleted NG2-glia also after a more extensive TBI has not yet been analyzed. Despite all these findings, many questions related to the response of NG2-glia to TBI remain unanswered. For example, it is not known if the demonstrated cellular homeostasis of NG2-glia is maintained during the acute phase of TBI, how long and to what extend the reactivity of NG2-glia remains and most importantly, what function this injury response might have. Furthermore, it is unknown if NG2-glia are enriched at the injury site, and if this enrichment is resulting from migration or proliferation. Therefore, repetitive *in vivo* 2-photon laser scanning microscopy after TBI in the somatosensory cortex of adult Sox10-iCreERT2 x CAG-eGFP mice was performed to study the detailed response behavior of NG2-glia. The subsequent analysis revealed that NG2-glia responded very fast following TBI (already observable at 2dpi) by hypertrophy, polarization and migration toward the injury, while proliferation as a later event, occurred mainly between 2 and 6dpi. Although the response behavior of NG2-glia is very heterogeneous and depends on the injury size and the distance to the injury, the majority of NG2-glia showed at least one of the defined reaction categories.

4.1 The impaired homeostatic control of NG2-glia after injury

Studying NG2-glia with *in vivo* imaging under physiological conditions demonstrated that they are evenly distributed within the cortex, building a dense cellular network with exclusive territories, which are maintained through self-repulsive behavior (Hughes et al., 2013). This homeostatic network is even preserved when NG2-glia differentiate or undergo apoptosis via proliferation and migration of neighboring NG2-glia replacing the missing cells and thereby keeping the cellular density constant (Hughes et al., 2013). However, analyzing the behavior of NG2-glia after a more intense TBI, massive proliferation and migration toward the lesion led to very high cell densities within and around the lesion core. This had the consequence, that NG2-glia get in very close proximity to each other and transiently overcome their homeostatic distribution. Those cells at the injury core responded with high levels of hypertrophy, migration and proliferation. As a result, a massive increase of NG2-glia number, exceeding NG2-glia in the periphery, occurred and despite their usual self-repulsive behavior those cells entered the territories of neighboring cells forming a dense cellular network (Figure 15). Finally, the cellular homeostasis together with the cellular density of NG2-glia is largely reestablished between 3 and 4 weeks after injury. This is achieved by reorientation of polarization and migration from NG2-glia beginning as early as one week following injury resulting in a progressive reduction of cell numbers with increasing post lesion times (Figure 8, Figure 16, Figure 17 and Figure 22). Also after Diphtheria Toxin induced depletion of NG2-glia in the GM of adult mice the cells were able to reestablish their cellular homeostasis within a month via increased proliferation of resident cells that escaped the depletion (Birey and Aguirre, 2015).

The change in proliferation behavior of NG2-glia does not seem to be a specific event only occurring after TBI but has also been seen in other diseases and injury models. NG2-glia in Alzheimer´s Disease (AD) mouse models (Behrendt et al., 2013) and in MS in human also show altered proliferation (Maeda et al., 2001; Cui et al., 2013), although the proliferative behavior varies between the different pathologies. In contrast to the increased density of NG2-glia after TBI and AD, NG2-glia number is strongly decreasing within some chronic demyelinating lesions in MS (Chang et al., 2002; Sim et al., 2002). This could possibly explain the failure of NG2-glia to counteract the demyelination process by eliciting a response mechanism leading to sufficient differentiation and replacement of missing oligodendrocytes in chronic MS lesions. All these different response behaviors of NG2-glia seem connected with an impaired NG2-glia homeostasis. However, these changes of NG2-glia homeostasis might be beneficial in terms of tissue integrity and wound closure after TBI or detrimental for regeneration after demyelinating events.

Therefore, it is essential to further investigate signals influencing or maintaining this homeostasis, to potentially improve therapies for pathological conditions.

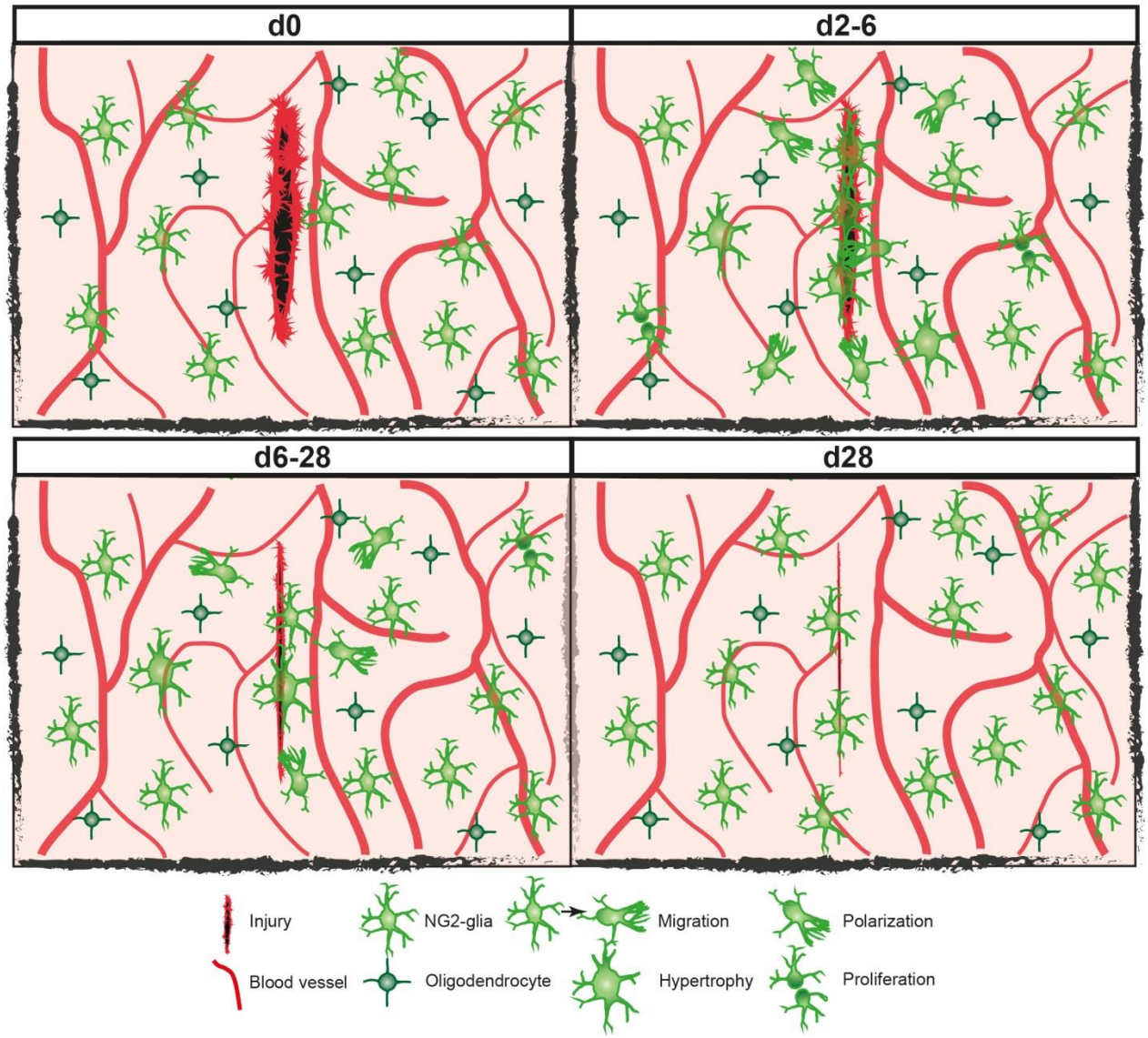

Figure 22 Schematic model of the reaction of NG2-glia at different timepoints after injury.

4.2 The morphological changes of NG2-glia after traumatic brain injury

As a part of their response behavior after acute brain injury, NG2-glia show morphological alterations already after a short period (1-2dpi; e.g. Figure 6 and Figure 23A). The first observed change in morphology was the expansion of the size of the cell soma and processes, termed hypertrophy (examples see Figure 9). The validation of this quick and transient event was

performed by our collaborator Felix Buggenthin, confirming the performed analysis and the existence of two distinct clusters of NG2-glia (hypertrophic and non-hypertrophic; Figure 23C). The hypertrophic cells showed a wide variety of their volume-fold enlargements (mean between 2-4 fold) compared to the previous timepoint analyzed (Figure 23B).

Trying to understand the function of this morphologic response, the most apparent relation to an enlargement of the cell soma would be a subsequent cell division. Indeed, hypertrophic NG2-glia had a higher likelihood of proliferating at the later timepoint compared with the non-hypertrophic cells (Figure 9) contributing to the compensatory proliferation that occurs in tissue repair (Tamori and Deng, 2014). Nevertheless, more than half of the hypertrophic NG2-glia did not undergo cell division later on, arguing for further effects of this cellular behavior.

Highlighting an alternative mechanism controlling tissue integrity and organ size, a recent study investigated the impact of cell apoptosis of follicle cells due to cell competition in the postmitotic follicular epithelium of *Drosophila* (Tamori and Deng, 2013). They demonstrated that neighboring cells compensated for the resulting loss of local tissue volume via compensatory cellular hypertrophy. This increase of cellular volume (2-4 fold larger than "normal cells") was the result of an accelerated endocycle, a variant cell cycle leading to increased DNA synthesis with gap phases but without active mitosis. These rounds of endoreplication seemed to be triggered via the insulin/insulin-like growth factor (IGF)-like signaling pathway (Tamori and Deng, 2013), which is connected to regulating cellular growth and endoreplication rates through nutrient sensing in various cell types (Hietakangas and Cohen, 2009; Tamori and Deng, 2014). Beside cellular competition, also tissue damage is an important trigger for compensatory mechanisms to retain tissue integrity. This was addressed by another recent study performing puncture wounds in the mitotically quiescent epithelial tissue of *Drosophila* (Losick et al., 2013). This tissue damage got repaired after forming an initial melanized scab within 2 days. Important contributors to this wound healing process were epithelial cells near the lesion site which fused to giant syncytiums containing up to 120 nuclei. Also under these conditions cells increased their endocycle after 24h with no subsequent cell division, leading to hypertrophy. Blocking the observed polyploidization and cell fusion via the knockdown of Cyclin E and the expression of a dominant negative form of the Rac GTPase RacN17 led to a large delay in wound closure suggesting an important role of these cellular events in stabilization of damaged tissue and tissue regeneration (Losick et al., 2013; Tamori and Deng, 2014).

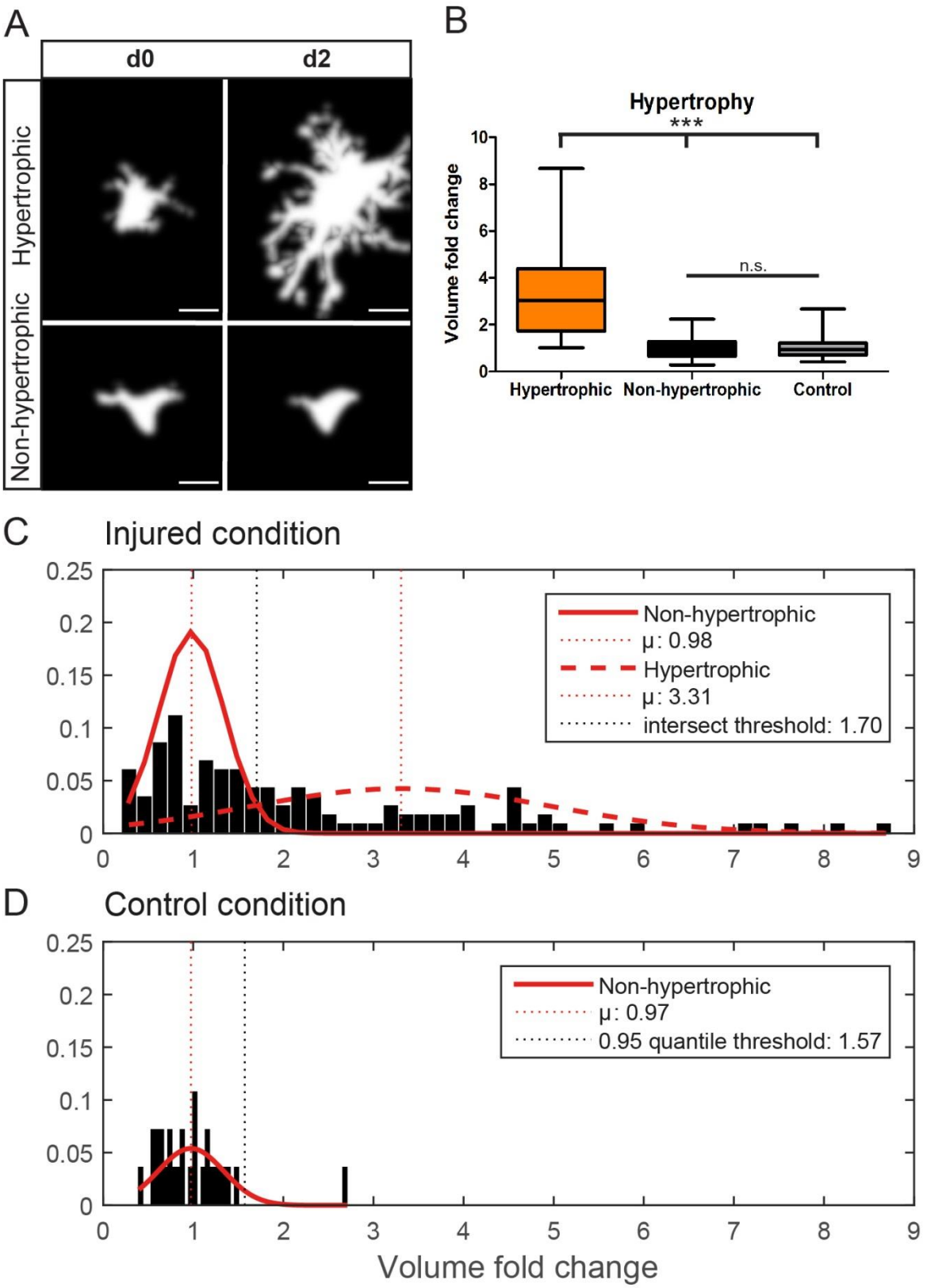

Figure 23 Cells classified as hypertrophic show a significant difference in volume fold change. (A) Exemplary images for a hypertrophic (top row) and a non-hypertrophic (bottom row) NG2-glia at two succeeding timepoints. (B) Boxplot comparison of n=64 hypertrophic and n=52 non-hypertrophic NG2-glia from 10 different mice with injury and n=28 cells from 3 control animals without a lesion (Values represented as mean with whiskers extended

to maximum and minimum of data). Cells classified as hypertrophic show a significant difference in volume fold change in comparison to non-hypertrophic and control cells. In contrast, the difference in the volume fold change of non-hypertrophic versus control cells is not significant (Wilcoxon Rank Sum Test: hypertrophic vs. control: p=8,2653e-11; hypertrophic vs. non-hypertrophic: p=2.7023e-13; non-hypertrophic vs. control: p=0.8520). (C) A Gaussian mixture model with two populations best describes the volume fold change of 116 cells after injury. The average fold change μ of the non-hypertrophic population (solid red fit) is 0.98, the average fold change μ of the hypertrophic population is 3.31 (dashed red fit). The threshold of the volume fold change between the two populations was determined as the intersection of the two distributions at 1.70. (D) The average fold change μ in a control set (n=28 cells from a non-injured sample) is 0.97. The 95 percentile of a fitted Gaussian distribution to the control population is 1.57 and can also be used as a fold change threshold. The two statistically determined fold change thresholds lead to a hypertrophic and a non-hypertrophic subpopulation that overlap with 88% (Gaussian mixture model) and 94% (95 percentile of the control set) with the visual classification, respectively. Scale bars represent 10μm. Graphs and data for the figure kindly provided by Felix Buggenthin.

Also in mammals, hypertrophy and polyploidization can be seen in liver hepatocytes, acting as a compensatory mechanism to retain homeostasis after cell loss or tissue damage (Miyaoka et al., 2012; Duncan, 2013) or corneal endothelial cells (Honda et al., 1982; Ikebe et al., 1988; Tamori and Deng, 2014). Like in *Drosophila*, IGF has been suggested to be involved in mechanical stretch-induced hypertrophy of rabbit cardiomyocytes (Blaauw et al., 2010). However, the exact molecular mechanisms eliciting hypertrophy are still unknown and have to be addressed in future studies. Even if polyploidization is unlikely in NG2-glia it cannot be excluded especially for some cells in the core of the injury due to their cellular amassment. Independent from the intracellular events leading to the observed hypertrophy, the tendency of higher numbers of hypertrophic cells in close proximity to the lesion core (Figure 14 and Figure 15) and at the acute phase after injury (Figure 8) argues for a contribution to the mechanical tissue stabilization after TBI, possibly contributing to a scaffold-like structure.

The second morphological alteration observed in NG2-glia after TBI was polarization. Polarization, also defined as the asymmetry of distribution and organization of cellular contents is involved in many important features of all living organisms, like asymmetric cell division and most importantly cell migration (Woodham and Machesky, 2014). Without these events no multicellular organism would be able to develop properly and to survive. Like hypertrophy cells quickly adapted this morphological change (1-2dpi) with a strong tendency to orientate toward the lesion core (Figure 8 and Figure 10). Due to the strong link between polarization and migration comprising the whole process of cytoskeletal reorganization, many factors and pathways, like the Rho GTPase polarity proteins (Hall, 1998; Raftopoulou and Hall, 2004; Etienne-Manneville, 2006), intermediate filaments (Leduc and Etienne-Manneville, 2015) and even electric currents (Cao et al., 2013) are considered to influence these cellular events.

However, even if many of the analyzed NG2-glia showing a polarized morphology migrated later on, more than half of the cells did not migrate at the subsequent timepoint (Figure 10). This

suggests other functions of polarization besides being a prerequisite for migration, even if in some cases the migratory behavior might be initialized but did not progress any further due to insufficient stimuli. As NG2-glia are screening their environment with filopodia located at their processes (Hughes et al., 2013), it is very likely that they re-orientate their sensing processes towards the direction containing a higher concentration of relevant cues, which are released from the lesion site. Also in Drosophila epidermis (Galko and Krasnow, 2004; Losick et al., 2013; Tamori and Deng, 2014) and mammalian corneal endothelium (Honda et al., 1982) cells at the margin of the injury site were shown to elongate and orientate themselves toward the damaged area as an early event of the wound-healing process. Recent *in-vivo* imaging of astrocytes after SWI also demonstrated a polarization of astrocytes without subsequent migration of this cell type (Bardehle et al., 2013), further supporting polarization also as a standalone cellular behavior after tissue damage. Therefore, it is of interest to further investigate polarization as an independent cellular response after brain injury, even if it will be challenging to dissect polarization from migration due to their shared cellular mechanisms.

4.3 NG2-glia display directional migration toward the lesion site

Highly motile filopodia of NG2-glia sensing their surrounding area for loss of NG2-glia or retraction of their processes are essential for the maintenance of the cellular homeostasis of NG2-glia (Hughes et al., 2013). Due to the exerted self-repulsive behavior, NG2-glia in the adult healthy brain remain in their distinct domains, show no long range migration and their movement has no directional bias (Hughes et al., 2013). In contrast to the physiological situation, NG2-glia after TBI migrate over longer distances toward the injury site for the first 6dpi. Our collaborators Felix Buggenthin and Carsten Marr used a registration technique based on the channel of the rather stable blood vessels to confirm that the movement was active migration and not just passive movement due to tissue alterations (Figure 24; examples for active migrating cells: white arrows Figure 24C').

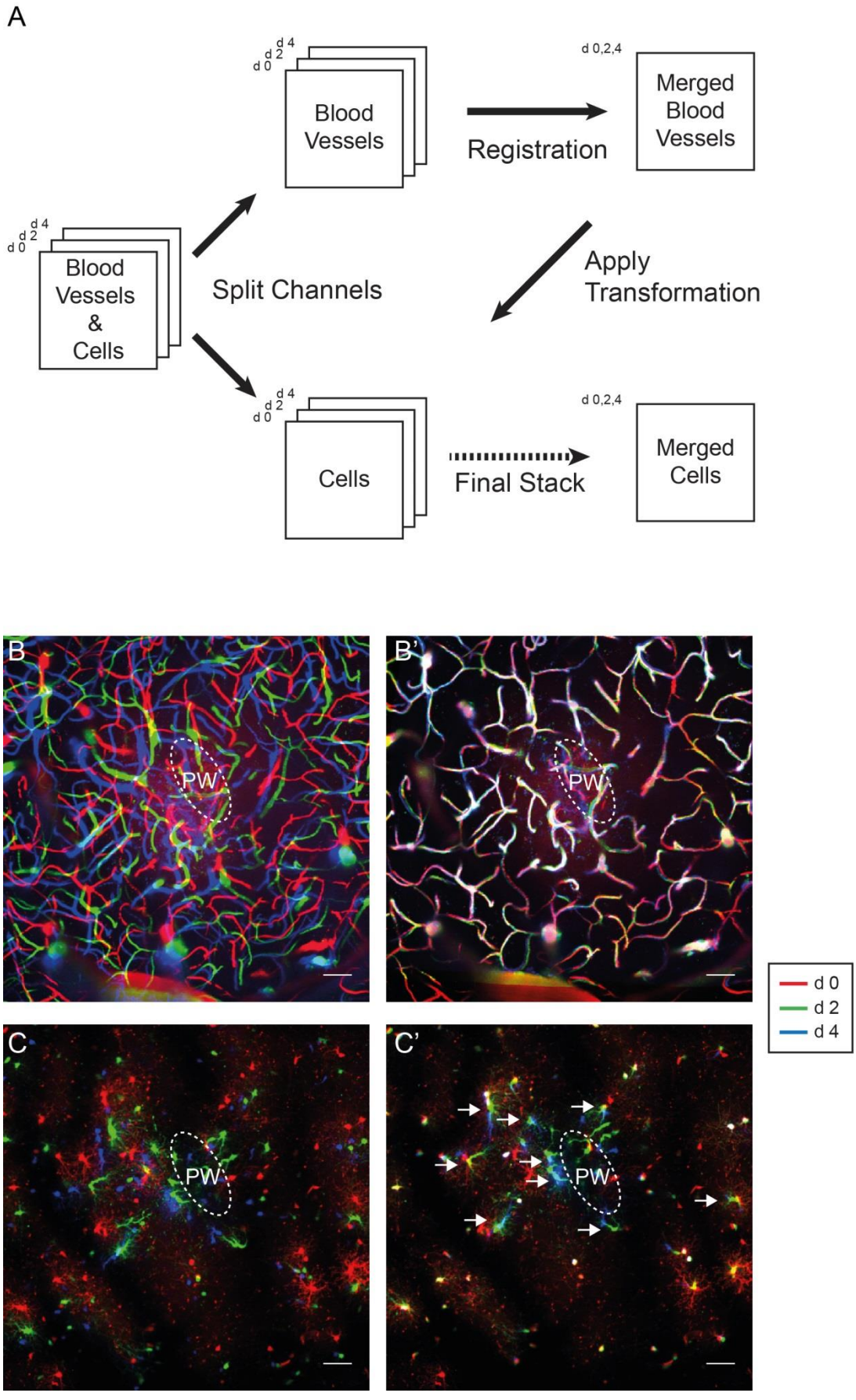
A
d 0
d 2
d 4
Blood Vessels
Registration
d 0,2,4
Merged Blood Vessels
Blood Vessels & Cells
Split Channels
Apply Transformation
Cells
Final Stack
Merged Cells
B
B'
C
C'
PW
d 0
d 2
d 4

Figure 24 Automated registration of 3D image stacks at 0, 2 and 4dpi indicates migration of NG2-glia toward lesion site. (A) Pipeline for registration of image stacks using blood vessels as landmarks (for details, see the methods section): At every timepoint, the image stack is split into two grayscale stacks to separate the landmarks (blood vessels) from the data of interest (GFP^+ cells). (B) Overlay of z-projections from 0dpi (red), 2dpi (green) and 4dpi (blue) showing stained blood vessels. Linear shifts due to slight changes of the imaging angle and non-linear shifts due to tissue swelling are observable. (C) Overlay of z-projections from 0dpi (red), 2dpi (green) and 4dpi (blue) showing GFP-labeled NG2-glia. Due to the systematic shifts between the timepoints, observation of migration might be spurious. (B') Overlay of z-projections of blood vessel stacks. After non-rigid registration, the blood vessels of all timepoints are adequately aligned. (C') Overlay of z-projections of GFP^+ cells after transforming the stacks from 2dpi and 4dpi in accordance to the computed registration parameters from the blood vessel stacks. After registration migration of cells toward the lesion site between the different timepoints is clearly observable (white arrows). Images show maximum intensity projections of 30µm. Scale bars represent 40µm. Figure kindly provided by Felix Buggenthin.

After the acute migratory response within the first days after insult, migration continues but the directionality of the movement returns to a more randomized orientation within the tissue (Figure 8). Finally, two weeks after injury the migration distance and velocity of NG2-glia return to physiological levels (Figure 11). Also during development progenitors of the oligodendrocyte lineage show directed migration over long distances from their places of origin to axonal tracts and other brain regions before they begin to differentiate (Kessaris et al., 2006). As a prerequisite for migration of NG2-glia or other cell types continual remodeling of the cytoskeleton, which can be controlled by Rho-GTPases like cdc42, RhoA and Rac has to occur (Etienne-Manneville and Hall, 2002). However, tissue-specific ablation of cdc42 did not affect NG2 proliferation, differentiation and directed migration *in vitro* (Thurnherr et al., 2006). Similar to the results obtained *in vitro*, also *in vivo* imaging of $cdc42^{fl/fl}$ x Sox10-$iCreER^{T2}$ x eGFP mice in this work did not show any obvious effects of cdc42 on the response behavior of NG2-glia after injury, including migration and polarization (Figure 20). These results cannot exclude, that cdc42 is involved in the underlying mechanisms for migration and polarization but it seems that either cdc42 has not such a strong effect in NG2-glia of the adult brain or can be compensated by another protein for these injury-triggered behaviors.

In contrast to the *in vitro* findings for cdc42 in NG2-glia, a recent study could show that the proteoglycan NG2 effects migration and polarization *in vitro* by regulating cell polarity via the RhoA/rho-associated, coiled-coil-containing protein kinase 1 (ROCK) pathway activation (Biname et al., 2013). This study demonstrated that NG2-glia in stab wounded NG2-EYFP knock-in mice lacking the NG2-proteoglycan showed an altered polarization toward the injury, however they did not study migration *in vivo* (Biname et al., 2013). In addition, other studies have proposed the influence of NG2 on migration and polarization of NG2-glia via proteins associated with cell motility (Chatterjee et al., 2008; Biname et al., 2013). However, the focus of these studies has been on the molecular pathways and interactions of NG2 with proteins like Syntenin-1, Rho-GTPases or polarity complex proteins associated with remodeling of the cytoskeleton, with the majority of

these results obtained *in vitro*. The only *in vivo* results by Biname et al. (2013) demonstrated a shift of polarized cells away from the injury site in NG2-EYFP knock-in mice (Biname et al., 2013). However, they solely distinguished between a longitudinal and a more roundish cell body often disregarding their processes. Thus, actual *in vivo* data about migration and polarization of NG2-glia after knocking out NG2 were still missing. Analyzing the response of NG2-glia after injury in NG2-CreER^{T2} x CAG-eGFP (Huang et al., 2014) mice lacking the NG2-protein with *in vivo* imaging showed that neither migration nor polarization seemed to be majorly effected. Similarly, NG2-glia of a NG2-EYFP knock-in mouse line (Karram et al., 2008) responded comparable to NG2-glia of control animals. The only stable effect detected in those mouse lines was a shift to an earlier peak in cell division, yet this was also seen in the heterozygous NG2-EYFP mouse (Figure 21). This outcome could reflect a dose dependent effect already visible in heterozygous animals or result from the different background of the NG2-KO mouse lines. Importantly, in both cdc42 and NG2 deficient mice the accumulation of NG2-glia in and around the injury core was comparable to the WT situation (Figure 20 and Figure 21). Therefore, both proteins, most likely involved in the protein cascade leading to reorganization of the cytoskeleton, seem to either have non-essential functions for the analyzed cell behavior categories after acute brain injury or they are substitutable by other proteins. Overall, the essential proteins and signal cascades leading to a directed remodeling of the cytoskeleton and migration of NG2-glia remain to be identified. Also the cues that are released after injury inducing this targeted migration are so far not known. bFGF has been suggested to be a chemo-attractant that was shown to be released e.g. by reactive astrocytes under various pathological situations like demyelination in multiple sclerosis or acute cortical insults (Rowntree and Kolb, 1997; Clemente et al., 2011). Moreover, a study employing immunohistochemistry could demonstrate a gradient of bFGF after SWI with high levels of the cytokine in and around the injury core and lower levels more distant (Biname et al., 2013). Also VEGF, released by endothelial cells after injury, could be a promoting factor for NG2-glia migration (Hayakawa et al., 2011). The here obtained observations that NG2-glia do exhibit directional migration toward the injury site - as opposed to astrocytes (Bardehle et al., 2013) - now prompts the search for factors and pathways responsible for mediating this migratory response. However, first results in cdc42 and NG2 deficient mice showed, that the identification of an essential part of the underlying signal cascade might be challenging due to the potential substitutability of proteins. Therefore combined approaches might be advisable for future projects.

4.4 NG2-glia increase their proliferation rate following injury

NG2-glia, are the major proliferative cell in the healthy adult brain parenchyma, with a long cell cycle length of several weeks in the GM (Psachoulia et al., 2009; Simon et al., 2011; Clarke et al., 2012). Upon traumatic injury they rapidly shorten their cell cycle length and show a general increase in proliferation (McTigue et al., 2001; Buffo et al., 2005; Simon et al., 2011). Employing repetitive *in vivo* imaging after TBI, this study could demonstrate for the first time that the majority of NG2-glia only divide once in the area around the lesion core during the first days after injury. Within the core of the injury cells most likely divide more often due to the rapid cellular increase. However, these elevated NG2-glia numbers also result from migration of this glial cell population toward the injury. In contrast to the other reaction categories, proliferation of NG2-glia was observed as a rather late event (peaking at 4dpi) and was not as dependent on the injury size and the distance to the injury. This highlights the idea that proliferation of NG2-glia after injury is not strictly triggered by stimuli released from the lesion site. The factors mediating NG2-glia proliferation have been studied *in vitro* and *in vivo*, mainly after demyelination identifying cytokines like tumor necrosis factor-α (TNF-α), interleukin-1β (IL1β) and interferon-γ (IFNγ) as well as the chemokine CXCL1 as potential effector molecules on NG2-glia proliferation (Arnett et al., 2001; Rhodes et al., 2006; Filipovic and Zecevic, 2008; Clemente et al., 2013; Moyon et al., 2015). However, if these factors also influence the proliferative behavior of NG2-glia after traumatic brain injury remains to be determined. This increase in proliferation of NG2-glia is not restricted to TBI, as it was also shown after sensory deprivation in the developing barrel cortex (Mangin et al., 2012) and in other types of injury like chronic plaque deposition (in general models of AD) or demyelination (Keirstead et al., 1998; Behrendt et al., 2013). Yet, as also shown for astrocytes and in contrast to microglia which react to all kinds of brain pathology, increase of NG2-glia proliferation seems to be mainly elicited after lesions including BBB damage, while cellular damage like ablation of half of the neurons in the adult mouse cerebral cortex (Cruz et al., 2003) does not trigger NG2-glia proliferation (Sirko et al., 2013). Therefore, these studies strongly support the concept that the response of macroglial cells reacting to injury is also influenced by blood-derived factors. Assessing the effect of direct vicinity to blood vessels on NG2-glia behavior after injury did not show any influence on proliferation (Figure 13). However, as NG2-glia are not a part of the neurovascular unit and have most likely no direct access to the blood vessels it is not surprising that they do not show an increased proliferation tendency, like seen for the juxtavascular astrocytes (Bardehle et al., 2013). Taken together, the regulation of NG2-glia proliferation is most likely influenced by both blood-derived factors emerging from the

area of tissue damage and other signaling molecules potentially released from neighboring NG2-glia or other cell types.

4.5 Heterogeneity in the cellular response of NG2-glia after injury

After TBI, NG2-glia in the somatosensory cortex showed a rather heterogeneous behavior, in contrast to the homogenous behavior observed under physiological conditions (Hughes et al., 2013). Whether this heterogeneous response is due to intrinsically different subsets of NG2-glia or due to their specific local environment including different concentration of signal molecules influencing their behavior, is not known. However, as cells in very close proximity to each other also displayed heterogeneous behavior despite receiving a similar input of released stimuli, the influence of the local environment alone is unlikely. On the other side, intrinsic heterogeneity of NG2-glia has already been reported between cells from the GM and WM of the cerebral cortex (Vigano et al., 2013). However, to which extent this heterogeneity is also playing a role within the same area, like here in the GM of the cerebral cortex, is still unclear. Yet, a recent study performing quantitative single cell RNA sequencing in mice from the primary somatosensory cortex and the hippocampal CA1 region identified six clusters of oligodendrocyte subpopulations. Most likely, the majority of these subclasses represent different maturation stages (from immature to myelinating), yet they also identified an intermediate population specifically in the somatosensory cortex that might be in a distinct cellular state (Zeisel et al., 2015). Additionally, only a subset of NG2-glia in the adult cerebral cortex expressed the G-protein coupled receptor, GPR17 (Boda et al., 2011; Vigano et al., 2015). Following acute brain injury these GPR17-expressing cells showed a higher differentiation rate compared to the remaining NG2-glia population, constituting a reserve pool for repair after injury (Vigano et al., 2015). Also different phases of cell cycle or maturation state in neighboring NG2-glia most likely contribute to the heterogeneous state of NG2-glia and to variations in gene expression. Indeed, the NG2-glia population was shown to divide heterogeneously, in terms of asymmetric and symmetric cell divisions and marker expression of sister cells. This distribution of cell cycle events was altered by aging, physical activity and also following acute injury (Boda et al., 2015). Overall, the heterogeneous response behavior of NG2-glia most likely results from a combination of both, intrinsic heterogeneity of the individual cells and local differences in the environment.

While the majority of NG2-glia around the injury core responded by showing at least one of the four observed reaction categories, some NG2-glia did not show any detectable alterations in

morphology or any migratory and proliferative behavior (static cells; Figure 6B-F and Figure 14D). This could be the result of an insufficient concentration of triggering molecules in the surrounding of those cells in relation to their e.g. metabolic and proliferative state. Additionally, the morphology of mature oligodendrocytes also labeled in the Sox10-iCreER^{T2} x eGFP mice was very stable after TBI, which was advantageous for their use as landmarks (additionally to the labeled blood vessels) during *in vivo* imaging. Even in direct proximity to the lesion core mature oligodendrocytes never displayed any drastic changes in morphology and only sparsely disappeared, showing that those cells are less plastic and highlighting the importance of oligodendrocytes to remain in their distinct networks. Therefore these results demonstrated that oligodendrocytes in the somatosensory cortex did not contribute morphologically to scar formation or wound healing following acute brain injury.

4.6 NG2-glia as a major reactive gliosis population contribute to wound closure

As described before, NG2-glia responded very fast to acute injury accumulating in the core of the lesion and probably contributing to a first cellular scaffold. However, what is the exact role of this NG2-glial accumulation? To address this question my colleague Sarah Schneider took advantage of the acetyl-transferase establishment of cohesion 1 homologue 2 (Esco2)$^{fl/fl}$ mouse line (Whelan et al., 2012b) crossed with the Sox10-iCreER^{T2} x CAG-eGFP mouse line. Esco2 is an important protein in the cell cycle regulating the proper cohesion of the sister chromatids and after loss of gene function proliferative cells undergo apoptosis (Whelan et al., 2012a). Therefore, in the Esco2$^{fl/fl}$ x Sox10-iCreER^{T2} x CAG-eGFP line induction led to the specifically ablation of proliferating NG2-glia. Strikingly, the resulting restraint of NG2-glia accumulation in the lesion core after acute brain injury caused a delayed wound closure in these animals (Figure 25). Due to the high levels of proliferation in close vicinity to the injury core, the reduction of recombined NG2-glia and hence the general NG2-glia number was especially reduced in that region compared with the WT control (Figure 25 A-C). Most likely due to this elicited prevention of NG2-glia accumulation the wound closure was clearly impaired at 4 and 7dpi (Figure 25 D and E). However, at 14dpi, when also NG2-glia numbers around the injury where comparable to the WT control, a sufficient wound closure could be observed (Figure 25C-E). Therefore, it is very likely that NG2-glia indeed play an important role in the first phase of scaffold formation, tissue remodeling and recovery after an acute injury. Also secondary functions of NG2-glia like signaling to other cell types are very likely

to contribute to the events following acute brain injury, as astrocytic reactivity after TBI is reduced when proliferating NG2-glia have been ablated (Schneider and Dimou, unpublished observations). Along the same line, abrogation of β-Catenin signaling in NG2-glia led to reduction of their proliferative behavior after SCI together with reduced accumulation of activated microglia/macrophages and astrocyte activity (Rodriguez et al., 2014). This argues for the importance of cell-cell interactions for the injury response and the specific contribution from various cell types of the brain for an efficient tissue recovery.

In summary, the intensity of the NG2-glia response increased depending on the injury size and distance from the lesion core. Overall, NG2-glia responded fast and strong within the first 2-6dpi resulting in a massive increase of cell number and cellular density directly within as well as in close vicinity to the injury core. Whereas the homeostasis of NG2-glia was transiently overcome within the lesion core it was maintained in more distant regions by neighboring NG2-glia replacing migrated cells with increased proliferation. The cellular scaffold of NG2-glia formed in the core of the injury seemed to improve tissue regeneration as ablation of proliferating NG2-glia impaired wound closure after acute brain injury. Already one week after injury the general reactivity of NG2-glia decreased. This concurred with a progressive restauration of the general cellular density, distribution and morphology of NG2-glia. Finally, three to four weeks after TBI physiological conditions of NG2-glia were restored in terms of morphology and distribution of cells (Figure 8 and Figure 16). This implies a new role of NG2-glia during the first phase of acute brain injury in tissue regeneration.

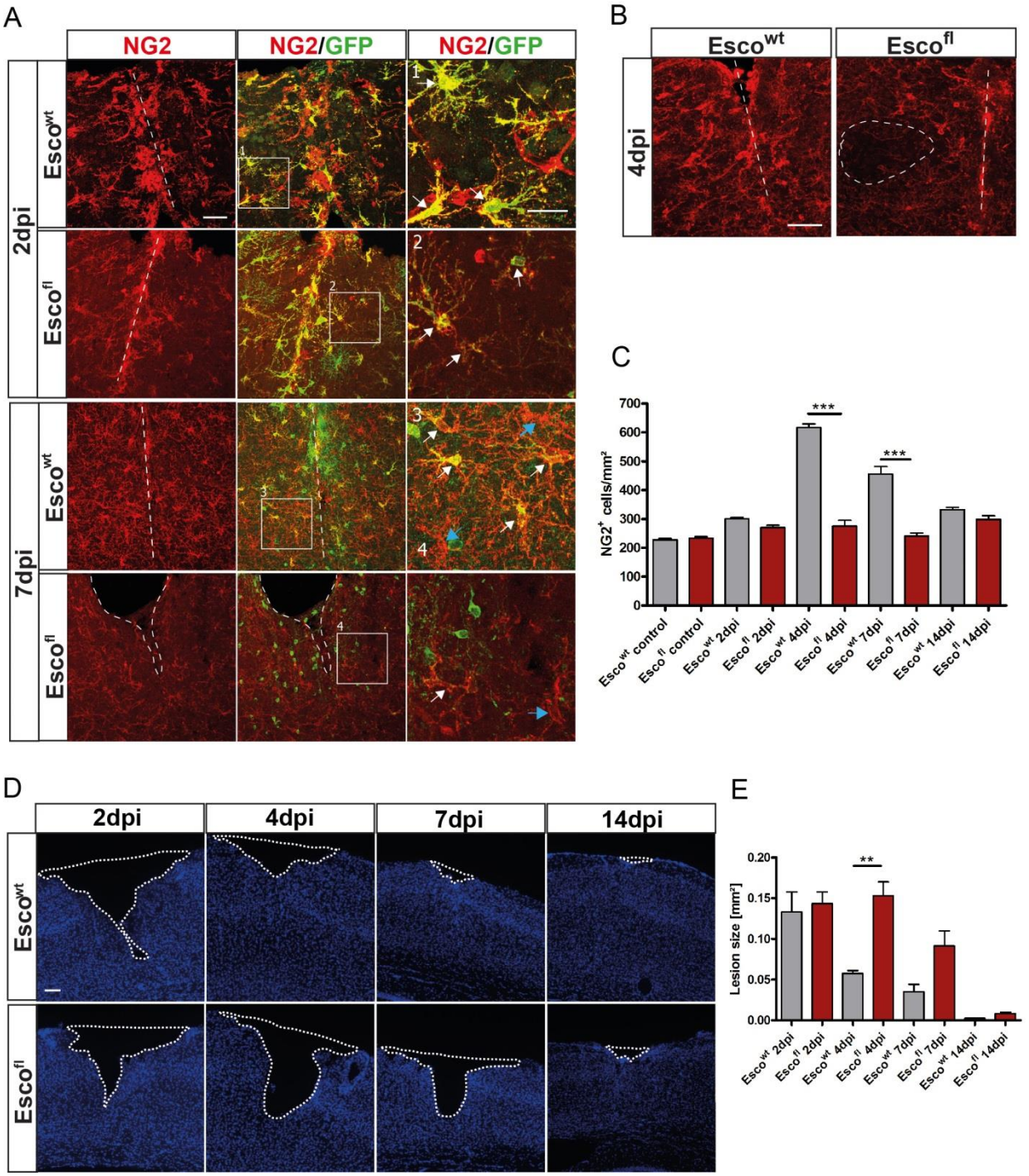

Figure 25 Depletion of NG2-glia after injury leads to impaired wound closure. (A) Confocal images of NG2+ cells in Esco^{wt} and Esco^{fl} animals at 2 and 7 dpi. (B) NG2-glia in Esco^{wt} and Esco^{fl} animals at 4dpi. In Esco^{fl} animals, areas with complete absence of NG2-glia can be observed (dashed ellipse). (C) Cell counts of NG2^{+} cells per mm^2 in Esco^{wt} and Esco^{fl} animals in control, non-lesioned brains and at different timepoints after the lesion. Esco^{fl} mice show a reduced cell number after injury (n=3 animals for each genotype and timepoint, cell counts are presented as mean+SEM; 1way ANOVA with Tukey post-test: *** indicates significance level of $p<0.0001$). (D) Lesion size in the cerebral cortex visualized by the lack of DAPI positive cells in Esco^{wt} and Esco^{fl} animals at different timepoints after the lesion. (E) Size of the lesion in mm^2 at 2, 4, 7 and 14dpi in Esco^{wt} and Esco^{fl} animals. Esco^{fl} animals show a significantly bigger lesion compared to Esco^{wt} control littermates. (n=3 for Esco^{wt} (2, 7 and 14dpi), n=4 for Esco^{wt} (4 and 14dpi), n=5 for Esco^{fl} (2dpi), n=6 for Esco^{fl} (4 and 7dpi) animals), data are presented as mean±SEM; 1way ANOVA with Tukey

post-test: ** indicates significance level of p<0.001. Scale bars represent 25µm in (A) blow-up, 50µm in (A) and (B), 100µm in (D). Figure kindly provided by Sarah Schneider.

4.7 The cellular response after brain injury

In general, several components are included in the complex and multifaceted events occurring in tissue regeneration following tissue damage. These include the systemic response and extracellular matrix deposition which are shared between various tissue types. Nevertheless, the CNS as a somehow privileged tissue type has its distinct cellular composition which results in tissue-specific events after injury, amongst others leading to an insufficient regenerative capacity (Shechter and Schwartz, 2013). This has a detrimental impact on the majority of CNS pathologies. Hence, it is of great importance to further investigate the cellular components and the underlying mechanisms contributing to the injury response and the regeneration in this tissue.

Until recently, astrocytes were the most likely candidates to contribute to the so called glial scar formation after CNS injury. However, results from this study as well as a recent study by Bardehle et al. (2013) challenge this concept. Indeed, as a first reaction to the injury, microglial cells start to respond and proliferate around the injury (Nimmerjahn et al., 2005), macrophages infiltrate (Anthony and Couch, 2014) and then NG2-glia start to react with roughly one day delay (e.g. Figure 6). In contrast, only a small proportion of astrocytes react at later timepoints with polarization and proliferation while migration could not be observed (Bardehle et al., 2013). This late and low level reaction of astrocytes renders them less important for the first steps of scar formation and tissue recovery in the cerebral cortex than it was assumed before. Though, an indirect role via signaling to other cells initializing their response for e.g. wound closure or scar formation preceding their cellular reaction cannot be excluded. One of the potential targets of astrocyte interaction after tissue damage are immune cells like T cells, which could be influenced via cytokines and other soluble factors released by astrocytes (Xie and Yang, 2015). In contrast to astrocytes, other cell types like neural stem cells were shown to be recruited to the injury site in the brain if the elicited damage extended to the white matter (Brill et al., 2009). Single-cell RNA sequencing of acutely isolated neural stem cells revealed a heterogeneous pool of cells with a distinct sub-population that became responsive after global forebrain ischemia (Llorens-Bobadilla et al., 2015). In the spinal cord where neural stem cells are recruited to the injury site in a similar manner, they differentiated into astrocytes contributing beneficially to wound healing (Sabelstrom et al., 2013). Also the injury responses of pericytes (Goritz et al., 2011) and perivascular fibroblasts (Soderblom et al., 2013) seem to advance the healing process in the spinal cord. A recent study

investigating the response of pericytes after different types of tissue injuries, like pulmonary, renal and cardiac injuries, claimed a response of this cell type after SCI and SWI in the cortex (Birbrair et al., 2014). Unfortunately, this study using NG2-DsRed mice, ignored the fact that NG2-glia were also shown to be responsive after injury by citing the study of Barnabé-Heider et al. (2010), which just stated that the response of NG2-glia after SCI was not as intense as the ones from astrocytes and ependymal cells (Barnabe-Heider et al., 2010). These flaws could therefore lead to a misleading conclusion about the rate of pericyte reactivity following injury. However, a general responsiveness of pericytes after several tissue injuries is very likely. Endothelial cells and endothelial progenitor cells were also shown to participate in revascularization and neuronal repair via cell-cell communication after extensive vascular damage like in stroke (Ma et al., 2015). Therefore, many of the resident brain cell types seem to participate in the injury response and the consecutive tissue repair. Resident microglia and invading immune cells are supposedly the first responders (0-1dpi) followed by NG2-glia, potentially fibroblast-like cells, pericytes (2-4dpi) and astrocytes (5-7dpi; Figure 26). Interestingly, a recent study could demonstrate that the cellular reaction after cortical brain injury differed between male and female mice. This gender difference was especially pronounced in the neuroinflammatory response, whereas astrocytes seemed less effected (Acaz-Fonseca et al., 2015). Whether additional cellular components also contribute to wound closure and if all those findings can be translated between different regions of the CNS is still not fully understood. Moreover, the discussion to what extent different cell types play a beneficial or detrimental role in wound healing and tissue regeneration remains a heavily discussed topic, which has to be further clarified for advancement of the treatment strategies in various CNS pathologies (Cregg et al., 2014).

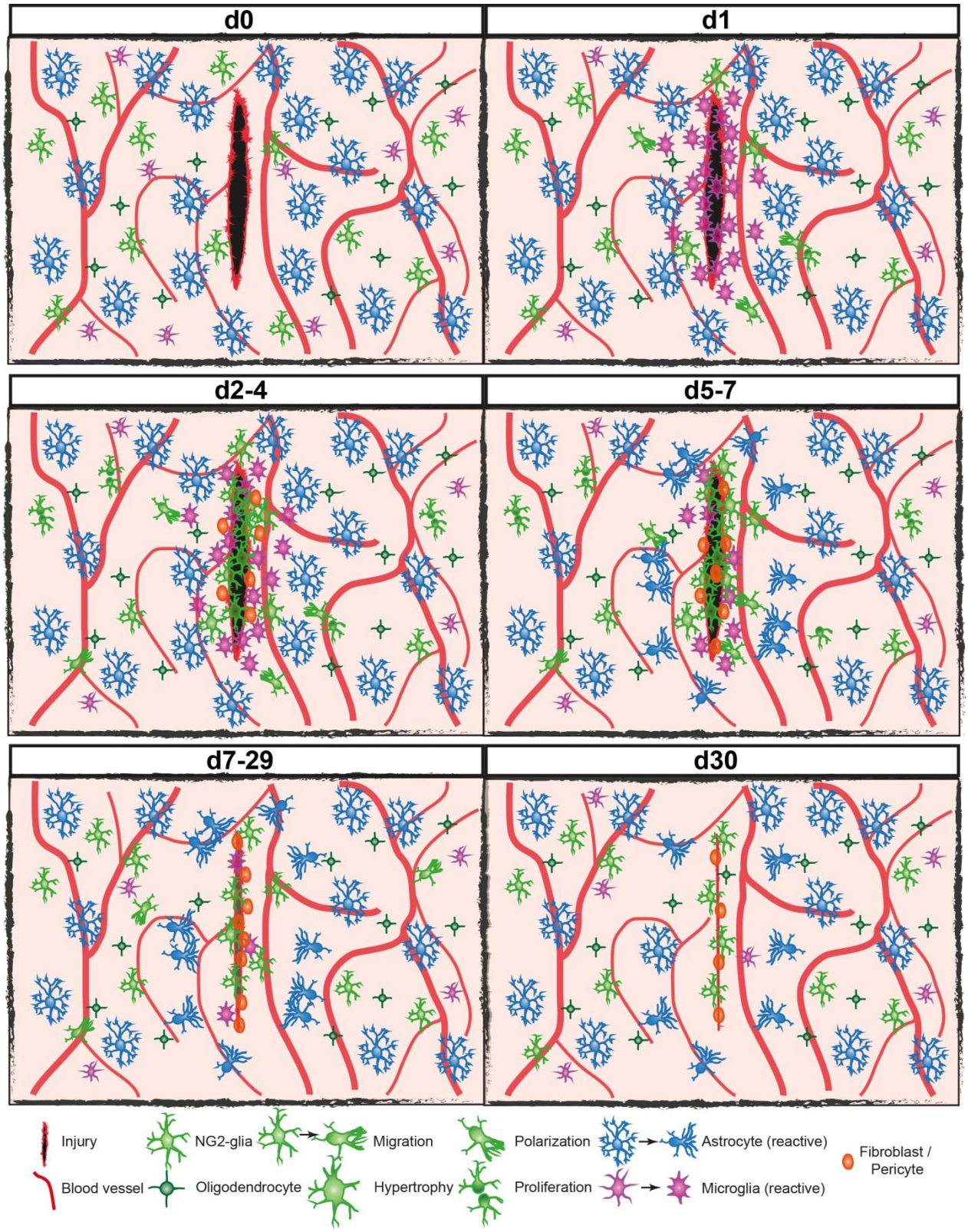

Figure 26 Cellular reactivity after brain injury. Different cell types become reactive upon injury showing proliferation, polarization, migration and hypertrophy. NG2-glia, microglia and probably fibroblast-like cells accumulate in and around the injury core and decrease at later timepoints, while astrocytes do not migrate but keep their reactive profile for a longer time.

4.8 NG2-glia and their injury response as a potential target for clinical application

Analyzing the functionality and capability of different cell types can help to better understand the pathological events in which those cells are involved. Hopefully, this could lead to an improved therapy and possibly even preventive measures to stop the disease course of interest. In the past decades the focus of clinical research associated with NG2-glia has been on their potential to substitute for lost oligodendrocytes during demyelinating diseases like MS (Hartley et al., 2014; Kremer et al., 2015). Despite the still existing prevalence of immunomodulatory drugs in MS treatment, some advances have been made in regard to improve remyelination (Kremer et al., 2015). In a large scale study employing an *in vitro* screen of 727 NIH approved drugs for differentiation and myelination of NG2-glia (Najm et al., 2011), two very promising targets were identified, ameliorating myelination *in vitro*, *in vivo* and in mouse models of MS (Najm et al., 2015). These promising results could be relevant for not just the classical demyelinating diseases but also for functional restoration after SCI. There, demyelination and oligodendrocyte loss occurs after disturbance of nodal organization and subsequent conduction blockage as a secondary damage (Papastefanaki and Matsas, 2015). Therefore, the emphasis of clinical research aiming to improve therapy after SCI shifted their focus from strictly enhancing neuronal regeneration to also provide protection for oligodendrocytes and enhance remyelination (Mekhail et al., 2012; Papastefanaki and Matsas, 2015). However, to achieve full functional recovery one has to bear in mind when boosting NG2-glia proliferation and differentiation after SCI, that the proteoglycan NG2 has been shown to have detrimental effects on axonal outgrowth and sensory recovery (Tan et al., 2005). Another critical aspect of NG2-glia manipulation is the high prevalence of this cell type in different types of gliomas (Chekenya and Pilkington, 2002; Liu et al., 2011; Xu et al., 2011). Due to their relatively high proliferation rate also in humans they are susceptible for oncogenic mutations, potentially leading to tumor formation (Visvader, 2011). Having high malignancy rates, very limited treatment options (Talibi et al., 2014; Venur et al., 2015) and therefore a poor probability of survival (Frosina, 2015), gliomas are a considerable risk for all kinds of effectors on NG2-glia behavior.

This also holds true for the recent advances in transplantation and reprogramming of NG2-glia to improve repair and regeneration after tissue damage. In these experimental approaches researchers are trying to manipulate a target cell type via altered gene expression to differentiate into a cell type of interest (e.g. neurons for neuronal reprogramming). Attempting to improve therapies for diffuse traumatic axonal injuries, human NG2-glia have been transplanted in a

corresponding mouse model which elicited massive migration and differentiation of those cells along the WM tracts (Xu et al., 2015). Also in a rat model for ischemic brain injury of periventricular leukomalacia, transplanted mouse NG2-glia led to ameliorated neuronal death, increased proliferation of neural stem cells and improved functional outcome (Chen et al., 2015). Additionally, first studies showed promising results of NG2-glia as a target cell type for neuronal reprogramming and thus representing an intrinsic source for new neurons (Heinrich et al., 2014). Despite these promising results, other aspects beside the risk of potential malignancy have to be considered, especially when manipulating the endogenous NG2-glia population. More and more findings contribute to the concept, that NG2-glia are not just sole progenitor cells waiting to be differentiated into myelinating oligodendrocytes or reprogrammed in other cell types without any further functions. Their communication with neurons have been already demonstrated for the so called neuro-glial synapses (Mangin and Gallo, 2011; Sakry et al., 2011) and this interplay has been furthered with the discovery of their production of neuromodulatory factors (Sakry et al., 2015) and the activity dependent ectodomain cleavage of NG2 (Sakry et al., 2014). In addition, this study now concurs to the findings showing NG2-glia as a major responsive element after all kinds of CNS injuries contributing to wound closure and potential functional recovery beyond the so called glial scar.

5 Materials

5.1 Equipment

Name	Company
Binocular MZ6	Leica
Centrifuge (table centrifuge)	Neolab
Cold-light source KL1300LCD	Leica
Cryostate CM 3050	Leica
Drill K1070 High Speed Rotary Micromotor Kit	Foredom
Geldoc™ XR	BIO-RAD
Hair trimmer	Philips
Heating Mat Thermo Control Professional	Verticare BV
Laminar flow	Bdk
Laser Mai Tai High-Performance Mode-Locked Ti-Sapphire	Spectra-Physics
Magnetic stirrer IKAMAG® RCT	Bachofer
Microscope AxioImager M2	Zeiss
Microscope Axiovert 40CFL	Zeiss
Microscope LSM700 (confocal microscope)	Zeiss
Microscope LSM7 MP (multiphoton microscope)	Zeiss
Microscope FV 1000MPE (multiphoton microscope)	Olympus
Microscope SZ61 (standing stereo operation microscope)	Olympus
Microwave	Privileg
Perfusion pump	Gilson
pH meter WTW	inoLab
Power supply EAPS 2016-100	Philips
Scale	Scaltec
Scale analytic (precision scale)	Sartorius
Shaker Duomax 1030	Heidolph
SMART Table UT2	Newport
Stage for 2PMS (self-build)	LMU
Stereotactic apparatus (Digital Standard)	Stoelting
Thermocycler 3000	Biometra

Thermomixer comfort	Eppendorf
Vortex-Genie	Vortex-Genie Bender & Hobein AG
Water bath	Haake

5.2 Consumables

Name	**Company**
Augen- und Nasensalbe	Bepanthen
Cellulose Swabs (Pur-Zellin)	Hartmann
Cooling Mixture CCL100	Nalco
Cotton buds (Rotilabo)	Roth
Cover Glasses (Menzel) 5mm	Thermo Scientific
Coverslips	Roth
Delicate Task Wipes	Kimtech Science
Dental Cement (Paladur; liquid + powder)	Heraeus
Drill heads (5+3)	Meisinger
Insulin needles, U-100, 1ml	BD Micro Fine
Liquid Blocker	Science Services
Filtropur S 0,2 Spritzenfilter	Sarstedt
Microscope slides	Roth
Microscope slides Superfrost	Thermo Scientific
Parafilm PM-996	Parafilm
Reaction tubes for PCR	Eppendorf
Reaction tubes (0.5 ml; 1.5 ml; 2 ml)	Plastibrand
Reaction tubes safelock (1.5 ml; 2 ml)	Eppendorf
Serological pipettes (5 ml; 10 ml; 15 ml)	Sarstedt
Sugi Sponge Strips (rectangular)	Kettenbach
Sugi Sponge Points	Kettenbach
Super glue (precision)	Loctite
Surgical blade (22)	Schreiber
Suture Vicryl Polyglactin 910	Ethicon
Syringe Omnifix-F Tuberculin 1ml	Braun
Syringe (50ml)	Braun
V-Lance™ Knife, 19 Gauge	Alco Surgical

Well-Plate, 24 wells	Orange Scientific

5.3 Chemicals and pharmaceuticals

Chemical	Company
Acetic acid	Roth
Atipamezol (Antisedan)	Orion Pharma
Agarose	Serva
Bromphenol blue	Sigma
Buprenorphine (Temgesic)	RB Pharmaceuticals
Calcium chloride dihydrate	Sigma
Carprofen (Rimadyl) 50mg	Pfizer
Citric acid monohydrate	Roth
Corn oil	Sigma
D(+)-glucose-monohydrate	Merck
4',6-diamidino-2-phenylindole, dilactate (DAPI)	Invitrogen
dNTPs	PeqLab
Ethanol	Roth
Ethidiumbromid	Roth
Ethylenediamine-tetraacetic acid (EDTA)	Sigma
Ethylene glycol	Sigma
Fentanyl citrate (Fentanyl)	Hexal
Flumazenil (Anexate)	Roche
Glycerol	Sigma
Glycine	Sigma
Goat Serum	Gibco
HEPES	Sigma
Hydrochloric acid	Merck
Ketaminhydrochlorid (Ketavet) 100 mg/ml	Pfizer
Lidocain (Xylocain) 0.2mg/ml pump spray	Astra Zeneca
Magnesium sulphate hexahydrate	Merck
Medetomidin (Domitor) 1mg/ml	Pfizer
Midazolam (Dormicum) 5mg/ml	Roche

Mounting solution (AquaPolymount)	Polysciences
0,9% NaCl solution (Saline)	Braun
Paraformaldehyde (PFA)	Sigma
PCR Reaction buffer 10 x	Qiagen
Protein kinase K	Roth
Potassium chloride	Sigma
Potassium dihydrogen phosphate	Merck
Saccharose	Merck
Sodium chloride	Sigma
Sodium dodecyl sulphate (SDS)	Sigma
di-sodium hydrogen phosphate dihydrate	Merck
Sodium hydroxide	Fluka
Tamoxifen	Sigma
Taq Polymerase	NEB
Triton X-100	Sigma
TRISbase	Sigma
TRISHCL	Sigma
Tween20	Sigma
Xylazinhydrochlorid (Rompun) 2%	Bayer
Xylene cyanole	Sigma

5.4 Buffers and solutions

5.4.1 DNA Preparation

- Lysis buffer

Substance	**Concentration**
NaCl	1M
TRISHCl, pH=8,5 (1.211g TRISBase/1l H_2O)	1M
SDS	10%
EDTA	0.5M
Protein kinase K (freshly added)	10mg/ml

Filled up with ddH_2O.

- 10x PCR Buffer uni

Substance	Concentration
KCl	500mM
TRISHCl	100mM

Filled up with ddH_2O and adjusted to pH=8.7

- dNTP mix

Substance	Concentration
dATP, dTTp, dCTP, dGTP	2.5mM each

Filled up to 1l with ddH_2O.

- 50x TAE buffer

Substance	Concentration
TRISBase	242g (121.14 g/mol)
Acetic Acid (100%)	57,1ml
$Na_2EDTA*H_2O$	37,2g (372.2 g/mol)

Filled up to 1l with ddH_2O and adjusted to pH=8.0.

- Ethidium bromide

Substance	Concentration
Ethidium bromide	100mg
H_2Odd	2ml

- 4x DNA loading buffer

Substance	Concentration
Glycerin (100%)	20ml
50x TAE buffer	1ml
Bromphenol blue	200µl
Xylene cyanol solution	500µl
H_2Odd	50ml

5.4.2 Immunohistochemistry

- 20% Paraformaldehyde (PFA)

Substance	Concentration
Na_2HPO_4	134g
PFA	400g
Sodium hydroxide solution	32%

Filtered through paper filter, filled up to 2l with H_2Odd and adjusted to pH=7.4

- 10x Phosphate buffered saline (PBS)

Substance	Concentration
Na_2HPO_4 x $2H_2O$	0.08M
KH_2PO_4	0.01M
NaCl	1.5M
KCl	0.03M

Filled up with 1l H_2Odd and adjusted to pH=7.4.

- 30% Saccharose solution for cryoprotection

Substance	Concentration
Saccharose	15g

Add 50ml of 1xPBS; mix thoroughly

- Storing solution for floating sections

Substance	Concentration
Glycerol	4M
Ethylene glycol	5.4M
Phosphate buffer, pH 7.2 - 7.4	25mM

- Blocking solution

Substance	Concentration
TritonX-100	0.5%
Goat Serum	10%

Dilute in 1xPBS

5.4.3 Animal handling and imaging

- Tamoxifen

Substance	Concentration
Tamoxifen	40mg/ml
Ethanol (100%)	10%
Cornoil	90%

For dissolution the preparation has to be shaken for 3-4h at 37°C.

- Rimadyl

Substance	stock (mg/ml)	dose (mg/kg)	ml/3ml
Carprofen (Rimadyl)	50	4	0.06
NaCl	0.9		2.94

- "Sleep mix"

Substance	stock (mg/ml)	dose (mg/kg)	ml/5ml
Fentanyl citrate (Fentanyl)	0.05	0.025	0.25
Midazolam (Dormicum)	5	5	0.5
Medetomidin (Domitor)	1	0.5	0.25
NaCl	0.9		4

- "Awake mix"

Substance	stock (mg/ml)	dose (mg/kg)	ml/5ml
Buprenorphine (Temgesic)	0.3	0.1	0.17
Flumazenil (Anexate)	0.1	0.5	2.5
Atipamezol (Antisedan)	5	2.5	0.25
NaCl	0.9		2.08

- Cortex buffer

Substance	mM	g/l	g/100ml
NaCl	125	7.21	0.72
KCl	5	0.372	0.037
Glucose	10	1.802	0.18
HEPEs	10	2.38	1ml (1M stock solution)
$CaCl_2$	2	2ml (1M stock solution)	0.2ml (1M stock solution)
$MgSO_4$	2	2ml (1M stock solution)	0.2ml (1M stock solution)

The mix was filled up to 100ml with ddH_20, adjusted to pH=7.4 and sterile filtered under the hood using Filtropur S 0.2µm (Sarstedt) filters. Aliquots of 10ml were stored at 4°C.

6 Methods

6.1 Animals

6.1.1 Mouse strains

All experiments were performed in accordance and under the Guidelines of Use of Animals and Humans in Neuroscience Research, revised and approved by the Society of Neuroscience, and licensed by the State of Upper Bavaria under license number 55.2-1-54-2532-171-11.

The mouse lines used for experiments:

1-Sox10-iCreER^{T2} x CAG-eGFP

2-Sox10-iCreER^{T2} x CAG-eGFP

1-Sox10-iCreER^{T2} x cdc42$^{fl/fl}$ x CAG-eGFP

NG2-CreER^{T2} x CAG-eGFP

NG2-EYFP

The 1-Sox10-iCreER^{T2} line as well as the 2-Sox10-iCreER^{T2} line were used for analysis, as both showed reliable and comparable recombination of cells from the oligodendrocyte lineage after induction in adult animals (Simon et al., 2012).

6.1.2 Genotyping

Colonies of experimental mice were kept and bred in the animal facility. Each mouse received a numbered ear clip (0001-9999) or was tagged via 99 ear punch system. To identify the genotype of each mouse small tail biopsies were taken for DNA isolation and a polymerase chain reaction

(PCR) was performed. Therefore, tail pieces were incubated in 500µl lysis buffer, shaking at 55°C over night. After a centrifugation step at 10000rpm for 5 minutes (min) for sedimentation of tissue residues the supernatant was transferred and DNA was precipitated via addition of 0.5ml isopropanol for 5min and pelleted by 10min centrifugation at10000 rpm. After discarding the supernatant the pellet was dried at room temperature (RT). The DNA was dissolved in 200µl 10mM Tris buffer at 55°C. For genotyping 2µl of DNA was used in a total of 25µl reaction mix. The standard reaction mix contained:

Substance	**Volume (µl)**
H_2O	11
MgCl	2.5
Buffer uni	2.5
Primer 1	0.5
Primer 2	0,5
Q-Solution	5
dNTP's	0.5
Taq Polymerase	0.5
DNA	2
Total	25

Following primer pairs were used:

Primer name	**Sequence (always 5'-3')**
GFP-II-Reporter	AG-2: CTG CTA ACC ATG TTC ATG CC CAT-2: GGT ACA TTG AGC AAC TGA CTG
Sox10-iCreER^{T2}	CS32: AAA CAC CCA CAC CTA GAG AC CS33: ACC ATT TCC TGT TGT TCA GC
Cdc42$^{fl/fl}$	Fw: TTG TAA TGT AGT GTC TGT CCA TTG G Rev: TGT CCT CTG CCA TCT ACA CAT ACA C
NGCE-Cre (NG2-CreER^{T2})	NG2Cre-fw: GGC AAA CCC AGA GCC CTG CC NG2wt-rev: GCT GGA GCT GAC AGC GGG TG NG2Cre-rev: GCC CGA ACC GAC GAT GAA GCA
GFP-ZEG (NG2-EYFP)	F2: CTA CGG CAA GCT GAC CCT GAA GTT C R2: GCC GAT GGG GGT GTT CTG CTG GTA G

Following the PCR loading buffer was added to the reaction mix and loaded on a 2% agarose gel (with 1xTBS buffer and 3 drops of Ethidium bromide) to detect the PCR products. The following PCR protocols were carried out:

6.1.3 Tamoxifen induction

Adult (3-4 months old) Sox10-iCreERT2xCAG-eGFP mice received three times every second day 0.4µg tamoxifen per gram of body weight by oral gavaging (stock solution: 40µg/ml tamoxifen in corn oil with 10% EtOH). For the analysis of altered induction rates and possibly resulting subtype specific recombination also a reduced amount (one time gavaging; 0.4µg tamoxifen per gram of body weight) was used to label fewer cells.

6.1.4 Operation

Starting at least 9 days after recombination the animals were operated introducing a cranial window. To reduce pain Rimadyl (containing Carprofen) in a NaCl solution was injected subcutaneously with a concentration of 4mg/kg bodyweight before the operation. Mice were anaesthetized by intraperitoneal injection of the "sleep mix" containing midazolam (5mg per kg of body weight), medetomidine (0.5mg per kg) and fentanyl (0.025mg per kg) and an unilateral craniotomy was performed using a high speed dental drill over the somatosensory cortex followed by a small punctate (depth of ~0.7mm and length of ~0.1mm) or a large stab wound injury (depth of ~0.7mm and length of ~1mm) using a 19 gauge lancet shaped knife. After flushing the resulting craniotomy with cortex buffer and cessation of potential bleeding a glass coverslip (5mm diameter) for the cranial window was fixed over the craniotomy and sealed with dental acrylic (Paladur). The control operations included all the previously described steps excluding the knife-induced injuries. For the longer imaging periods after injury (starting from 4dpi) the craniotomy and injury was performed like described before, but instead of sealing the tissue with a cranial window the skull piece was re-placed on the craniotomy and closed with a suture. Four days later, in a subsequent operation, the skull piece was removed again and the craniotomy sealed with a cranial window as described above. For the control operations a craniotomy followed by the placement of a cranial window was performed as described above without any further injury. Following all these operations, a metal head bar was attached on top of the contralateral hemisphere with super glue to allow the fixation of the mouse head during imaging and 50µl of a Texas-Red-conjugated dextran (70kDa) containing solution (10mg ml^{-1}) was intravenously injected (tail vein) to label blood vessels. After surgery and imaging, antagonization of the anesthesia was induced

via injection of the "awake mix" containing atipamezol (2.5mg per kg), flumazenil (0.5mg per kg) and buprenorphine (0.1mg per kg).

6.2 In vivo two-photon microscopy

Anaesthetized animals were fixed with the help of the metal head bar on a custom made, heated stereotactic stage, orientated perpendicular to the optical axis of the microscope and imaging was performed with an Olympus FV 1000MPE or Zeiss LSM7 MP microscope each equipped with a multi-photon, near infrared, pulsed MaiTai High-Performance Mode-Locked Ti-Sapphire DeepSee laser (Spectra Physics). The Olympus setup contained a 20x water immersion objective (1.0 numerical aperture [NA]), a FV10-MROPT filter (BA=420-500nm for detection of second harmonic signals; BA=515-560nm for detection of GFP; BA=590-650 for detection of Texas-Red) and internal photomultiplier tube detectors. The Zeiss setup contained a 10x air based and a 20x water immersion objective (1.0 NA), comparable filter sets (BA=445-500, BA=520-560nm and BA=570-610nm) and BiG as well as LSM 710 NDD detection modules. The laser was tuned to 910nm and laser intensity was adjusted depending on tissue depth (<50mW). Emission of green fluorescence of intrinsic eGFP expression of recombined Sox10 expressing cells, red fluorescence of Texas-red labeled blood vessels and blue second harmonic signal (detectable at half the emission wavelength ~460nm) of fiber-like structures like the dura were detected and optical sections with the resolution of 1024x1024 in the x-y dimension were recorded every 2µm to a depth of maximal 600µm below the dura. The orientation of the image plain was controlled by scanning the dura mater prior to each imaging session. To re-identify and re-image the area of interest at later timepoints the labeled blood vessels and the stable oligodendrocytes were used as landmarks. The first imaging session was performed on the day of the operation (0dpi; ~30 minutes after operation) and imaging was repeated at day 2, 4, 6/7, 8, 11, 14, 21 and 28.

6.2.1 Image processing and analysis

Recorded image stacks were processed and analyzed using the Fiji (based on ImageJ 1.48i) software. To reduce technical noise, stacks were slightly smoothed using two-dimensional Gaussian filter (sigma=0.7–1.0) and in some cases background was reduced using Subtract Background (radius=50-500). Cells of interest were identified and the channel showing the blood vessels together with the stable oligodendrocytes were used to re-identify the cells at the different timepoints. For each cell and timepoint the approximate distance to the dura (visible due to second harmonic signal in the blue channel) and to the injury core was measured and the morphological characteristics and position changes were analyzed. A cell was considered as polarized, when the

majority of processes are orientated towards one direction, often combined with a transformation and elongation of the cell body. The directionality of the polarization was assessed by subdividing the area surrounding the cell in 4 quadrants. The quadrant, in which the lesion site was placed in the center, was considered as PW direction and the remaining 3 quadrants as not PW direction. Cells were then categorized according to their reaction and timepoint and for each group percentages of the respective traits were calculated and compared to the other groups. For the assessment if a reaction category was new or old (Figure 8) the traits of the mother cell were counted for the two daughter cells as preliminary reaction. For the reaction profiles (Figure 6E and F) and the distance analysis (Figure 14F and G) 254 cells from 8 animals were pooled for d0-d2 (Figure 6E) and 222 cells from 6 animals for d2-d4 (Figure 14F). Also for the different reaction profiles (Figure 8D-I) 254 cells from 8 animals and 222 cells from 6 animals were analyzed for 2 and 4dpi respectively. Additionally 144 cells from 4 animals (6dpi), 148 cells from 4 animals (8dpi), 115 cells from 3 animals (11dpi), 151 cells from 4 animals (21dpi), 110 animals from 3 animals (28dpi) and 199 cells from 3 animals for the control were analyzed for the later timepoints. For the stab wound paradigm (Figure 14C and D) 121 cells from 3 animals were compared to the 254 cells (2dpi; PWI). The analysis of the cells in the injury core (Figure 15B and C) includes 34 cells from 7 animals (2dpi) and 23 cells from 4 animals (4dpi). The velocity and maximum migration (Figure 11E and F) assays comprise 115 cells from 3 animals (14dpi) additionally to the cells used for Figure 8D-I. For the follow-up profiling (Figure 9, Figure 10, Figure 11 and Figure 12) 157 cells from 6 animals were analyzed.

6.2.2 Hypertrophy analysis

For the analysis of volume change in hypertrophic cells 116 cells (n=64 hypertrophic cells and n=52 non-hypertrophic cells) from 10 different animals were selected for the injured conditions. For the control conditions n=28 cells from 3 animals were selected. Each cell was identified at the first and the consecutive imaging timepoint and a small stack containing the cell body together with the major processes was cut out for each timepoint. These pairs of stacks of each cell were then further processed and analyzed by Felix Buggenthin.

6.3 Immunohistochemistry

Animals at different timepoints after the injury (2, 4, 7, 14, 28 dpi and nonlesioned site) were anaesthetized and transcardially perfused with 4% paraformaldehyde (PFA). The collected brains were postfixed in 4% PFA for 30 minutes followed by cryoprotection in 30% sucrose. 30µm thick

sections were cut and stained, after blocking with the goat serum containing blocking solution and subsequent washing steps with PBS, with the following primary antibodies: rabbit (rb)-NG2 (1:500, AB5320 Millipore), m-GFAP (1:500, G3893 Sigma-Aldrich) and chick-GFP (1:500, GFP-1020 Aves Lab). After incubation over night at 5°C, secondary antibodies were chosen: anti-chick A488 (1:500, A11039 Life Technologies), anti-rb Cy3 or A647 (1:500, 711-165-152 or 111-605-144 Dianova) and anti-m Cy3 or Dylight 649 (1:500, 115-165-003 or 115-496-072 Dianova) according to the primary antibodies fluorochrome conjugated and the sections were incubated with the secondary antibodies for 2 hours at room temperature. Additionally nuclei were stained with DAPI (4',6-diamidino-2-phenylindole, 1:10000, D9564 Sigma Aldrich). Multi-channel confocal images were obtained using a Zeiss confocal microscope system (LSM 710) and analyzed using the cell counter plug-in for FIJI (http://fiji.sc/Fiji based on ImageJ 1.48i). Analysis was performed on 3 sections of 3 animals for each timepoint. The area spanning 50µm around the lesion core (identified using GFAP staining) was counted until up to ~350µm below the pial surface with an image depth of ~10µm. A total number of 1167 cells were counted. The numbers of NG2+ cells at the different timepoints after injury were statistically tested using one-way ANOVA combined with a Tukey post-test.

6.4 Statistics

Statistics was performed on the non-pooled datasets. Results are represented as means or as mean+SEM. The sample size ($n \geq 3$ animals) was justified by experience from previous studies and no exclusion of data points or datasets were performed. For the analysis no randomization was used and the investigator was not blinded to the group allocation during the experiment or analysis. As we expect our data to be normally distributed and the majority of assessable experiments including at least 5 data points passed the Kolmogorov-Smirnov test (with Dallal-Wilkinson-Lilliefor P-value) for a Gaussian distribution, we used unpaired t-test or one-way ANOVA with Tukey post-test for grouped analysis. For the data which was not normally distributed Wilcoxon Rank Sum Test was used. The sample size of $n \geq 3$ was justified by the experience from previous studies. Data were considered as significant with $p<0.05$ *, $p<0.01$ ** and $p<0.0001$ ***. Statistics was performed with GraphPad Prism 5.0.

7 References

Abbott NJ (2002) Astrocyte-endothelial interactions and blood-brain barrier permeability. J Anat 200:629-638.

Acaz-Fonseca E, Duran JC, Carrero P, Garcia-Segura LM, Arevalo MA (2015) Sex differences in glia reactivity after cortical brain injury. Glia 63:1966-1981.

Agresti C, Meomartini ME, Amadio S, Ambrosini E, Serafini B, Franchini L, Volonte C, Aloisi F, Visentin S (2005) Metabotropic P2 receptor activation regulates oligodendrocyte progenitor migration and development. Glia 50:132-144.

Aguirre A, Gallo V (2004) Postnatal neurogenesis and gliogenesis in the olfactory bulb from NG2-expressing progenitors of the subventricular zone. J Neurosci 24:10530-10541.

Aguirre AA, Chittajallu R, Belachew S, Gallo V (2004) NG2-expressing cells in the subventricular zone are type C-like cells and contribute to interneuron generation in the postnatal hippocampus. J Cell Biol 165:575-589.

Allen WE, Zicha D, Ridley AJ, Jones GE (1998) A role for Cdc42 in macrophage chemotaxis. J Cell Biol 141:1147-1157.

Anthony DC, Couch Y (2014) The systemic response to CNS injury. Exp Neurol 258:105-111.

Anthony DC, Couch Y, Losey P, Evans MC (2012) The systemic response to brain injury and disease. Brain Behav Immun 26:534-540.

Arai K, Lok J, Guo S, Hayakawa K, Xing C, Lo EH (2011) Cellular mechanisms of neurovascular damage and repair after stroke. J Child Neurol 26:1193-1198.

Arnett HA, Mason J, Marino M, Suzuki K, Matsushima GK, Ting JP (2001) TNF alpha promotes proliferation of oligodendrocyte progenitors and remyelination. Nat Neurosci 4:1116-1122.

Back SA (2014) Cerebral white and gray matter injury in newborns: new insights into pathophysiology and management. Clin Perinatol 41:1-24.

Bacon C, Lakics V, Machesky L, Rumsby M (2007) N-WASP regulates extension of filopodia and processes by oligodendrocyte progenitors, oligodendrocytes, and Schwann cells-implications for axon ensheathment at myelination. Glia 55:844-858.

Balasingam V, Tejada-Berges T, Wright E, Bouckova R, Yong VW (1994) Reactive astrogliosis in the neonatal mouse brain and its modulation by cytokines. J Neurosci 14:846-856.

Banerjee S, Bhat MA (2008) Glial ensheathment of peripheral axons in Drosophila. J Neurosci Res 86:1189-1198.

Bardehle S, Kruger M, Buggenthin F, Schwausch J, Ninkovic J, Clevers H, Snippert HJ, Theis FJ, Meyer-Luehmann M, Bechmann I, Dimou L, Gotz M (2013) Live imaging of astrocyte responses to acute injury reveals selective juxtavascular proliferation. Nat Neurosci 16:580-586.

Barnabe-Heider F, Goritz C, Sabelstrom H, Takebayashi H, Pfrieger FW, Meletis K, Frisen J (2010) Origin of new glial cells in intact and injured adult spinal cord. Cell Stem Cell 7:470-482.

Barres BA, Koroshetz WJ, Swartz KJ, Chun LL, Corey DP (1990) Ion channel expression by white matter glia: the O-2A glial progenitor cell. Neuron 4:507-524.

Batchelor PE, Tan S, Wills TE, Porritt MJ, Howells DW (2008) Comparison of Inflammation in the Brain and Spinal Cord following Mechanical Injury. J Neurotrauma 25:1217-1225.

Bauer NG, Richter-Landsberg C, Ffrench-Constant C (2009) Role of the oligodendroglial cytoskeleton in differentiation and myelination. Glia 57:1691-1705.

Baumann N, Pham-Dinh D (2001) Biology of oligodendrocyte and myelin in the mammalian central nervous system. Physiol Rev 81:871-927.

Behrendt G, Baer K, Buffo A, Curtis MA, Faull RL, Rees MI, Gotz M, Dimou L (2013) Dynamic changes in myelin aberrations and oligodendrocyte generation in chronic amyloidosis in mice and men. Glia 61:273-286.

Belachew S, Chittajallu R, Aguirre AA, Yuan X, Kirby M, Anderson S, Gallo V (2003) Postnatal NG2 proteoglycan-expressing progenitor cells are intrinsically multipotent and generate functional neurons. J Cell Biol 161:169-186.

Bercury KK, Macklin WB (2015) Dynamics and mechanisms of CNS myelination. Dev Cell 32:447-458.

Bergles DE, Roberts JD, Somogyi P, Jahr CE (2000) Glutamatergic synapses on oligodendrocyte precursor cells in the hippocampus. Nature 405:187-191.

Biname F, Sakry D, Dimou L, Jolivel V, Trotter J (2013) NG2 regulates directional migration of oligodendrocyte precursor cells via Rho GTPases and polarity complex proteins. J Neurosci 33:10858-10874.

Birbrair A, Zhang T, Files DC, Mannava S, Smith T, Wang ZM, Messi ML, Mintz A, Delbono O (2014) Type-1 pericytes accumulate after tissue injury and produce collagen in an organ-dependent manner. Stem Cell Res Ther 5:122.

Birey F, Aguirre A (2015) Age-Dependent Netrin-1 Signaling Regulates NG2+ Glial Cell Spatial Homeostasis in Normal Adult Gray Matter. J Neurosci 35:6946-6951.

Blaauw E, van Nieuwenhoven FA, Willemsen P, Delhaas T, Prinzen FW, Snoeckx LH, van Bilsen M, van der Vusse GJ (2010) Stretch-induced hypertrophy of isolated adult rabbit cardiomyocytes. J Cardiovasc Transl Red 6: 861-869.

Blakemore WF, Franklin RJ (2008) Remyelination in experimental models of toxin-induced demyelination. Curr Top Microbiol Immunol 318:193-212.

Blaustein MP, Lederer WJ (1999) Sodium/calcium exchange: its physiological implications. Physiol Rev 79:763-854.

Boda E, Di Maria S, Rosa P, Taylor V, Abbracchio MP, Buffo A (2015) Early phenotypic asymmetry of sister oligodendrocyte progenitor cells after mitosis and its modulation by aging and extrinsic factors. Glia 63:271-286.

Boda E, Vigano F, Rosa P, Fumagalli M, Labat-Gest V, Tempia F, Abbracchio MP, Dimou L, Buffo A (2011) The GPR17 receptor in NG2 expressing cells: focus on in vivo cell maturation and participation in acute trauma and chronic damage. Glia 59:1958-1973.

Bouzier-Sore AK, Pellerin L (2013) Unraveling the complex metabolic nature of astrocytes. Front Cell Neurosci 7:179.

Brill MS, Ninkovic J, Winpenny E, Hodge RD, Ozen I, Yang R, Lepier A, Gascon S, Erdelyi F, Szabo G, Parras C, Guillemot F, Frotscher M, Berninger B, Hevner RF, Raineteau O, Gotz M (2009) Adult generation of glutamatergic olfactory bulb interneurons. Nat Neurosci 12:1524-1533.

Buffo A (2007) Fate determinant expression in the lesioned brain: Olig2 induction and its implications for neuronal repair. Neurodegener Dis 4:328-332.

Buffo A, Vosko MR, Erturk D, Hamann GF, Jucker M, Rowitch D, Gotz M (2005) Expression pattern of the transcription factor Olig2 in response to brain injuries: implications for neuronal repair. Proc Natl Acad Sci U S A 102:18183-18188.

Buffo A, Rite I, Tripathi P, Lepier A, Colak D, Horn AP, Mori T, Gotz M (2008) Origin and progeny of reactive gliosis: A source of multipotent cells in the injured brain. Proc Natl Acad Sci U S A 105:3581-3586.

Burda JE, Sofroniew MV (2014) Reactive gliosis and the multicellular response to CNS damage and disease. Neuron 81:229-248.

Burnside ER, Bradbury EJ (2014) Review: Manipulating the extracellular matrix and its role in brain and spinal cord plasticity and repair. Neuropathol Appl Neurobiol 40:26-59.

Busch SA, Horn KP, Cuascut FX, Hawthorne AL, Bai L, Miller RH, Silver J (2010) Adult NG2+ cells are permissive to neurite outgrowth and stabilize sensory axons during macrophage-induced axonal dieback after spinal cord injury. J Neurosci 30:255-265.

Bush TG, Puvanachandra N, Horner CH, Polito A, Ostenfeld T, Svendsen CN, Mucke L, Johnson MH, Sofroniew MV (1999) Leukocyte infiltration, neuronal degeneration, and neurite outgrowth after ablation of scar-forming, reactive astrocytes in adult transgenic mice. Neuron 23:297-308.

Butt AM (2011) ATP: a ubiquitous gliotransmitter integrating neuron-glial networks. Semin Cell Dev Biol 22:205-213.

Cai J, Qi Y, Hu X, Tan M, Liu Z, Zhang J, Li Q, Sander M, Qiu M (2005) Generation of oligodendrocyte precursor cells from mouse dorsal spinal cord independent of Nkx6 regulation and Shh signaling. Neuron 45:41-53.

Camand E, Morel MP, Faissner A, Sotelo C, Dusart I (2004) Long-term changes in the molecular composition of the glial scar and progressive increase of serotoninergic fibre sprouting after hemisection of the mouse spinal cord. Eur J Neurosci 20:1161-1176.

Cao L, Wei D, Reid B, Zhao S, Pu J, Pan T, Yamoah E, Zhao M (2013) Endogenous electric currents might guide rostral migration of neuroblasts. EMBO reports 14:184-190.

Cappello S, Attardo A, Wu X, Iwasato T, Itohara S, Wilsch-Brauninger M, Eilken HM, Rieger MA, Schroeder TT, Huttner WB, Brakebusch C, Gotz M (2006) The Rho-GTPase cdc42 regulates neural progenitor fate at the apical surface. Nat Neurosci 9:1099-1107.

Carlen M, Meletis K, Goritz C, Darsalia V, Evergren E, Tanigaki K, Amendola M, Barnabe-Heider F, Yeung MSY, Naldini L, Honjo T, Kokaia Z, Shupliakov O, Cassidy RM, Lindvall O, Frisen J (2009) Forebrain ependymal cells are Notch-dependent and generate neuroblasts and astrocytes after stroke. Nat Neurosci 12:259-267.

Casano AM, Peri F (2015) Microglia: multitasking specialists of the brain. Dev Cell 32:469-477.

Cau J, Hall A (2005) Cdc42 controls the polarity of the actin and microtubule cytoskeletons through two distinct signal transduction pathways. J Cell Sci 118:2579-2587.

Cernak I, Vink R, Zapple DN, Cruz MI, Ahmed F, Chang T, Fricke ST, Faden AI (2004) The pathobiology of moderate diffuse traumatic brain injury as identified using a new experimental model of injury in rats. Neurobiol Dis 17:29-43.

Chang A, Tourtellotte WW, Rudick R, Trapp BD (2002) Premyelinating oligodendrocytes in chronic lesions of multiple sclerosis. N Engl J Med 346:165-173.

Chang A, Nishiyama A, Peterson J, Prineas J, Trapp BD (2000) NG2-positive oligodendrocyte progenitor cells in adult human brain and multiple sclerosis lesions. J Neurosci 20:6404-6412.

Chatterjee N, Stegmuller J, Schatzle P, Karram K, Koroll M, Werner HB, Nave KA, Trotter J (2008) Interaction of syntenin-1 and the NG2 proteoglycan in migratory oligodendrocyte precursor cells. J Biol Chem 283:8310-8317.

Chekenya M, Pilkington GJ (2002) NG2 precursor cells in neoplasia: functional, histogenesis and therapeutic implications for malignant brain tumours. J Neurocytol 31:507-521.

Chen LX, Ma SM, Zhang P, Fan ZC, Xiong M, Cheng GQ, Yang Y, Qiu ZL, Zhou WH, Li J (2015) Neuroprotective effects of oligodendrocyte progenitor cell transplantation in premature rat brain following hypoxic-ischemic injury. PloS one 10:e0115997.

Chen Y, Wu H, Wang S, Koito H, Li J, Ye F, Hoang J, Escobar SS, Gow A, Arnett HA, Trapp BD, Karandikar NJ, Hsieh J, Lu QR (2009) The oligodendrocyte-specific G protein-coupled receptor GPR17 is a cell-intrinsic timer of myelination. Nat Neurosci 12:1398-1406.

Chittajallu R, Aguirre A, Gallo V (2004) NG2-positive cells in the mouse white and grey matter display distinct physiological properties. J Physiol 561:109-122.

Clarke LE, Young KM, Hamilton NB, Li H, Richardson WD, Attwell D (2012) Properties and fate of oligodendrocyte progenitor cells in the corpus callosum, motor cortex, and piriform cortex of the mouse. J Neurosci 32:8173-8185.

Clemente D, Ortega MC, Arenzana FJ, de Castro F (2011) FGF-2 and Anosmin-1 are selectively expressed in different types of multiple sclerosis lesions. J Neurosci 31:14899-14909.

Clemente D, Ortega MC, Melero-Jerez C, de Castro F (2013) The effect of glia-glia interactions on oligodendrocyte precursor cell biology during development and in demyelinating diseases. Front Cell Neurosci 7:00268.

Cregg JM, DePaul MA, Filous AR, Lang BT, Tran A, Silver J (2014) Functional regeneration beyond the glial scar. Exp Neurol 253:197-207.

Cruz JC, Tseng HC, Goldman JA, Shih H, Tsai LH (2003) Aberrant Cdk5 activation by p25 triggers pathological events leading to neurodegeneration and neurofibrillary tangles. Neuron 40:471-483.

Cui QL, Fogle E, Almazan G (2006) Muscarinic acetylcholine receptors mediate oligodendrocyte progenitor survival through Src-like tyrosine kinases and PI3K/Akt pathways. Neurochem Int 48:383-393.

Cui QL, Kuhlmann T, Miron VE, Leong SY, Fang J, Gris P, Kennedy TE, Almazan G, Antel J (2013) Oligodendrocyte progenitor cell susceptibility to injury in multiple sclerosis. Am J Pathol 183:516-525.

Dalkara T, Gursoy-Ozdemir Y, Yemisci M (2011) Brain microvascular pericytes in health and disease. Acta Neuropathol 122:1-9.

Dawson MR, Levine JM, Reynolds R (2000) NG2-expressing cells in the central nervous system: are they oligodendroglial progenitors? J Neurosci Res 61:471-479.

Dawson MR, Polito A, Levine JM, Reynolds R (2003) NG2-expressing glial progenitor cells: an abundant and widespread population of cycling cells in the adult rat CNS. Mol Cell Neurosci 24:476-488.

De Biase LM, Nishiyama A, Bergles DE (2010) Excitability and synaptic communication within the oligodendrocyte lineage. J Neurosci 30:3600-3611.

Dean JM, Shi Z, Fleiss B, Gunn KC, Groenendaal F, van Bel F, Derrick M, Juul SE, Tan S, Gressens P, Mallard C, Bennet L, Gunn AJ (2015) A Critical Review of Models of Perinatal Infection. Dev Neurosci 37:289-304.

Del Bigio MR (2010) Ependymal cells: biology and pathology. Acta neuropathologica 119:55-73.

DeRuiter MC, Poelmann RE, VanMunsteren JC, Mironov V, Markwald RR, Gittenberger-de Groot AC (1997) Embryonic endothelial cells transdifferentiate into mesenchymal cells expressing smooth muscle actins in vivo and in vitro. Circ Res 80:444-451.

Di Bello IC, Dawson MR, Levine JM, Reynolds R (1999) Generation of oligodendroglial progenitors in acute inflammatory demyelinating lesions of the rat brain stem is associated with demyelination rather than inflammation. J Neurocytol 28:365-381.

Dimou L, Gotz M (2014) Glial cells as progenitors and stem cells: new roles in the healthy and diseased brain. Physiol Rev 94:709-737.

Dimou L, Gallo V (2015) NG2-glia and their functions in the central nervous system. Glia 63:1429-1451.

Dimou L, Simon C, Kirchhoff F, Takebayashi H, Gotz M (2008) Progeny of Olig2-expressing progenitors in the gray and white matter of the adult mouse cerebral cortex. J Neurosci 28:10434-10442.

Dore-Duffy P, Katychev A, Wang X, Van Buren E (2006) CNS microvascular pericytes exhibit multipotential stem cell activity. J Cereb Blood Flow Metab 26:613-624.

Dore-Duffy P, Balabanov R, Beaumont T, Hritz MA, Harik SI, LaManna JC (1999) Endothelial activation following prolonged hypobaric hypoxia. Microvasc Res 57:75-85.

Dore-Duffy P, Mehedi A, Wang X, Bradley M, Trotter R, Gow A (2011) Immortalized CNS pericytes are quiescent smooth muscle actin-negative and pluripotent. Microvasc Res 82:18-27.

Duncan AW (2013) Aneuploidy, polyploidy and ploidy reversal in the liver. Semin Cell Dev Biol 24:347-356.

Eisenmann KM, McCarthy JB, Simpson MA, Keely PJ, Guan JL, Tachibana K, Lim L, Manser E, Furcht LT, Iida J (1999) Melanoma chondroitin sulphate proteoglycan regulates cell spreading through Cdc42, Ack-1 and p130cas. Nat Cell Biol 1:507-513.

Etienne-Manneville S (2006) In vitro assay of primary astrocyte migration as a tool to study Rho GTPase function in cell polarization. Methods Enzymol 406:565-578.

Etienne-Manneville S, Hall A (2002) Rho GTPases in cell biology. Nature 420:629-635.

Fabry Z, Fitzsimmons KM, Herlein JA, Moninger TO, Dobbs MB, Hart MN (1993) Production of the cytokines interleukin 1 and 6 by murine brain microvessel endothelium and smooth muscle pericytes. J Neuroimmunol 47:23-34.

Faulkner JR, Herrmann JE, Woo MJ, Tansey KE, Doan NB, Sofroniew MV (2004) Reactive astrocytes protect tissue and preserve function after spinal cord injury. J Neurosci 24:2143-2155.

Fawcett JW, Asher RA (1999) The glial scar and central nervous system repair. Brain Res Bull 49:377-391.

Feeney DM, Boyeson MG, Linn RT, Murray HM, Dail WG (1981) Responses to cortical injury: I. Methodology and local effects of contusions in the rat. Brain Res 211:67-77.

Fenstermacher J, Gross P, Sposito N, Acuff V, Pettersen S, Gruber K (1988) Structural and functional variations in capillary systems within the brain. Ann N Y Acad Sci 529:21-30.

Fern RF, Matute C, Stys PK (2014) White matter injury: Ischemic and nonischemic. Glia 62:1780-1789.

Fernandez-Klett F, Offenhauser N, Dirnagl U, Priller J, Lindauer U (2010) Pericytes in capillaries are contractile in vivo, but arterioles mediate functional hyperemia in the mouse brain. Proc Natl Acad Sci U S A 107:22290-22295.

Filipovic R, Zecevic N (2008) The effect of CXCL1 on human fetal oligodendrocyte progenitor cells. Glia 56:1-15.

Filous AR, Tran A, Howell CJ, Busch SA, Evans TA, Stallcup WB, Kang SH, Bergles DE, Lee SI, Levine JM, Silver J (2014) Entrapment via Synaptic-Like Connections between NG2 Proteoglycan+ Cells and Dystrophic Axons in the Lesion Plays a Role in Regeneration Failure after Spinal Cord Injury. J Neurosci 34:16369-16384.

Franklin RJ, Ffrench-Constant C (2008) Remyelination in the CNS: from biology to therapy. Nat Rev Neurosci 9:839-855.

Freitas-Andrade M, Naus CC (2015) Astrocytes in neuroprotection and neurodegeneration: The role of connexin43 and pannexin1. Neuroscience 323:207-221.

Frohlich N, Nagy B, Hovhannisyan A, Kukley M (2011) Fate of neuron-glia synapses during proliferation and differentiation of NG2 cells. J Anat 219:18-32.

Frosina G (2015) Limited advances in therapy of glioblastoma trigger re-consideration of research policy. Crit Rev Oncol Hematol 96:257-261.

Fuchs S, Herzog D, Sumara G, Buchmann-Moller S, Civenni G, Wu X, Chrostek-Grashoff A, Suter U, Ricci R, Relvas JB, Brakebusch C, Sommer L (2009) Stage-specific control of neural crest stem cell proliferation by the small rho GTPases Cdc42 and Rac1. Cell Stem Cell 4:236-247.

Fukushi J, Makagiansar IT, Stallcup WB (2004) NG2 proteoglycan promotes endothelial cell motility and angiogenesis via engagement of galectin-3 and alpha3beta1 integrin. Mol Biol Cell 15:3580-3590.

Funfschilling U, Supplie LM, Mahad D, Boretius S, Saab AS, Edgar J, Brinkmann BG, Kassmann CM, Tzvetanova ID, Mobius W, Diaz F, Meijer D, Suter U, Hamprecht B, Sereda MW, Moraes CT, Frahm J, Goebbels S, Nave KA (2012) Glycolytic oligodendrocytes maintain myelin and long-term axonal integrity. Nature 485:517-521.

Galko MJ, Krasnow MA (2004) Cellular and genetic analysis of wound healing in Drosophila larvae. PLoS biology 2:E239.

Gallo V, Mangin JM, Kukley M, Dietrich D (2008) Synapses on NG2-expressing progenitors in the brain: multiple functions? J Physiol 586:3767-3781.

Garvalov BK, Flynn KC, Neukirchen D, Meyn L, Teusch N, Wu X, Brakebusch C, Bamburg JR, Bradke F (2007) Cdc42 regulates cofilin during the establishment of neuronal polarity. J Neurosci 27:13117-13129.

Gensert JM, Goldman JE (1997) Endogenous progenitors remyelinate demyelinated axons in the adult CNS. Neuron 19:197-203.

Ghiani CA, Eisen AM, Yuan X, DePinho RA, McBain CJ, Gallo V (1999) Neurotransmitter receptor activation triggers p27(Kip1)and p21(CIP1) accumulation and G1 cell cycle arrest in oligodendrocyte progenitors. Development 126:1077-1090.

Gibson EM, Purger D, Mount CW, Goldstein AK, Lin GL, Wood LS, Inema I, Miller SE, Bieri G, Zuchero JB, Barres BA, Woo PJ, Vogel H, Monje M (2014) Neuronal activity promotes oligodendrogenesis and adaptive myelination in the mammalian brain. Science 344:1252304.

Ginhoux F, Greter M, Leboeuf M, Nandi S, See P, Gokhan S, Mehler MF, Conway SJ, Ng LG, Stanley ER, Samokhvalov IM, Merad M (2010) Fate mapping analysis reveals that adult microglia derive from primitive macrophages. Science 330:841-845.

Giorgio A, Watkins KE, Douaud G, James AC, James S, De Stefano N, Matthews PM, Smith SM, Johansen-Berg H (2008) Changes in white matter microstructure during adolescence. NeuroImage 39:52-61.

Go AS et al. (2014) Heart disease and stroke statistics--2014 update: a report from the American Heart Association. Circulation 129:e28-e292.

Gomez Perdiguero E, Klapproth K, Schulz C, Busch K, Azzoni E, Crozet L, Garner H, Trouillet C, de Bruijn MF, Geissmann F, Rodewald HR (2015) Tissue-resident macrophages originate from yolk-sac-derived erythro-myeloid progenitors. Nature 518:547-551.

Goritz C, Dias DO, Tomilin N, Barbacid M, Shupliakov O, Frisen J (2011) A pericyte origin of spinal cord scar tissue. Science 333:238-242.

Greenhalgh AD, David S (2014) Differences in the phagocytic response of microglia and peripheral macrophages after spinal cord injury and its effects on cell death. J Neurosci 34:6316-6322.

Greenwood K, Butt AM (2003) Evidence that perinatal and adult NG2-glia are not conventional oligodendrocyte progenitors and do not depend on axons for their survival. Mol Cell Neurosci 23:544-558.

Gudz TI, Komuro H, Macklin WB (2006) Glutamate stimulates oligodendrocyte progenitor migration mediated via an alphav integrin/myelin proteolipid protein complex. J Neurosci 26:2458-2466.

Guo F, Maeda Y, Ma J, Xu J, Horiuchi M, Miers L, Vaccarino F, Pleasure D (2010) Pyramidal neurons are generated from oligodendroglial progenitor cells in adult piriform cortex. J Neurosci 30:12036-12049.

Gurtner GC, Werner S, Barrandon Y, Longaker MT (2008) Wound repair and regeneration. Nature 453:314-321.

Gyoneva S, Ransohoff RM (2015) Inflammatory reaction after traumatic brain injury: therapeutic potential of targeting cell-cell communication by chemokines. Trends Pharmacol Sci 36:471-480.

Hall A (1998) Rho GTPases and the actin cytoskeleton. Science 279:509-514.

Hall A (2005) Rho GTPases and the control of cell behaviour. Biochem Soc Trans 33:891-895.

Hamilton N, Vayro S, Wigley R, Butt AM (2010) Axons and astrocytes release ATP and glutamate to evoke calcium signals in NG2-glia. Glia 58:66-79.

Hampton DW, Rhodes KE, Zhao C, Franklin RJ, Fawcett JW (2004) The responses of oligodendrocyte precursor cells, astrocytes and microglia to a cortical stab injury, in the brain. Neuroscience 127:813-820.

Hanisch UK, Kettenmann H (2007) Microglia: active sensor and versatile effector cells in the normal and pathologic brain. Nat Neurosci 10:1387-1394.

Hartley MD, Altowaijri G, Bourdette D (2014) Remyelination and multiple sclerosis: therapeutic approaches and challenges. Curr Neurol Neurosci Rep 14:014-0485.

Hayakawa K, Pham LD, Som AT, Lee BJ, Guo S, Lo EH, Arai K (2011) Vascular endothelial growth factor regulates the migration of oligodendrocyte precursor cells. J Neurosci 31:10666-10670.

Heinrich C, Bergami M, Gascon S, Lepier A, Vigano F, Dimou L, Sutor B, Berninger B, Gotz M (2014) Sox2-mediated conversion of NG2 glia into induced neurons in the injured adult cerebral cortex. Stem Cell Reports 3:1000-1014.

Herculano-Houzel S (2009) The human brain in numbers: a linearly scaled-up primate brain. Front Hum Neurosci 3:31.

Hietakangas V, Cohen SM (2009) Regulation of Tissue Growth through Nutrient Sensing. Annu Rev Genet 43:389-410.

Hildebrand C, Remahl S, Persson H, Bjartmar C (1993) Myelinated nerve fibres in the CNS. Prog Neurobiol 40:319-384.

Hill RA, Natsume R, Sakimura K, Nishiyama A (2011) NG2 cells are uniformly distributed and NG2 is not required for barrel formation in the somatosensory cortex. Mol Cell Neurosci 46:689-698.

Hill RA, Patel KD, Medved J, Reiss AM, Nishiyama A (2013) NG2 cells in white matter but not gray matter proliferate in response to PDGF. J Neurosci 33:14558-14566.

Hill RA, Patel KD, Goncalves CM, Grutzendler J, Nishiyama A (2014) Modulation of oligodendrocyte generation during a critical temporal window after NG2 cell division. Nat Neurosci 17:1518-1527.

Hines DJ, Hines RM, Mulligan SJ, Macvicar BA (2009) Microglia processes block the spread of damage in the brain and require functional chloride channels. Glia 57:1610-1618.

Holtje M, Hoffmann A, Hofmann F, Mucke C, Grosse G, Van Rooijen N, Kettenmann H, Just I, Ahnert-Hilger G (2005) Role of Rho GTPase in astrocyte morphology and migratory response during in vitro wound healing. J Neurochem 95:1237-1248.

Honda H, Ogita Y, Higuchi S, Kani K (1982) Cell movements in a living mammalian tissue: Long-term observation of individual cells in wounded corneal endothelia of cats. J Morphol 174:25-39.

Horner PJ, Thallmair M, Gage FH (2002) Defining the NG2-expressing cell of the adult CNS. J Neurocytol 31:469-480.

Horner PJ, Power AE, Kempermann G, Kuhn HG, Palmer TD, Winkler J, Thal LJ, Gage FH (2000) Proliferation and differentiation of progenitor cells throughout the intact adult rat spinal cord. J Neurosci 20:2218-2228.

Hostenbach S, Cambron M, D'Haeseleer M, Kooijman R, De Keyser J (2014) Astrocyte loss and astrogliosis in neuroinflammatory disorders. Neurosci Lett 565:39-41.

Huang W, Zhao N, Bai X, Karram K, Trotter J, Goebbels S, Scheller A, Kirchhoff F (2014) Novel NG2-CreERT2 knock-in mice demonstrate heterogeneous differentiation potential of NG2 glia during development. Glia 62:896-913.

Hughes EG, Kang SH, Fukaya M, Bergles DE (2013) Oligodendrocyte progenitors balance growth with self-repulsion to achieve homeostasis in the adult brain. Nat Neurosci 16:668-676.

Ikebe H, Takamatsu T, Itoi M, Fujita S (1988) Changes in nuclear DNA content and cell size of injured human corneal endothelium. Exp Eye Res 47:205-215.

Johansson CB, Momma S, Clarke DL, Risling M, Lendahl U, Frisén J (1999) Identification of a Neural Stem Cell in the Adult Mammalian Central Nervous System. Cell 96:25-34.

Joyce NC, Haire MF, Palade GE (1985) Contractile proteins in pericytes. II. Immunocytochemical evidence for the presence of two isomyosins in graded concentrations. J Cell Biol 100:1387-1395.

Kang SH, Fukaya M, Yang JK, Rothstein JD, Bergles DE (2010) NG2+ CNS glial progenitors remain committed to the oligodendrocyte lineage in postnatal life and following neurodegeneration. Neuron 68:668-681.

Kang SH, Li Y, Fukaya M, Lorenzini I, Cleveland DW, Ostrow LW, Rothstein JD, Bergles DE (2013) Degeneration and impaired regeneration of gray matter oligodendrocytes in amyotrophic lateral sclerosis. Nat Neurosci 16:571-579.

Karadottir R, Hamilton NB, Bakiri Y, Attwell D (2008) Spiking and nonspiking classes of oligodendrocyte precursor glia in CNS white matter. Nat Neurosci 11:450-456.

Karram K, Goebbels S, Schwab M, Jennissen K, Seifert G, Steinhauser C, Nave KA, Trotter J (2008) NG2-expressing cells in the nervous system revealed by the NG2-EYFP-knockin mouse. Genesis 46:743-757.

Keirstead HS, Levine JM, Blakemore WF (1998) Response of the oligodendrocyte progenitor cell population (defined by NG2 labelling) to demyelination of the adult spinal cord. Glia 22:161-170.

Kermer P, Klocker N, Bahr M (1999) Neuronal death after brain injury. Models, mechanisms, and therapeutic strategies in vivo. Cell Tissue Res 298:383-395.

Kessaris N, Fogarty M, Iannarelli P, Grist M, Wegner M, Richardson WD (2006) Competing waves of oligodendrocytes in the forebrain and postnatal elimination of an embryonic lineage. Nat Neurosci 9:173-179.

Kettenmann H, Hanisch UK, Noda M, Verkhratsky A (2011) Physiology of microglia. Physiol Rev 91:461-553.

Kierdorf K et al. (2013) Microglia emerge from erythromyeloid precursors via Pu.1- and Irf8-dependent pathways. Nat Neurosci 16:273-280.

Kigerl K, Popovich P (2006) Drug evaluation: ProCord - a potential cell-based therapy for spinal cord injury. IDrugs 9:354-360.

Klein MA, Moller JC, Jones LL, Bluethmann H, Kreutzberg GW, Raivich G (1997) Impaired neuroglial activation in interleukin-6 deficient mice. Glia 19:227-233.

Komitova M, Serwanski DR, Lu QR, Nishiyama A (2011) NG2 cells are not a major source of reactive astrocytes after neocortical stab wound injury. Glia 59:800-809.

Kou Z, VandeVord PJ (2014) Traumatic white matter injury and glial activation: from basic science to clinics. Glia 62:1831-1855.

Koushik SV, Wang J, Rogers R, Moskophidis D, Lambert NA, Creazzo TL, Conway SJ (2001) Targeted inactivation of the sodium-calcium exchanger (Ncx1) results in the lack of a heartbeat and abnormal myofibrillar organization. FASEB J 15:1209-1211.

Kremer D, Kury P, Dutta R (2015) Promoting remyelination in multiple sclerosis: current drugs and future prospects. Mult Scler 21:541-549.

Krenning G, Zeisberg EM, Kalluri R (2010) The origin of fibroblasts and mechanism of cardiac fibrosis. J Cell Physiol 225:631-637.

Krikorian JG, Guth L, Donati EJ (1981) Origin of the connective tissue scar in the transected rat spinal cord. Exp Neurol 72:698-707.

Krueger M, Bechmann I (2010) CNS pericytes: concepts, misconceptions, and a way out. Glia 58:1-10.

Kukley M, Dietrich D (2009) Kainate receptors and signal integration by NG2 glial cells. Neuron Glia Biol 5:13-20.

Lalancette-Hebert M, Gowing G, Simard A, Weng YC, Kriz J (2007) Selective ablation of proliferating microglial cells exacerbates ischemic injury in the brain. J Neurosci 27:2596-2605.

Lang B, Liu HL, Liu R, Feng GD, Jiao XY, Ju G (2004) Astrocytes in injured adult rat spinal cord may acquire the potential of neural stem cells. Neuroscience 128:775-783.

Leduc C, Etienne-Manneville S (2015) Intermediate filaments in cell migration and invasion: the unusual suspects. Curr Opin Cell Biol 32:102-112.

Lee H, McKeon RJ, Bellamkonda RV (2010) Sustained delivery of thermostabilized chABC enhances axonal sprouting and functional recovery after spinal cord injury. Proc Natl Acad Sci U S A 107:3340-3345.

Lehmann R (2001) Cell migration in invertebrates: clues from border and distal tip cells. Curr Opin Genet Dev 11:457-463.

Levine J (2015) The reactions and role of NG2 glia in spinal cord injury. Brain Res 1638:199-208.

Levine JM (1994) Increased expression of the NG2 chondroitin-sulfate proteoglycan after brain injury. J Neurosci 14:4716-4730.

Levine JM, Reynolds R (1999) Activation and proliferation of endogenous oligodendrocyte precursor cells during ethidium bromide-induced demyelination. Exp Neurol 160:333-347.

Levine JM, Reynolds R, Fawcett JW (2001) The oligodendrocyte precursor cell in health and disease. Trends Neurosci 24:39-47.

Lin SC, Bergles DE (2004) Synaptic signaling between GABAergic interneurons and oligodendrocyte precursor cells in the hippocampus. Nat Neurosci 7:24-32.

Lin SC, Huck JH, Roberts JD, Macklin WB, Somogyi P, Bergles DE (2005) Climbing fiber innervation of NG2-expressing glia in the mammalian cerebellum. Neuron 46:773-785.

Liu C, Sage Jonathan C, Miller Michael R, Verhaak Roel GW, Hippenmeyer S, Vogel H, Foreman O, Bronson Roderick T, Nishiyama A, Luo L, Zong H (2011) Mosaic Analysis with Double Markers Reveals Tumor Cell of Origin in Glioma. Cell 146:209-221.

Liu J, Dietz K, DeLoyht JM, Pedre X, Kelkar D, Kaur J, Vialou V, Lobo MK, Dietz DM, Nestler EJ, Dupree J, Casaccia P (2012) Impaired adult myelination in the prefrontal cortex of socially isolated mice. Nat Neurosci 15:1621-1623.

Llorens-Bobadilla E, Zhao S, Baser A, Saiz-Castro G, Zwadlo K, Martin-Villalba A (2015) Single-Cell Transcriptomics Reveals a Population of Dormant Neural Stem Cells that Become Activated upon Brain Injury. Cell stem cell 17:329-340.

Losick Vicki P, Fox Donald T, Spradling Allan C (2013) Polyploidization and Cell Fusion Contribute to Wound Healing in the Adult Drosophila Epithelium. Curr Biol 23:2224-2232.

Ma F, Morancho A, Montaner J, Rosell A (2015) Endothelial progenitor cells and revascularization following stroke. Brain Res 1623:150-159.

Madison RD, Macklis JD (1993) Noninvasively induced degeneration of neocortical pyramidal neurons in vivo: selective targeting by laser activation of retrogradely transported photolytic chromophore. Exp Neurol 121:153-159.

Maeda Y, Solanky M, Menonna J, Chapin J, Li W, Dowling P (2001) Platelet-derived growth factor-alpha receptor-positive oligodendroglia are frequent in multiple sclerosis lesions. Ann Neurol 49:776-785.

Majumdar M, Vuori K, Stallcup WB (2003) Engagement of the NG2 proteoglycan triggers cell spreading via rac and p130cas. Cell Signal 15:79-84.

Makagiansar IT, Williams S, Dahlin-Huppe K, Fukushi J, Mustelin T, Stallcup WB (2004) Phosphorylation of NG2 proteoglycan by protein kinase C-alpha regulates polarized membrane distribution and cell motility. J Biol Chem 279:55262-55270.

Mangin JM, Gallo V (2011) The curious case of NG2 cells: transient trend or game changer? ASN Neuro 3:e00052.

Mangin JM, Kunze A, Chittajallu R, Gallo V (2008) Satellite NG2 progenitor cells share common glutamatergic inputs with associated interneurons in the mouse dentate gyrus. J Neurosci 28:7610-7623.

Mangin JM, Li P, Scafidi J, Gallo V (2012) Experience-dependent regulation of NG2 progenitors in the developing barrel cortex. Nat Neurosci 15:1192-1194.

Marmarou A, Foda MA, van den Brink W, Campbell J, Kita H, Demetriadou K (1994) A new model of diffuse brain injury in rats. Part I: Pathophysiology and biomechanics. J Neurosurg 80:291-300.

Masahira N, Takebayashi H, Ono K, Watanabe K, Ding L, Furusho M, Ogawa Y, Nabeshima Y, Alvarez-Buylla A, Shimizu K, Ikenaka K (2006) Olig2-positive progenitors in the embryonic spinal cord give rise not only to motoneurons and oligodendrocytes, but also to a subset of astrocytes and ependymal cells. Dev Biol 293:358-369.

Mato S, Alberdi E, Ledent C, Watanabe M, Matute C (2009) CB1 cannabinoid receptor-dependent and -independent inhibition of depolarization-induced calcium influx in oligodendrocytes. Glia 57:295-306.

McQueen J, Reimer MM, Holland PR, Manso Y, McLaughlin M, Fowler JH, Horsburgh K (2014) Restoration of oligodendrocyte pools in a mouse model of chronic cerebral hypoperfusion. PloS one 9:e87227.

McTigue DM, Wei P, Stokes BT (2001) Proliferation of NG2-positive cells and altered oligodendrocyte numbers in the contused rat spinal cord. J Neurosci 21:3392-3400.

Mekhail M, Almazan G, Tabrizian M (2012) Oligodendrocyte-protection and remyelination post-spinal cord injuries: a review. Prog Neurobiol 96:322-339.

Menon DK, Schwab K, Wright DW, Maas AI (2010) Position statement: definition of traumatic brain injury. Arch Phys Med Rehabil 91:1637-1640.

Mills CD (2015) Anatomy of a discovery: m1 and m2 macrophages. Front Immunol 6:212.

Ming GL, Song H (2011) Adult neurogenesis in the mammalian brain: significant answers and significant questions. Neuron 70:687-702.

Miyaoka Y, Ebato K, Kato H, Arakawa S, Shimizu S, Miyajima A (2012) Hypertrophy and Unconventional Cell Division of Hepatocytes Underlie Liver Regeneration. Curr Biol 22:1166-1175.

Moffett JR, Arun P, Ariyannur PS, Garbern JY, Jacobowitz DM, Namboodiri AM (2011) Extensive aspartoacylase expression in the rat central nervous system. Glia 59:1414-1434.

Morales DM, Marklund N, Lebold D, Thompson HJ, Pitkanen A, Maxwell WL, Longhi L, Laurer H, Maegele M, Neugebauer E, Graham DI, Stocchetti N, McIntosh TK (2005) Experimental models of traumatic brain injury: do we really need to build a better mousetrap? Neuroscience 136:971-989.

Morell P, Norton WT (1980) Myelin. Sci Am 242:88-96.

Moyon S, Dubessy AL, Aigrot MS, Trotter M, Huang JK, Dauphinot L, Potier MC, Kerninon C, Melik Parsadaniantz S, Franklin RJ, Lubetzki C (2015) Demyelination causes adult CNS progenitors to revert to an immature state and express immune cues that support their migration. J Neurosci 35:4-20.

Murray JA, Blakemore WF (1980) The relationship between internodal length and fibre diameter in the spinal cord of the cat. J Neurol Sci 45:29-41.

Najm FJ, Zaremba A, Caprariello AV, Nayak S, Freundt EC, Scacheri PC, Miller RH, Tesar PJ (2011) Rapid and robust generation of functional oligodendrocyte progenitor cells from epiblast stem cells. Nat Meth 8:957-962.

Najm FJ et al. (2015) Drug-based modulation of endogenous stem cells promotes functional remyelination in vivo. Nature 522:216-220.

Niemeier JP, Grafton LM, Chilakamarri T (2015) Treating persons with traumatic brain injury: history and updates. N C Med J 76:105-110.

Nimmerjahn A, Kirchhoff F, Helmchen F (2005) Resting microglial cells are highly dynamic surveillants of brain parenchyma in vivo. Science 308:1314-1318.

Nishiyama A, Yu M, Drazba JA, Tuohy VK (1997) Normal and reactive NG2+ glial cells are distinct from resting and activated microglia. J Neurosci Res 48:299-312.

Nobes CD, Hall A (1995) Rho, rac, and cdc42 GTPases regulate the assembly of multimolecular focal complexes associated with actin stress fibers, lamellipodia, and filopodia. Cell 81:53-62.

Nunes MC, Roy NS, Keyoung HM, Goodman RR, McKhann G, 2nd, Jiang L, Kang J, Nedergaard M, Goldman SA (2003) Identification and isolation of multipotential neural progenitor cells from the subcortical white matter of the adult human brain. Nat Med 9:439-447.

Oldendorf WH, Cornford ME, Brown WJ (1977) The large apparent work capability of the blood-brain barrier: a study of the mitochondrial content of capillary endothelial cells in brain and other tissues of the rat. Ann Neurol 1:409-417.

Osmani N, Vitale N, Borg JP, Etienne-Manneville S (2006) Scrib controls Cdc42 localization and activity to promote cell polarization during astrocyte migration. Curr Biol 16:2395-2405.

Overman JJ, Clarkson AN, Wanner IB, Overman WT, Eckstein I, Maguire JL, Dinov ID, Toga AW, Carmichael ST (2012) A role for ephrin-A5 in axonal sprouting, recovery, and activity-dependent plasticity after stroke. Proc Natl Acad Sci U S A 109:E2230-2239.

Pachner AR (2011) Experimental models of multiple sclerosis. Curr Opin Neurol 24:291-299.

Papastefanaki F, Matsas R (2015) From demyelination to remyelination: the road toward therapies for spinal cord injury. Glia 63:1101-1125.

Parras CM, Hunt C, Sugimori M, Nakafuku M, Rowitch D, Guillemot F (2007) The proneural gene Mash1 specifies an early population of telencephalic oligodendrocytes. J Neurosci 27:4233-4242.

Pekny M, Pekna M (2014) Astrocyte reactivity and reactive astrogliosis: costs and benefits. Physiol Rev 94:1077-1098.

Pelvig DP, Pakkenberg H, Stark AK, Pakkenberg B (2008) Neocortical glial cell numbers in human brains. Neurobiol Aging 29:1754-1762.

Penderis J, Shields SA, Franklin RJ (2003) Impaired remyelination and depletion of oligodendrocyte progenitors does not occur following repeated episodes of focal demyelination in the rat central nervous system. Brain 126:1382-1391.

Persidsky Y, Ramirez SH, Haorah J, Kanmogne GD (2006) Blood-brain barrier: structural components and function under physiologic and pathologic conditions. J Neuroimmune Pharmacol 1:223-236.

Psachoulia K, Jamen F, Young KM, Richardson WD (2009) Cell cycle dynamics of NG2 cells in the postnatal and ageing brain. Neuron Glia Biol 5:57-67.

Rabchevsky AG, Weinitz JM, Coulpier M, Fages C, Tinel M, Junier MP (1998) A role for transforming growth factor alpha as an inducer of astrogliosis. J Neurosci 18:10541-10552.

Raff MC, Miller RH, Noble M (1983) A glial progenitor cell that develops in vitro into an astrocyte or an oligodendrocyte depending on culture medium. Nature 303:390-396.

Raftopoulou M, Hall A (2004) Cell migration: Rho GTPases lead the way. Dev Biol 265:23-32.

Ransohoff RM, Kivisakk P, Kidd G (2003) Three or more routes for leukocyte migration into the central nervous system. Nat Rev Immunol 3:569-581.

Redwine JM, Armstrong RC (1998) In vivo proliferation of oligodendrocyte progenitors expressing PDGFalphaR during early remyelination. J Neurobiol 37:413-428.

Reier PJ, Golder FJ, Bolser DC, Hubscher C, Johnson R, Schrimsher GW, Velardo MJ (2002) Gray matter repair in the cervical spinal cord. Prog Brain Res 137:49-70.

Remahl S, Hildebrand C (1990) Relations between axons and oligodendroglial cells during initial myelination. II. The individual axon. J Neurocytol 19:883-898.

Reynolds BA, Weiss S (1992) Generation of neurons and astrocytes from isolated cells of the adult mammalian central nervous system. Science 255:1707-1710.

Rhodes KE, Raivich G, Fawcett JW (2006) The injury response of oligodendrocyte precursor cells is induced by platelets, macrophages and inflammation-associated cytokines. Neuroscience 140:87-100.

Richards LJ, Kilpatrick TJ, Bartlett PF (1992) De novo generation of neuronal cells from the adult mouse brain. Proc Natl Acad Sci U S A 89:8591-8595.

Richardson WD, Kessaris N, Pringle N (2006) Oligodendrocyte wars. Nat Rev Neurosci 7:11-18.

Rivers LE, Young KM, Rizzi M, Jamen F, Psachoulia K, Wade A, Kessaris N, Richardson WD (2008) PDGFRA/NG2 glia generate myelinating oligodendrocytes and piriform projection neurons in adult mice. Nat Neurosci 11:1392-1401.

Robel S, Bardehle S, Lepier A, Brakebusch C, Gotz M (2011) Genetic deletion of cdc42 reveals a crucial role for astrocyte recruitment to the injury site in vitro and in vivo. J Neurosci 31:12471-12482.

Rodriguez JP, Coulter M, Miotke J, Meyer RL, Takemaru K, Levine JM (2014) Abrogation of beta-catenin signaling in oligodendrocyte precursor cells reduces glial scarring and promotes axon regeneration after CNS injury. J Neurosci 34:10285-10297.

Rowntree S, Kolb B (1997) Blockade of basic fibroblast growth factor retards recovery from motor cortex injury in rats. Eur J Neurosci 9:2432-2441.

Sa-Pereira I, Brites D, Brito MA (2012) Neurovascular unit: a focus on pericytes. Mol Neurobiol 45:327-347.

Sabelstrom H, Stenudd M, Reu P, Dias DO, Elfineh M, Zdunek S, Damberg P, Goritz C, Frisen J (2013) Resident neural stem cells restrict tissue damage and neuronal loss after spinal cord injury in mice. Science 342:637-640.

Sahinkaya FR, Milich LM, McTigue DM (2014) Changes in NG2 cells and oligodendrocytes in a new model of intraspinal hemorrhage. Exp Neurol 255:113-126.

Sakry D, Karram K, Trotter J (2011) Synapses between NG2 glia and neurons. J Anat 219:2-7.

Sakry D, Yigit H, Dimou L, Trotter J (2015) Oligodendrocyte precursor cells synthesize neuromodulatory factors. PloS one 10:e0127222.

Sakry D, Neitz A, Singh J, Frischknecht R, Marongiu D, Biname F, Perera SS, Endres K, Lutz B, Radyushkin K, Trotter J, Mittmann T (2014) Oligodendrocyte precursor cells modulate the neuronal network by activity-dependent ectodomain cleavage of glial NG2. PLoS biology 12:e1001993.

Sauer B (1998) Inducible gene targeting in mice using the Cre/lox system. Methods 14:381-392.

Schnell L, Fearn S, Klassen H, Schwab ME, Perry VH (1999) Acute inflammatory responses to mechanical lesions in the CNS: differences between brain and spinal cord. Eur J Neurosci 11:3648-3658.

Schulz C, Gomez Perdiguero E, Chorro L, Szabo-Rogers H, Cagnard N, Kierdorf K, Prinz M, Wu B, Jacobsen SE, Pollard JW, Frampton J, Liu KJ, Geissmann F (2012) A lineage of myeloid cells independent of Myb and hematopoietic stem cells. Science 336:86-90.

Sedlakova R, Shivers RR, Del Maestro RF (1999) Ultrastructure of the blood-brain barrier in the rabbit. J Submicrosc Cytol Pathol 31:149-161.

Sellers DL, Maris DO, Horner PJ (2009) Postinjury niches induce temporal shifts in progenitor fates to direct lesion repair after spinal cord injury. J Neurosci 29:6722-6733.

Shechter R, Schwartz M (2013) CNS sterile injury: just another wound healing? Trends Mol Med 19:135-143.

Shepro D, Morel NM (1993) Pericyte physiology. FASEB J 7:1031-1038.

Shi J, Marinovich A, Barres BA (1998) Purification and characterization of adult oligodendrocyte precursor cells from the rat optic nerve. J Neurosci 18:4627-4636.

Silver J, Schwab ME, Popovich PG (2015) Central nervous system regenerative failure: role of oligodendrocytes, astrocytes, and microglia. Cold Spring Harb Perspect Biol 7:a020602.

Sim FJ, Zhao C, Penderis J, Franklin RJ (2002) The age-related decrease in CNS remyelination efficiency is attributable to an impairment of both oligodendrocyte progenitor recruitment and differentiation. J Neurosci 22:2451-2459.

Simon C, Gotz M, Dimou L (2011) Progenitors in the adult cerebral cortex: cell cycle properties and regulation by physiological stimuli and injury. Glia 59:869-881.

Simon C, Lickert H, Gotz M, Dimou L (2012) Sox10-iCreERT2 : a mouse line to inducibly trace the neural crest and oligodendrocyte lineage. Genesis 50:506-515.

Sirko S, Irmler M, Gascon S, Bek S, Schneider S, Dimou L, Obermann J, De Souza Paiva D, Poirier F, Beckers J, Hauck SM, Barde YA, Gotz M (2015) Astrocyte reactivity after brain injury-: The role of galectins 1 and 3. Glia 63:2340-2361.

Sirko S et al. (2013) Reactive glia in the injured brain acquire stem cell properties in response to sonic hedgehog. [corrected]. Cell Stem Cell 12:426-439.

Skipor J, Thiery JC (2008) The choroid plexus--cerebrospinal fluid system: undervaluated pathway of neuroendocrine signaling into the brain. Acta Neurobiol Exp 68:414-428.

Smith DH, Soares HD, Pierce JS, Perlman KG, Saatman KE, Meaney DF, Dixon CE, McIntosh TK (1995) A model of parasagittal controlled cortical impact in the mouse: cognitive and histopathologic effects. J Neurotrauma 12:169-178.

Snaidero N, Simons M (2014) Myelination at a glance. J Cell Sci 127:2999-3004.

Soderblom C, Luo X, Blumenthal E, Bray E, Lyapichev K, Ramos J, Krishnan V, Lai-Hsu C, Park KK, Tsoulfas P, Lee JK (2013) Perivascular fibroblasts form the fibrotic scar after contusive spinal cord injury. J Neurosci 33:13882-13887.

Sofroniew MV, Bush TG, Blumauer N, Lawrence K, Mucke L, Johnson MH (1999) Genetically-targeted and conditionally-regulated ablation of astroglial cells in the central, enteric and peripheral nervous systems in adult transgenic mice. Brain Res 835:91-95.

Somjen GG (1988) Nervenkitt: notes on the history of the concept of neuroglia. Glia 1:2-9.

Sriram K, Benkovic SA, Hebert MA, Miller DB, O'Callaghan JP (2004) Induction of gp130-related cytokines and activation of JAK2/STAT3 pathway in astrocytes precedes up-regulation of glial fibrillary acidic protein in the 1-methyl-4-phenyl-1,2,3,6-tetrahydropyridine model of neurodegeneration: key signaling pathway for astrogliosis in vivo? J Biol Chem 279:19936-19947.

Stallcup WB, Dahlin-Huppe K (2001) Chondroitin sulfate and cytoplasmic domain-dependent membrane targeting of the NG2 proteoglycan promotes retraction fiber formation and cell polarization. J Cell Sci 114:2315-2325.

Stelzer S, Ebnet K, Schwamborn JC (2010) JAM-A is a novel surface marker for NG2-Glia in the adult mouse brain. BMC Neurosci 11:27.

Sugiarto S, Persson AI, Munoz EG, Waldhuber M, Lamagna C, Andor N, Hanecker P, Ayers-Ringler J, Phillips J, Siu J, Lim DA, Vandenberg S, Stallcup W, Berger MS, Bergers G, Weiss WA, Petritsch C (2011) Asymmetry-defective oligodendrocyte progenitors are glioma precursors. Cancer Cell 20:328-340.

Sullivan HG, Martinez J, Becker DP, Miller JD, Griffith R, Wist AO (1976) Fluid-percussion model of mechanical brain injury in the cat. J Neurosurg 45:521-534.

Sun W, Dietrich D (2013) Synaptic integration by NG2 cells. Front Cell Neurosci 7:255.

Tajiri N, Dailey T, Metcalf C, Mosley YI, Lau T, Staples M, van Loveren H, Kim SU, Yamashima T, Yasuhara T, Date I, Kaneko Y, Borlongan CV (2013) In vivo animal stroke models: a rationale for rodent and non-human primate models. Transl Stroke Res 4:308-321.

Talibi SS, Aweid B, Aweid O (2014) Prospective therapies for high-grade glial tumours: A literature review. Ann Med Surg 3:55-59.

Tamori Y, Deng W-M (2013) Tissue Repair through Cell Competition and Compensatory Cellular Hypertrophy in Postmitotic Epithelia. Dev Cell 25:350-363.

Tamori Y, Deng WM (2014) Compensatory cellular hypertrophy: the other strategy for tissue homeostasis. Trends Cell Biol 24:230-237.

Tan AM, Zhang W, Levine JM (2005) NG2: a component of the glial scar that inhibits axon growth. J Anat 207:717-725.

Tan AM, Colletti M, Rorai AT, Skene JH, Levine JM (2006) Antibodies against the NG2 proteoglycan promote the regeneration of sensory axons within the dorsal columns of the spinal cord. J Neurosci 26:4729-4739.

Tang X, Davies JE, Davies SJ (2003) Changes in distribution, cell associations, and protein expression levels of NG2, neurocan, phosphacan, brevican, versican V2, and tenascin-C during acute to chronic maturation of spinal cord scar tissue. J Neurosci Res 71:427-444.

Tatsumi K, Takebayashi H, Manabe T, Tanaka KF, Makinodan M, Yamauchi T, Makinodan E, Matsuyoshi H, Okuda H, Ikenaka K, Wanaka A (2008) Genetic fate mapping of Olig2 progenitors in the injured adult cerebral cortex reveals preferential differentiation into astrocytes. J Neurosci Res 86:3494-3502.

Thurnherr T, Benninger Y, Wu X, Chrostek A, Krause SM, Nave KA, Franklin RJ, Brakebusch C, Suter U, Relvas JB (2006) Cdc42 and Rac1 signaling are both required for and act synergistically in the correct formation of myelin sheaths in the CNS. J Neurosci 26:10110-10119.

Tong Y, Wang P, Xia Z, Xia X, Xu X (2009) [Color pattern reversal visual evoked potentials in primary open angle and angle closure glaucoma]. Zhong Nan Da Xue Xue Bao Yi Xue Ban 34:771-775.

Vallstedt A, Klos JM, Ericson J (2005) Multiple dorsoventral origins of oligodendrocyte generation in the spinal cord and hindbrain. Neuron 45:55-67.

Velez-Fort M, Audinat E, Angulo MC (2009) Functional alpha 7-containing nicotinic receptors of NG2-expressing cells in the hippocampus. Glia 57:1104-1114.

Ventura RE, Goldman JE (2006) Telencephalic oligodendrocytes battle it out. Nat Neurosci 9:153-154.

Venur V, Peereboom D, Ahluwalia M (2015) Current Medical Treatment of Glioblastoma. In: Current Understanding and Treatment of Gliomas (Raizer J, Parsa A, eds), pp 103-115: Springer International Publishing.

Verbeek MM, Westphal JR, Ruiter DJ, de Waal RM (1995) T lymphocyte adhesion to human brain pericytes is mediated via very late antigen-4/vascular cell adhesion molecule-1 interactions. J Immunol 154:5876-5884.

Vigano F, Mobius W, Gotz M, Dimou L (2013) Transplantation reveals regional differences in oligodendrocyte differentiation in the adult brain. Nat Neurosci 16:1370-1372.

Vigano F, Schneider S, Cimino M, Bonfati E, Gelosa P, Sironi L, Abbracchio MP, Dimou L (2015) GPR17 expressing NG2-glia: oligodendrocyte progenitors serving as a reserve pool after injury. Glia 64:287-299.

Visvader JE (2011) Cells of origin in cancer. Nature 469:314-322.

Voskuhl RR, Peterson RS, Song B, Ao Y, Morales LB, Tiwari-Woodruff S, Sofroniew MV (2009) Reactive astrocytes form scar-like perivascular barriers to leukocytes during adaptive immune inflammation of the CNS. J Neurosci 29:11511-11522.

Wang DD, Bordey A (2008) The astrocyte odyssey. Prog Neurobiol 86:342-367.

Wang JB, Sonn R, Tekletsadik YK, Samorodnitsky D, Osman MA (2009) IQGAP1 regulates cell proliferation through a novel CDC42-mTOR pathway. J Cell Sci 122:2024-2033.

Wang S, Young KM (2014) White matter plasticity in adulthood. Neuroscience 276:148-160.

Warner SJ, Yashiro H, Longmore GD (2010) The Cdc42/Par6/aPKC polarity complex regulates apoptosis-induced compensatory proliferation in epithelia. Curr Biol 20:677-686.

Whelan G, Kreidl E, Peters JM, Eichele G (2012a) The non-redundant function of cohesin acetyltransferase Esco2: some answers and new questions. Nucleus 3:330-334.

Whelan G, Kreidl E, Wutz G, Egner A, Peters JM, Eichele G (2012b) Cohesin acetyltransferase Esco2 is a cell viability factor and is required for cohesion in pericentric heterochromatin. Embo J 31:71-82.

Wigley R, Butt AM (2009) Integration of NG2-glia (synantocytes) into the neuroglial network. Neuron Glia Biol 5:21-28.

Winter CG, Saotome Y, Levison SW, Hirsh D (1995) A role for ciliary neurotrophic factor as an inducer of reactive gliosis, the glial response to central nervous system injury. Proc Natl Acad Sci U S A 92:5865-5869.

Wolswijk G, Noble M (1989) Identification of an adult-specific glial progenitor cell. Development 105:387-400.

Woodham EF, Machesky LM (2014) Polarised cell migration: intrinsic and extrinsic drivers. Curr Opin Cell Biol 30:25-32.

Wrathall JR (1992) Spinal cord injury models. J Neurotrauma 9 Suppl 1:S129-134.

Wren D, Wolswijk G, Noble M (1992) In vitro analysis of the origin and maintenance of O-2Aadult progenitor cells. J Cell Biol 116:167-176.

Xie L, Yang SH (2015) Interaction of astrocytes and T cells in physiological and pathological conditions. Brain Res 1623:63-73.

Xu JP, Zhao J, Li S (2011) Roles of NG2 glial cells in diseases of the central nervous system. Neurosci Bull 27:413-421.

Xu L, Ryu J, Hiel H, Menon A, Aggarwal A, Rha E, Mahairaki V, Cummings BJ, Koliatsos VE (2015) Transplantation of human oligodendrocyte progenitor cells in an animal model of diffuse traumatic axonal injury: survival and differentiation. Stem Cell Res Ther 6:93.

Yamashima T, Tonchev AB, Vachkov IH, Popivanova BK, Seki T, Sawamoto K, Okano H (2004) Vascular adventitia generates neuronal progenitors in the monkey hippocampus after ischemia. Hippocampus 14:861-875.

Young KM, Psachoulia K, Tripathi RB, Dunn SJ, Cossell L, Attwell D, Tohyama K, Richardson WD (2013) Oligodendrocyte dynamics in the healthy adult CNS: evidence for myelin remodeling. Neuron 77:873-885.

Yuan X, Eisen AM, McBain CJ, Gallo V (1998) A role for glutamate and its receptors in the regulation of oligodendrocyte development in cerebellar tissue slices. Development 125:2901-2914.

Zamanian JL, Xu L, Foo LC, Nouri N, Zhou L, Giffard RG, Barres BA (2012) Genomic analysis of reactive astrogliosis. J Neurosci 32:6391-6410.

Zawadzka M, Rivers LE, Fancy SP, Zhao C, Tripathi R, Jamen F, Young K, Goncharevich A, Pohl H, Rizzi M, Rowitch DH, Kessaris N, Suter U, Richardson WD, Franklin RJ (2010) CNS-resident glial progenitor/stem cells produce Schwann cells as well as oligodendrocytes during repair of CNS demyelination. Cell Stem Cell 6:578-590.

Zeisel A, Munoz-Manchado AB, Codeluppi S, Lonnerberg P, La Manno G, Jureus A, Marques S, Munguba H, He L, Betsholtz C, Rolny C, Castelo-Branco G, Hjerling-Leffler J, Linnarsson S (2015) Brain structure. Cell types in the mouse cortex and hippocampus revealed by single-cell RNA-seq. Science 347:1138-1142.

Zhang B, Gensel JC (2014) Is neuroinflammation in the injured spinal cord different than in the brain? Examining intrinsic differences between the brain and spinal cord. Exp Neurol 258:112-120.

Zhang Y, Chen K, Sloan SA, Bennett ML, Scholze AR, O'Keeffe S, Phatnani HP, Guarnieri P, Caneda C, Ruderisch N, Deng S, Liddelow SA, Zhang C, Daneman R, Maniatis T, Barres BA, Wu JQ

(2014) An RNA-sequencing transcriptome and splicing database of glia, neurons, and vascular cells of the cerebral cortex. J Neurosci 34:11929-11947.

Zhao C, Fancy SPJ, Kotter MR, Li W-W, Franklin RJM (2005) Mechanisms of CNS remyelination—the key to therapeutic advances. J Neurol Sci 233:87-91.

Zhu X, Bergles DE, Nishiyama A (2008) NG2 cells generate both oligodendrocytes and gray matter astrocytes. Development 135:145-157.

Zhu X, Hill RA, Dietrich D, Komitova M, Suzuki R, Nishiyama A (2011) Age-dependent fate and lineage restriction of single NG2 cells. Development 138:745-753.

Zlokovic BV (2008) The blood-brain barrier in health and chronic neurodegenerative disorders. Neuron 57:178-201.

8 Acknowledgements

I would like to thank:

First and foremost **Leda Dimou** for giving me the opportunity to work in her group and trusting me with this great project and the complex imaging technique. She supported me throughout the years with great discussions, technical and conceptual supervision and in the stressful periods of writing the manuscript. Furthermore she gave me the opportunity to join many interesting meetings and conferences.

Magdalena Götz for the opportunity to work on the project and be a part of her big group and sharing her fascination and energy for science. She provided me the possibility to work with a vast array of methods and the shared insights to many fascinating projects. Also as part of my TAC she helped me with many new ideas and concepts for my project.

Benedikt Grothe for taking over the supervision of my work for the biological faculty.

Martin Kerschensteiner and especially **Hannelore Ehrenreich** who supported me not only as part of my TAC with helpful discussions, motivation and ideas.

Christian Leibold, **Wolfgang Enard**, **Thomas Ott**, **Hans Straka** and **Heinrich Leonhardt** for the examination of my thesis.

Sarah and **Francesca** for sharing the office with me, a lot of helpful input in all science-related matters and beyond, the mental and emotional support and the nice time in- and outside the lab over the past years.

Christoph for starting this great project, his patience in teaching me this challenging technique, sharing the office with me and a lot of helpful discussions in and outside the lab.

Felix and **Carsten** for many helpful discussions and the great collaboration.

Marisa and **Sven** for a great time and so many good advices in the fields of science, biking, hiking, travelling and all the rest.

Sofia and **Nicole** for being part of the office and listening or sharing science-related or un-related stories and problems.

Detlef, Gabi, Carmen, Ines, Tatiana, Michaela and Manja for the great technical assistance and the solutions for so many questions in the lab.

All the animal caretakers for doing such a great and challenging job and being always supportive.

The new members of the NG2-group for bringing new life in this scientific field and asking the right questions.

All other people in the LMU and the Helmholtz for being great colleagues and the support when needed.

And last but definitely not least **Romina** and **my parents** for their endless support over all those years. Without you this would not have been possible.

9 Appendix

9.1 Detailed Statistics

Detailed Statistics of data represented in Figure 8

Category	Test	p-value	Comparisons	dF
Hypertrophy	ANOVA+Tukey post-test	p<0.05	d2 vs. d4	dF=32
Hypertrophy	ANOVA+Tukey post-test	p<0.01	Control vs. d4; d4 vs. d6	dF=32
Hypertrophy	ANOVA+Tukey post-test	p<0.0001	Control vs. d2; d2 vs. d6; d2 vs. d8; d2 vs. d11; d2 vs. d21; d2 vs. d28	dF=32
Polarization	ANOVA+Tukey post-test	p<0.05	d2 vs. d11; d4 vs. d28; d6 vs. d21; d8 vs. d28	dF=32
Polarization	ANOVA+Tukey post-test	p<0.01	Control vs. d4; Control vs. d6; Control vs. d8; d2 vs. d21; d6 vs. d28	dF=32
Polarization	ANOVA+Tukey post-test	p<0.0001	Control vs. d2; d2 vs. d28	dF=32
Proliferation	ANOVA+Tukey post-test	p<0.01	d2 vs. d4	dF=32
Proliferation	ANOVA+Tukey post-test	p<0.0001	Control vs. d4; d4 vs. d8; d4 vs. d11; d4 vs. d21; d4 vs. d28	dF=32
Migration	ANOVA+Tukey post-test	p<0.05	Control vs. d2; Control vs. d4; Control vs. d11	dF=32
Migration	ANOVA+Tukey post-test	p<0.01	Control vs. d6	dF=32

Detailed Statistics of data represented in Figure 11

Category	Test	p-value	Comparisons	dF
Velocity	ANOVA+Tukey post-test	p<0.05	Control vs. d2; Control vs. d4; d2 vs. d28; d4 vs. d14	dF=35
Velocity	ANOVA+Tukey post-test	p<0.01	d2 vs. d21; d4 vs. d21; d2 vs. d28	dF=35
Max. Migration distance	ANOVA+Tukey post-test	p<0.05	Control vs. d2; Control vs. d4; d2 vs. d14; d4 vs. d14; d8 vs. d28	dF=35
Max. Migration distance	ANOVA+Tukey post-test	p<0.01	d6 vs. d21; d6 vs. d28; d8 vs. d21	dF=35
Max. Migration distance	ANOVA+Tukey post-test	p<0.0001	d2 vs. d21; d2 vs. d28; d4 vs. d21; d4 vs. d28	dF=35

9.2 List of Figures

9.3 Abbreviations

2PLSM	Two-photon laser scanning microscopy
AChR	Acetylcholine receptor
AD	Alzheimers disease
AEP	Anterior entopeduncular area
ALS	Amyotrophic lateral sclerosis
AMPA	α-amino-3-hydroxy-5-methyl-4-isoxazolepropionic acid
aPKC	Atypical Protein kinase C
APC	Adenomatous polyposis coli
Ascl1	Achaete-scute homolog 1
ASPA	Aspartoacylase
ATP	Adenosine triphosphate
BBB	Blood brain barrier
bFGF	Basic fibroblast growth factor
CC	*Corpus callosum*
CC-1	See APC
CCL2	Ccl2 chemokine
cdc42	Cell division control protein 42 homolog
CGE	Caudal ganglionic eminence
CNS	Central nervous tissue
$CreER^{T2}$	Cre recombinase fused to a truncated estrogen receptor
CSPG	Chondroitin sulfate proteoglycan
d	Day
DAPI	4’,6-Diamidino-2-phenylindol
DNA	Deoxyribonucleic acid
dNTPs	Deoxynucleoside triphosphates
dpi	Days post injury
dpp	Days post proliferation
E	Embryonic day
EAE	Experimental autoimmune encephalomyelitis
ECM	Extracellular matrix
e.g.	Exempli gratia
EPSC	Excitatory postsynaptic potential
Esco2	Acetyl-transferase establishment of cohesion 1 homologue 2
EYFP	Enhanced yellow fluorescent protein
FGF	Fibroblast growth factor
GABA	γ-Aminobutyric acid
GDP	Guanosine diphosphate
GFAP	Glial fibrillary acidic protein
GFP	Green fluorescent protein
GM	Grey matter
GPR17	G-protein coupled receptor 17
GSTπ	Glutathione-S-transferase π
GTP	Guanosine-5'-triphosphate
h	Hour
IFNγ	Interferon-γ
IL	Interleukin
IGF	Insulin-like growth factor
IPSC	Inhibitory postsynaptic potential

JAMA	Junctional adhesion molecule A
JNK	c-Jun N-terminal kinases
kDa	Kilo Dalton
kg	Kilogram
KO	Knockout
LGE	Lateral ganglionic eminence
LIF	Leukemia inhibitory factor
LT	Long term
MAG	Myelin-associated glycoprotein
MAPK	Mitogen-activated protein kinase
MBP	Myelin basic protein
min	Minutes
mm	Millimeter
MOG	Myelin oligodendrocyte
MS	Multiple sclerosis
mTOR	Mechanistic target of rapamycin
µm	Micrometer
µl	Microliter
NA	Numerical aperture
NG2	Neuron-glia antigen 2
nm	Nanometer
NMDA	N-Methyl-D-aspartate
NO	Nitric oxide
OPC	Oligodendrocyte progenitor cell
Par6	Partitioning defective 6 homolog alpha
P	Postnatal day
PBS	Phosphate buffered saline
PCR	Polymerase chain reaction
PDGFRα	Platelet-derived growth factor receptor α
PFA	Paraformaldehyde
PKC	Protein kinase C
PLP	Proteolipid protein
PWI	Punctate wound injury
RhoA	Ras homolog gene family member A
ROCK	Rho-associated, coiled-coil-containing protein kinase 1
RT	Room temperature
SCI	Spinal cord injury
SDS	Sodium dodecyl sulphate
ST	Short term
STAT3	Signal transducer and activator of transcription 3
Syx1	Syntaxin 1
SWI	Stab wound injury
TBI	Traumatic brain injury
TGF-α	Transforming growth factor alpha
TNF-α	Tumor necrosis factor-α
VEGF	Vascular endothelial growth factor
WASp	Wiskott-Aldrich Syndrome protein
WM	White matter
WT	Wild type

9.4 Eidesstattliche Erklärung

Ich versichere hiermit an Eides statt, dass die vorgelegte Dissertation von mir selbständig und ohne unerlaubte Hilfe angefertigt ist.

München, den 01.08.2016 Axel von Streitberg

(Unterschrift)

Erklärung

Hiermit erkläre ich, *

[X] dass die Dissertation nicht ganz oder in wesentlichen Teilen einer anderen Prüfungskommission vorgelegt worden ist.

[X] dass ich mich anderweitig einer Doktorprüfung ohne Erfolg nicht unterzogen habe.

[ ] dass ich mich mit Erfolg der Doktorprüfung im Hauptfach .....
und in den Nebenfächern .....
bei der Fakultät für ..... der .....
(Hochschule/Universität)
unterzogen habe.

[ ] dass ich ohne Erfolg versucht habe, eine Dissertation einzureichen oder mich der Doktorprüfung zu unterziehen.

München, den 01.08.2016 Axel von Streitberg

(Unterschrift)

*) Nichtzutreffendes streichen